Alasmarya Islamic University
College of Science
Department of Chemistry

Experimental, Simulation and Bonding Properties Studies of Some Frist and Second –Row Carbonyl Transition Metal and their Biology Application

Submitted by: Fatheya Mohammad AL-triky

Under Supervision

Prof. Salem El-tuhami Ashoor
Professor

Prof . Khalifa Abdulsalam Alfallous
Professor

A THESIS SUBMITTED IN PARTIAL FULFILLMENT OF THE REQUIREMENTS FOR THE DEGREE OF MASTER OF SCIENCE

Academic year: (2024 - 2025)

الجامعة الأسمرية الإسلامية
الإدارة العامة
إدارة الدراسات العليا والتدريب

نموذج د ع (31)
التاريخ: / /
الموافق: 14 / 6 / 2025م

قرار لجنة مناقشة رسالة الإجازة العالية (الماجستير)

عملاً بقرار السيد/ رئيس الجامعة رقم (279) لسنة 2025 م. الصادر في 06 / 5 / 2025م. القاضي بتشكيل لجنة لمناقشة رسالة علمية للحصول على درجة الإجازة العالية (الماجستير) في تخصص الكيمياء المقدمة من الطالبة : فتحية محمد امحمد التريكي . كلية العـــلوم وعنوانها:

(دراسات تجريبية ومحاكاة خصائص الترابط لبعض المعادن الانتقالية المحتوية على الكربونيل من الصف الأول والثاني وتطبيقاتها البيولوجية)

وتتكون اللجنة من الاساتذة:

1. أ.د. سالم التهامي عاشور	الجامعة:	مصراتة	مشرفا و مقررا.
2. أ.د. خليفة عبدالسلام الفلوس	الجامعة:	الأسمرية الإسلامية	مشرف ثان.
3. د. سليمة علي المبروك	الجامعة:	الأسمرية الإسلامية	عضوا داخليا.
4. أ.د. محمد سعد مفتاح محمد	الجامعة:	بني وليد	عضوا خارجيا.

عقدت اللجنة جلسة علنية على تمام الساعة: الحادية عشر من صباح يوم: السبت الموافق: 14 / 6 / 2025م، بقاعة الاجتماعات بالكلية لمناقشة الرسالة و تقويم مستواها العلمي و المنهج الذي اتبعته الباحثة و المصادر التي استخدمتها في دراستها، وقررت ما يلي:

بعد اتمام الطالبة: فتحية محمد امحمد التريكي لمتطلبات الدراسات العليا و اجتياز امتحاناتها و مناقشة رسالتها و تقويمها تقرر:

1. اجتيازها بدون ملاحظات (✓) بتقدير: // وبنسبة (//).
2. اجتيازها بملاحظات (//) بتقدير: // وبنسبة (//) وتمنح الطالبة فرصة للتعديل و الأخذ بالملاحظات خلال: // من تاريخ المناقشة.
3. عدم إجازتها (//).

توقيعات أعضاء لجنة المناقشة:

1. أ.د. سالم التهامي عاشور	الجامعة:	مصراتة	التوقيع
2. أ.د. خليفة عبدالسلام الفلوس	الجامعة:	الأسمرية الإسلامية	التوقيع
3. د. سليمة علي المبروك	الجامعة:	الأسمرية الإسلامية	التوقيع
4. أ.د. محمد سعد مفتاح محمد	الجامعة:	بني وليد	التوقيع

يعتمد:

عميد الكلية

رئيس الجامعة

يعد من عشرة (10) نسخ

بِسْمِ اللَّهِ الرَّحْمَنِ الرَّحِيمِ

﴿وَفَوْقَ كُلِّ ذِي عِلْمٍ عَلِيمٌ﴾

صَدَقَ اللهُ الْعَظِيمِ

سورة يوسف (76)

الإهـــــداء...

إلى روح والديّ الكريمين

أحاطكما المولى برحمته، وأنار قبريكما، بنوره العظيم،

وأدخلكما الفردوس الأعلى دون حساب ولا عذاب.

اللهم اجمعني بهما في جنات النعيم، واجعل عملي هذا صدقة جارية لهما يا عفو يا كريم ...

شكر وتقدير

الحمد لله الذي جعل العلم النافع طريقا موصلا لرضاه، وصراطا يتبعه من أراد هداه، ويحيد عنه من ضل واتبع هواه، وأشهد أن لا إله إلا الله، وحده لا شريك لـه وان محمدا عبده ورسوله، صلى الله عليه وعلى اله واصحابه الهداة التقاه ومن سار على نهجه الى يوم لقاه.

وبعد:

أتقدّم بخالص الشكر والتقدير إلى أستاذيَّ المشرفين: الأستاذ الدكتور سالم التهامي عاشور، والأستاذ الدكتور خليفة عبد السلام الفلوس، لما قدّماه من إشرافٍ علمي وتوجيهٍ منهجي أسهما إسهامًا فاعلًا في إنجاز هذا البحث وإخراجه بالصورة العلمية المطلوبة.

كما أتوجّه بجزيل الشكر إلى كلية العلوم بالجامعة الأسمرية الإسلامية على ما وفرته من دعمٍ أكاديمي وبيئةٍ علمية مناسبة، ولا سيما مبادرتها بفتح برامج الدراسات العليا، مما أتاح لي فرصة مواصلة الدراسة وإنجاز هذا العمل.

وأعرب عن امتناني لأسرتي الكريمة، من إخوتي وأخواتي وأبناء أخي، لما قدّموه من دعمٍ وتشجيعٍ خلال فترة إعداد البحث، كما أشكر إدارة ثانوية الزهراء وزملائي وزميلاتي، وكل من أسهم بالمساندة أو التيسير أو التشجيع.

وأسأل الله التوفيق والسداد، وأن يجعل هذا العمل نافعًا ومحققًا لأهدافه العلمية.

الباحثة

LIST OF CONTENTS

Subject	Page
the Quranic verse……..……....	II
Dedication…….……	III
Thanks and appreciation…….……..…	IV
Contents ……...……	V
List of Tables ……...……	VII
List of Figures ……..…….…..	VIII
List of Schemes…….,……...……...…	X
Abstract ((English) …….……...…….	XI
Chapter One **INTRODUCTIN**	
Introduction……..……	2
Chapter Two **EXPERIMENTAL AND METHODE**	
2.1. General Procedures …….……..…	28
2.1.1 Reagents and Materials……..……	28
2.1.2 Spectroscopic Techniques …….....……	28
2. 1.3 Theoretical calculations…….....……	28
2.1.4 Microwave instrument…….....……	29
2.2 Experimental……..……...…..……	29
2.2.1 Method of preparation and work steps:: …….	29
2.2.2 Synthesis of [Mo(CO)$_2$ (dpg)(dppm)]……...……..	29
2.2.3 -Synthesis of [Mo(CO)$_2$ (dppm)…….……..…	29
2.2.4 -Synthesis of [Mo(CO)$_2$ (dppm) (2-aminopy)] (dppm)]……..……	30
2.2.5 Synthesis of [Cr (CO)$_2$ (dppm) (DPG)] (dppm)]……..…… …	30
2.2.6- Synthesis of [Cr (CO)$_2$ (dppm) (8-HQ)] (dppm)] ……	31
2.2.7- Synthesis of [Cr (CO)$_2$ (dppm) (2-aminopy)] (dppm)] ……	31
2.3 Determination of potential cytotoxicity of novel Chromium moly-bdenum complexes with DPPM ligand……	32
2.3.1 Principle……..……...…..……	32

Subject	Page
2.3.2 Reagents and buffers…….…..	32
2.4 Measurement Of Biological Activity …….……...…	32
2.4.1 Procedure:…… …….…...…….……..	32
2.4.2 Calculation:…… ……...……..	33
CHAPTER THREE **Results and Discussion**	
3.1. Spectroscopic Studies Of Molybdenum (0) complexes …….……..…	36
3.2. Results and diagnosis of chromium (0) complexes ……..	48
3.3. Biological activity……...……...…….	61
3 . 4. Molecular docking studies …….…….	62
3.5. Conclusions ……...……	67
References……	68
Abstract ((Arabc) …….……...…….	78

LIST TABLES

Subject	Page
Table (1)The elemental analysis data of molybdenum complexes.....	34
Table(2)The elemental analysis data of chromium complexes……..……	34
Table (3) Absorbed vibrational frequencies of molybdenum complexes $Mo(CO)_2$(dppm)(dpg) ……..……..……	37
Table (4) Absorbed vibrational frequencies of molybdenum complexes [$Mo(CO)_2$(dppm)(8- HQ)]……..……..…..…	38
Table (5) Absorbed vibrational frequencies of molybdenum complexes [$Mo(CO)_2$(dppm)(2- aminopy)]……..……...……..……..	40
Table (6) Absorbed vibrational frequencies of chromium complexes [Cr $(CO)_2$(dppm)(dpg]……....	49
Table (7) Absorbed vibrational frequencies of chromium complexes Cr (CO)2(dppm)(8- HQ)……...…….……..	50
Table (8) Absorbed vibrational frequencies of chromium complexes Cr $(CO)_2$(dppm)(2-aminopy)……..….	52
Table (9) Effect of Chromium Molybdenum complexes with DPPM ligand on HepG2 cell survival and IC50 values after 48 hours of treatment……..……..	61
Table (10). Energy values during molecular docking analysis between complexes prepared as ligand molecule against 4PYP as target molecules……...……..…	63

LIST FIGURES

Subject	Page
Fig 1: Form of Metal carbonyl $M(CO)_6$ …….……...	5
Fig. 2: form of Metallocene ……...……...…	8
Fig 3 : Dichlorobismolybdenum (IV) (molybdocene dichloride)……...…	8
Fig .4: Form of $[Mo(NO)_2(amphp\text{-}aap)(OH)]$ ……...……...…	9
Fig . 5: Structural formula of 1,1-bis (diphenylphospino) methane (dppm)…….. ……..…..	12
Fig.6 : structure planar of M_2P_4(I) and cis $M_2(dpm)_2$ (II) (III) ...……...……	13
Fig .7: General structure of dppm bridge complexes between two different or identical transition metal centers ……..…..…	15
Fig .8 : structure of 2-Aminopyridine …….……...	17
Fig . 9: Chelating and bridging coordination modes of aminopyridinato ligands ……..…..	20
Fig. 10: structure of 8-Hydroxyquinoline (8HQ) ……...……	22
Fig . 11: Structural formula DPG ……...….	24
Fig.12: Mass spectrum for $[Mo(CO)_2(dppm)(dpg)]$ ……	37
Fig.13: Mass spectrum for $[Mo(CO)_2(dppm)(8\text{-}HQ)]$ …….……	39
Fig.14: Mass spectrum for $[Mo(CO)_2(dppm)(2\text{-}aminopy)]$…….……..	40
Fig .15 : Infrared spectrum of [$Mo(CO)_2(dppm)(DPG)$]……..…….	42
Fig. 16 : Infrared spectrum of $[Mo(CO)_2(dppm)(8HQ)]$……	42
Fig .17: Infrared spectrum of $[Mo(CO)_2(dppm)(2\text{-}aminopy)]$…….……	43
Fig .18: H^1 NMR spectrum of $[Mo(CO)_2(dpg)(dppm)]$…….……	44
Fig.19: ^{1} HNMR spectrum of $[Mo(CO)_2(8\text{-}HQ)(dppm)]$ ……..…	44
Fig .20 : H^1 NMR spectrum of $[Mo(CO)_2(2\text{-}aminopy)(dppm)]$…….	45
Fig.21 : Electronic spectrum of $[Mo(Co)_2(DPG)(dppm)]$……..….....	46
Fig. 22: Electronic spectrum of $[Mo(Co)_2(8\text{-}HQ)(dppm)]$……..…	47
Fig.23: Electronic spectrum of $[Mo(CO)_2(2\text{-}aminopy)(dppm)$……...……	48
Fig. 24: Mass spectrum for $[Cr(CO)_2(dppm)(dpg)$ …….....	49
Fig .25: Mass spectrum for $[Cr(CO)_2(dppm)(8\text{-}HQ)]$……..	51

Subject	Page
Fig.26: Mass spectrum for [$Cr(CO)_2$ (dppm)(2-aminopy)]……..……..	53
Fig.27: Infrared spectrum of [$Cr(CO)_2$(DPG)(dppm)] ……..…….....	54
Fig .28: Infrared spectrum of [$Cr(CO)_2$(dppm)(8-HQ)]……...	55
Fig .29: Infrared spectrum of [Cr ($CO)_2$(dppm)(2-aminopy)] …….....	55
Fig .30: ^{1} HNMR spectrum of [Mo ($CO)_2$(dpg)(dppm)] ……	56
Fig.31: H^1 NMR spectrum of [Mo ($CO)_2$(8- HQ)(dppm)] ……...…..	57
Fig .32 : ^{1}HNMR spectrum of [Mo ($CO)_2$(2-aminopy)(dppm)] (F6)……..	57
Fig.33 : Electronic spectrum of [Cr ($Co)_2$ (DPG)(dppm)] ……..…	58
Fig.34 : Electronic spectrum of [Cr ($Co)_2$ (8-HQ)(dppm)] ……..…....	59
Fig.35 : Electronic spectrum of [$Cr(Co)_2$ (2-aminoyp)(dppm)]……	60
Fig.36: Shows Surviving fraction and IC50 of HEPG-2 cells treated with Chromium-Molybdenum with DPPMligand for 48 hours……..	62
Fig.37: Docking Interaction of amino acid residues of PDB Id: 4PYP with F1, F4 and F6 …….……	65
Fig.38: Docking Interaction of amino acid residues of PDB Id: 4PYP with F2, F3 and F5 ……...…….	66

LIST SCHEMES

Subject	Page
scheme (1) Catalytic mechanism of catalyst CPS-[$MoO_2(ALGL)_2$] in epoxidation of cyclohexene to cyclohexene oxide by TBHP ..…….....	7
Scheme (2). Synthesis of the cis-disubstituted complex …….……	10
scheme (3). Synthesis [Cr(HL)(ADMPY)(H_2O)Cl_2] H_2O…..……	11
scheme (4) The proposed structure of metal complexes M: Co(II), Cr(III), Cu(II),Mn(II), Ni(II) with Schiff bases……..…	11
Scheme(5) Synthesis of diphenylphosphino)methane…….	12
Scheme (6. A.B) synthesis of [ClAu(m dppm)AuCl] as reported by Mirabelli et al and reported by Brandys et al.…….	14
Scheme(7). Synthesis of [(μ^6-C_6H_6)$RuCl_2$(μ-dppm)Fe(CO)I(μ^5-C_5H_5)] (I) [(μ^6-p-cymene)$RuCl_2$(μ-dppm)Fe(CO)I(h_5-C_5H_5)](II) ……..…	16
scheme (8) Synthesis of Mo(PN)(CO)4 where PN = N(diisopropylpho-sphanyl)-2-aminopyridine (PN-iPr)(PN-Ph, PN-iPr,PN-BIPOL, and PN-TARMe)……...……...……..	17
Scheme (9) Synthesis of Mo-(PN-iPr)(η3-CH2CHCH2)(CO)2Br (2)…	18
Scheme (10) Synthesis of Mo(PN-iPr)(CO)4(1b) ……...	19
Scheme (11). Synthesis of aminopyridine Fe complexes …….……	21
scheme 12.1: Preparation of [Zr(HQ)(Glu)$(Cl)_2$] [1]……..…	22
scheme 12.2: Preparation of [Zr(HQ)(Fru)(Cl)2] [2]…….	22
scheme (13)synthesized three complexes of (Cu,Ni, Co) containing 8-hydroxyquinoline (8-HQ) …….	23
scheme (14) Formation of a complex of cobalt(II) and nickel(II) with 2-hydroxy-5-nitrothiophenol and diphenylguanidine…….…….	25
Scheme (15) Synthesis of [$Mo(CO)_2$ (dpg)(dppm)] (F 1)……..……..…	29
Scheme(16) Synthesis of [$Mo(CO)_2$ (8-HQ) (dppm)] (F 2)…..…… …	30
Scheme(17) Synthesis of [$Mo(CO)_2$ (2-aminopy)(dppm)] (F 3)..…...…	30
Scheme (18) Synthesis of [Cr ($CO)_2$ (DPG) (dppm)](F 4)……...……..	31
Scheme (19) Synthesis of [Cr ($CO)_2$(8-HQ)(dppm)] (F 5)…….……	31
Scheme (20) Synthesis of [Cr ($CO)_2$ (2-aminopy) (dppm)] (F 6)…..…	32

ABSTRACT

The microwave-assisted green pathway was successfully employed to synthesize a series of novel transition metal carbonyl complexes from the first and second series, incorporating the chelating ligand dppm (bis(diphenylphosphino)methane) along with secondary ligands including diphenylguanidine (DPG), 8-hydroxyquinoline (8-HQ), and 2-aminopyridine (2-aminoPy), coordinated to $[Cr(CO)_6]$ and $[Mo(CO)_6]$ through the C=O moiety. The resulting complexes belong to the following types: $[M(CO)_2(dpg)(dppm)]$, $[M(CO)_2$ (8-HQ)(dppm)], $[Mo(CO)_2$ (2-aminopy)(dppm)] (M = Cr, Mo)

where.These complexes were characterized using ultraviolet (UV) spectroscopy, infrared (IR) spectroscopy, mass spectrometry (MS), elemental analysis (CHN), and ^1H NMR spectroscopy. Their biological activity was evaluated against the HepG2 liver cancer cell line, and all compounds exhibited growth-inhibitory effects. Notably, complexes F5 and F3 demonstrated the highest potency, with IC_{50} values of 180 and 207 μM, respectively, indicating the potential of these compounds as scaffolds for developing novel anticancer agents.

Furthermore, density functional theory (DFT) calculations were applied to molybdenum and chromium complexes to estimate the total system energy by approximating it to the electron density. Molecular docking studies of all complexes (F1–F6) on the estrogen receptor (PDB ID: 4PYP) revealed that complexes F1, F4, and F6 possess the highest binding affinity at the active site, with binding energies of –8.43, –8.54, and –8.85 kcal/mol, respectively, suggesting higher stability and stronger interaction compared to the other complexes. Computational simulations thus provided deeper insights into the nature of these interactions and the potential mechanism of action on cancer cells.

CHAPTER ONE
INTRODUCTIN

Introduction

Organometallic chemistry is a scientific discipline that thoroughly examines the properties, synthesis, and reactions of organometallic compounds, which are chemical compounds that inherently possess at least one chemical bond between a carbon atom of an organic molecule and a metal, encompassing a wide range of metals including alkali metals, alkaline earth metals, and transition metals, and sometimes even extending to include metalloids like boron, silicon, and selenium, as well as other related elements that exhibit intermediate properties between metals and nonmetals. The study of organometallic compounds is essential for understanding synthetic flexibility and creating new bonds in organic compounds [1, 2].

After the early 1970s, there was a sudden, remarkable, and unprecedented surge of activity in the realm of transition metal organometallic chemistry, which ultimately led to groundbreaking, phenomenal, and far-reaching developments that had a profound impact on various branches of mainstream chemistry as well as interfacial chemistry.

This new wave of scientific innovation was marked by extraordinary achievements, and the significance of these efforts was fully recognized when several Nobel Prizes were awarded to pioneers in this field in recent times. Specifically, the Nobel Prize in Chemistry was awarded to Yves Chauvin, Richard R. Schrock, and Robert H. Grubbs in 2005 for their groundbreaking work on olefin metathesis, a fundamental process in organic chemistry. Similarly, in 2010, the Nobel Prize in Chemistry was bestowed upon Akira Suzuki, Richard F. Heck, and Ei-ichi Negishi for their pioneering contributions to the development of palladium-catalyzed carbon-carbon cross-coupling reactions in organic synthesis, a crucial area of research that has revolutionized the field of organic chemistry. [3].

The 20^{th} century is characterized by the rapid development of organometallic chemistry. It opened possibilities for the synthesis and investigation of new heterocyclic systems. The initial application of organometallic compounds The exploration of biological systems started in 1985 and marked the emergence of the term "organometallic biochemistry " [4, 5].

G. Jaouen was the first to introduce the term organometallic biochemistry in 1993 and definite it as (organometallic complexes study with bio-ligands). Its use in a variety of applications and research studies, including the use of coordination compounds such

as cis-platen as a treatment for anti-tumor [6]. Which are becoming increasing numbers, especially for the light atoms (first row) transition metals, the due for a stability whose structural and magnetic property are reminiscent of Werner-type complexes even though they are less than 18 valence shell electrons.

The prefer to use the term “Werner-type coordination compounds” rather than “classical coordination compounds because the field of low-Valente organometallic complexes can also be considered as classical in many respects”. Obviously, “8-electron organometallics and Werner type complexes are the two extremes of a more general picture and the open-shell organometallic compounds” represent the “gray area” between these two extremes. The greater technical difficulty chemistry associated of these compounds especially “handling of these compounds (instability toward air, moisture, and thermal conditions) with respect to the Werner-type complexes, and the less effective use of spectroscopic tools of characterization relative to the chemistry of these compounds has remained comparatively little explored, the main reasons being perhaps" diamagnetic, low-Valente organometallics [7].

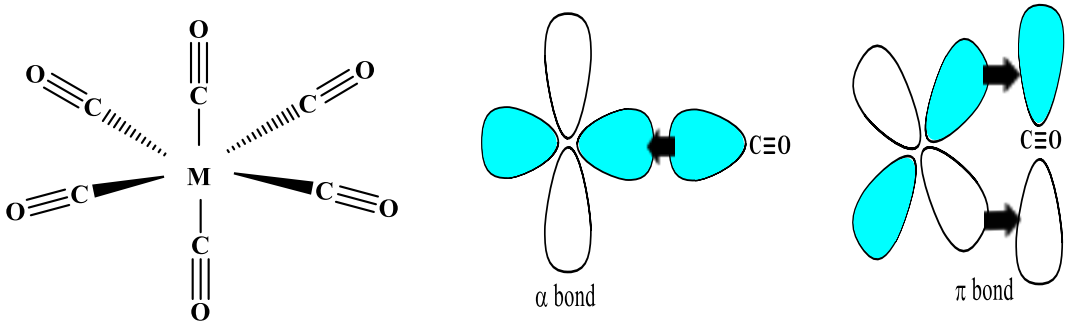
The idea of combining Many researchers have proposed combining two distinct disciplines, chemistry and biology, each of which could pave the way for a new realm of organic biomineral research. The interdisciplinary nature of this new field has led to the development of organometallic complexes for a range of biomedical applications. Some emerging biomedical applications from advances in organic biochemistry research are anticancers [8, 9] radiopharmaceuticals [10, 11]. Particulate matter[12, 13]. Biobacteria [14, 15] and organic trace metals in Non-isotype immunoassays [16-18] genetic sensors [19, 20] organometallic bioreaction center models [21, 22] and host supramolecular processes. [23, 24].

Organometallic complexes stand out from conventional organic compounds due to their unique features. They display a wide range of unusual structures not commonly found in organic molecules, making them crucial in modern chemical research and applications. The diverse structures of organometallic compounds allow chemists to manipulate their stereochemistry. For instance, a metal ion coordinated with six different bonds can exhibit up to 30 stereoisomers. Additionally, the presence of d orbitals in metal ions enables various geometries, offering novel approaches to address limitations in cancer treatment. [25].

The usual heterocyclic compounds contain only one of the three heteroatoms - oxygen, sulfur, or nitrogen, or their combinations. Insertion of the other heteroatoms into the ring permits one to prepare an enormous amount of new heterocyclic including metallacycles. The term "Organometallic" generally denotes compound in which organic groups are directly linked to the metal through at least one carbon atom. The bonding is ionic or covalent or delocalised between organic groups and a metal atom [26].

Many organic chemists now use organometallic compounds as catalysts under mild conditions as well as reagents to create high-quality selective super materials in interactions. The void is now being considered as important developments in these areas It relies heavily on organic mineral reagents[27]. Since the mid- 1950s, application to low-Valente metal cluster chemistry has received thriving area attention, and their practical applications in organic synthesis and industrial catalysis, this were from impact that N-heterocyclic carbine (NHC) ligands have had on organometallic chemistry and some of group 8 with have proven to be the most fertile area of cluster chemistry via the reaction tri carbonyl precursors such " $[M_3(CO)_{12}]$ (M = Fe, Ru, Os) with NHCs, largely due to their ease of accessibility and the well-known differences in properties that are seen upon descending the group"[28, 29].

Metal carbonyl complexes have been studied for a long time Among the most famous organometallic compounds are metallic carbonyl compounds, especially hexagonal compounds, which have been used as base materials in the preparation of many complexes, including the complexes studied here (Fig . 1). The CO bonds are tightly bound to the metal center using a synergistic mechanism that involves the donation of a lone ligand pair to the metal followed by the posterior donation of a π from a filled metal orbital to a free C−O* bond of the CO ligand orbital. Metal carbonyl complexes are prepared in several ways. Metal carbonyl complexes are usually stabilized by metal centers in low oxidation states [4].



(Fig 1): Form of Metal carbonyl $M(CO)_6$

These complexes may be homogeneous, containing only carbon dioxide bonds, such as nickel tetracarbonyl [$Ni(CO)_4$], but most commonly metallic carbonyl compounds are heterocyclic and contain a mixture of bonds. As in our study. Either these complexes are mononuclear containing only one metal atom as the central atom. Or metal carbonyl complexes are polynuclear containing a metal-metal bond. Complexes that contain different metals but only one type of bonding are called insulators.

Currently, despite the advancement of medical technology and various approaches to combat the dreaded disease, chemotherapy remains the most widely prescribed and commonly utilized form of treatment that a substantial majority of cancer patients undergo, often in conjunction with surgical intervention and/or radiotherapeutic procedures. Meanwhile, a significant proportion of cytotoxic platinum-based drugs, specifically cisplatin, carboplatin, and oxaliplatin, continue to play a pivotal role in more than half of the treatment regimens that are administered during the chemotherapy process, which is a clear indication of their widespread acceptance and applicability in the field of oncology [30] .

“Given the emergence of platinum resistance and the severe side effects associated with existing platinum-based treatments (such as neurotoxicity, hepatotoxicity, and nephrotoxicity), there is an urgent need to discover alternative drugs that can effectively suppress cancer tumor growth.” [31].

Calvin PohHwa Tiong mentioned in his book (Transition Metal Carbonyl Complexes for Biomedical Applications 2016) “Given the limitations of platinum-based drugs, chemists are exploring alternative transition metals to create anticancer drugs.” [25].

CALVIN POH HWA TIONG also added in his book "that incorporating carbonyl bonds in the development of anti-cancer treatments offers two major advantages :

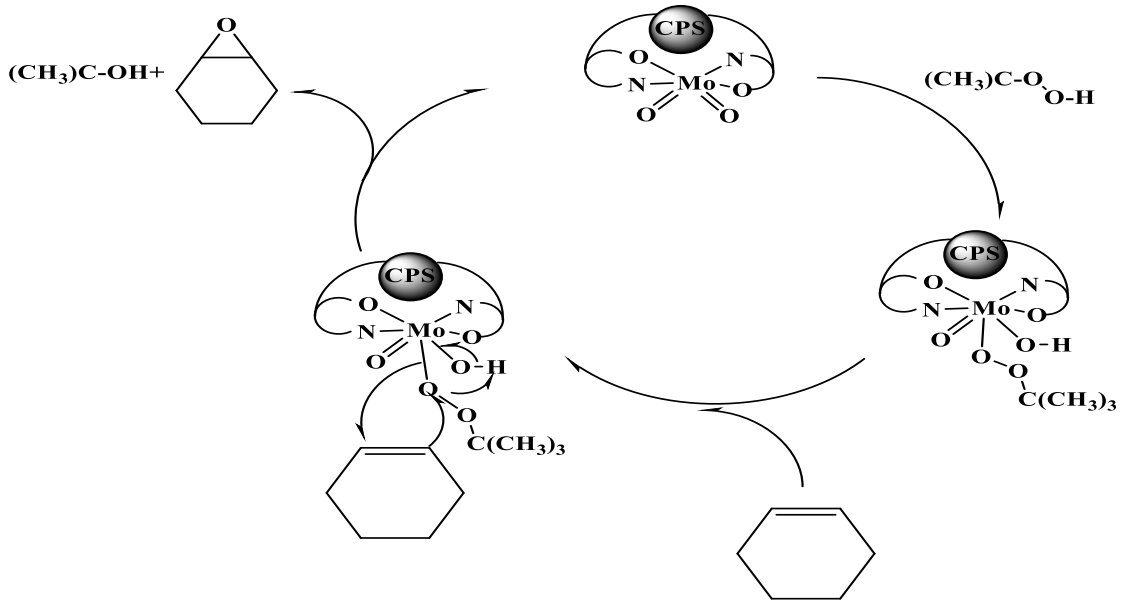
First: the intracellular fate of the metal complex can be easily traced using infrared spectroscopy, as the carbonyl groups generate a strong infrared signal in the 1900 cm^{-1} to 2100 cm^{-1} range.

Second : the carbonyl ligands are labile enough to allow diverse substitutions with different ligands (e.g. phosphenes, alkenes, pyridines, amines and thiols), allowing the cytotoxic properties of the resulting mineral complex to be tailored"[31].

The complexes have the necessary thermal stability to be used as catalysts in reactions taking Michiels[32], In order to address the specificity issues linked to platinum complexes, efforts have broadened to explore molybdenum-containing compounds which have demonstrated confirmed potential as antitumor agents [33-36].

Moreover, studies by F.T. GARZONa and colleagues "found that adding Na2MoO4 to the diet can prevent the carcinogenic effect of N-nitrosarcosine ethyl ester (NSEE), which is known to cause esophageal cancer in rats. Notably, experiments conducted thirty years ago using $Mo(bzac)_2Cl2$ (where bzac = 1-phenylbutane-1,3-dione) on colorectal cancer in Sprague Dawley (SD) rats led to a sudden increase in tumor growth".[35, 37].

In a study conducted by Baojiao et al. in 2015, "a series of Diodexo molybdenum (VI) complexes were tested as catalysts. The researchers found that the prepared heterogeneous catalyst exhibited high reactivity in the epoxidation of unfunctionalized olefins. Additionally, these catalysts demonstrated superior stability and reusability in redox reactions, as they could be reused up to ten times without significant loss in activity. The oxidative system used in this study showed excellent photocatalysis for the epoxidation of a-methylstyrene. Notably, this system did not require any expensive ligands or chiral additives, while effectively enhancing the catalytic reaction process" (scheme.1) [38].



Scheme (1) Catalytic mechanism of catalyst CPS-[$MoO_2(ALGL)_2$]

in epoxidation of cyclohexene to cyclohexene oxide by TBHP

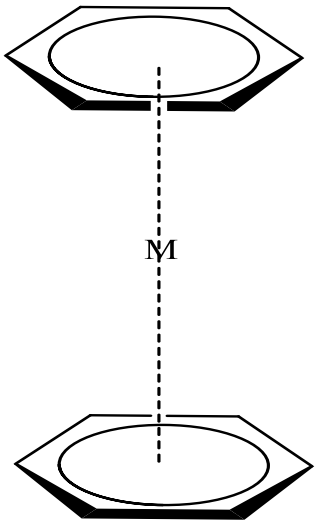
In 1960, scientists found that cisplatin, an inorganic compound containing cis-diammine-dichloroplatinum (III), exhibited anti-tumor properties. Today, cisplatin is extensively employed as a potent but toxic medication for cancer treatment in clinical settings.

Cisplatin, a platinum-derived medication, has become an essential component in cancer therapy due to its efficacy against cancerous cells. Nevertheless, its toxicity requires careful administration and monitoring. [39, 40].

The development of cisplatin has made it the most effective drug in the treatment of solid cancers. In order to improve the global anti-cancer study, the question comes, what effect does molybdenum play? "According to Nair et al., the biological applications of molybdenum complexes were due to the ability of the fused linkers to hydrolyze with a trace metal ion (molybdenum ion), their rare mechanisms of action, and their ability to produce a large amount of harmful reactive oxygen species (ROS).) that can disrupt the redox balance of a system leading to increased DNA damage, DNA protein-binding formation, lipid peroxidation, cytotoxicity, or misinitiation of cellular signaling path ways"[40, 41].

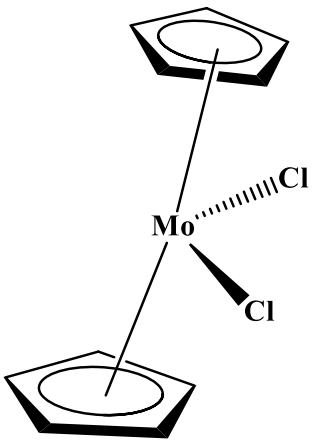
Their results confirmed that Mo(V) had more cytotoxic activities than Mo(VI). On another note, Melendez indicated that "metal- ´locenes are target specific drugs for cancer treatment. A metallocene (Fig.2) is an organometallic compound, which usually

consists of two cyclopentadienyl anions ($C_5H_5^-$, with Cp abbreviation) bound to a central metal (M)" [40](Fig. 2).



(Fig. 2). form of Metallocene

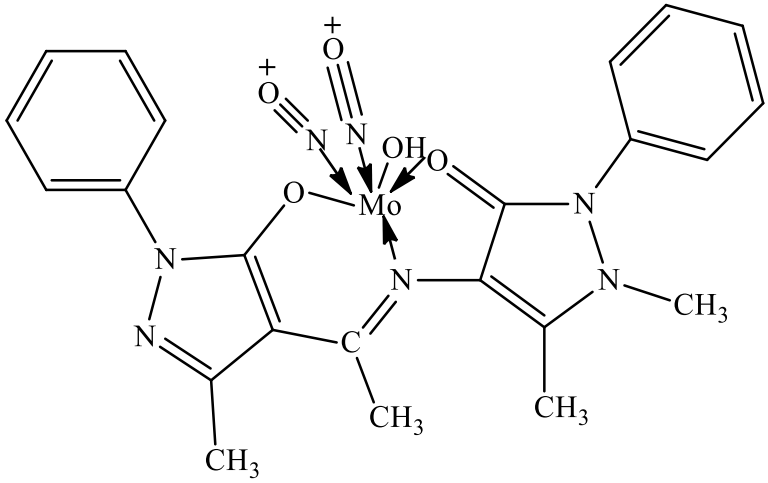
Marin et al. suggested extra optimization of these "metallocenes for them to be used as anticancer agents in chemotherapy[40, 42](40, 42)[40, 42][40, 42][40, 42](Martins, Marques et al. 2014, Odularu, Ajibade et al. 2019)[40, 42][40, 42](40, 42)[40, 42][40, 42][40, 42][40, 42](40, 42)[40, 42][40, 42][40, 42][40, 42][40, 42][40, 42][40, 42][40, 42][40, 42](40, 42)[40, 42][64, 76][40, 42][40, 42][64, 76][40, 42][40, 42][40, 42](Martins et al., 2014; Odularu et al., 2019)[40, 42][40, 42]. Molybdocene is a metallocene with a molybdenum atom. Molybdocene dichloride is the organomolybdenum which has the formula of $(\eta 5\text{-}C_5H_5)_2MoCl_2$" (**Fig. 3)**[40, 43].



(Fig 3) : Dichlorobismolybdenum(IV) (molybdocene dichloride)

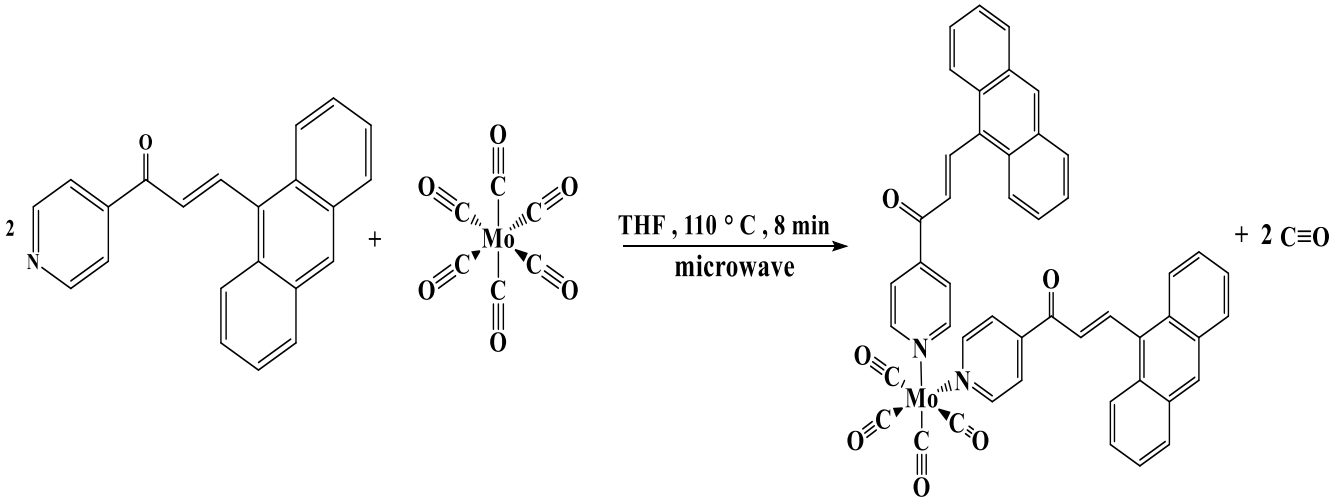
It was worked on by Jan Mohammad Mir and others "to make and study three molybdenum dinitrosyl-Schiff basic complexes with the formula $[Mo(NO)_2(L)(OH)]$. L

can be N-(dehydroacetic acid)-4-aminoantipyrene (dha-aapH), N-(4-acetylidene-3-methyl-1-phenyl-2-pyrazolin-5-one)-4-aminoantipyrine (amphp-aapH), or N-(3 methyl-1-phenyl-4-propionylidene-2-pyrazoline)-5-one)-4amino antipyrine (mphpp-aapH) (Fig.4). Spectral studies, magnetic susceptibility readings, molar conductivity behavior, and DFT calculations were used to come up with the combinations. In addition to looking at the structures and temperatures of the complexes, the study also looks at how well they fight bacteria and cancer in the lab. The results showed that the molecule that contained dha-aapH had strong biological qualities. The IC value for base Schiff was 53.13 mg/mL and the IC value for the substance in question was 10.51 mg/L. The tests were done on the human cancer cell line COLO-205 using 3-(4,5-dimethylthiazol-2-yl)-2,5-diphenyl-2Htetrazolium bromide (MTT). However, the same substance has also been shown to be useful against Aspergillus, Pseudomonas, E. coli, and Streptococcus. The results showed that it worked better against Pseudomonas and Streptococcus than against the other two types of bacteria" [44] .



(Fig .4) Form of [Mo(NO)2(amphp-aap)(OH)]

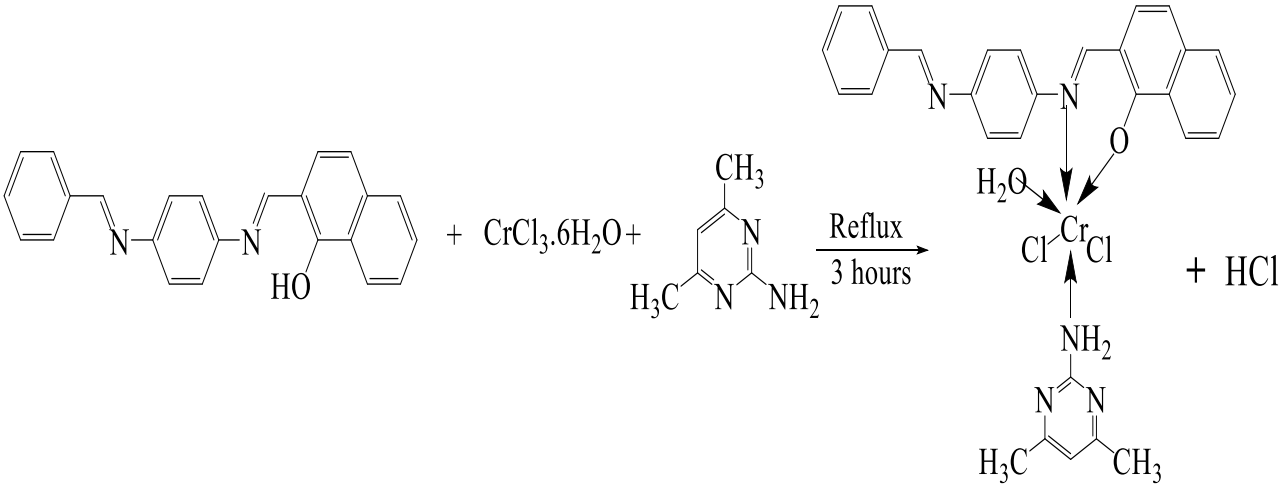
Lim Kar Ern Samuel, Ang Kang Yu Daniel "found the microwave-assisted reaction of $Mo(CO)_6$ with pyridyl anthryl isomers 1a-f chalcones Six new molybdenum carbonyl complexes have been awarded 2a–f. Complexes 2a-f were Characterized by infrared and ^{1}HNMR spectroscopy, f The structures of 2a–d are revealed as unresolved complexes with a general formula The intercalation abilities of $Mu(KO)_4L2.2a$-d towards DNA were examined using a tetramer Fluorescent displacement assay (FID)" scheme (2)[45] .



Scheme (2). Synthesis of the cis-disubstituted complex

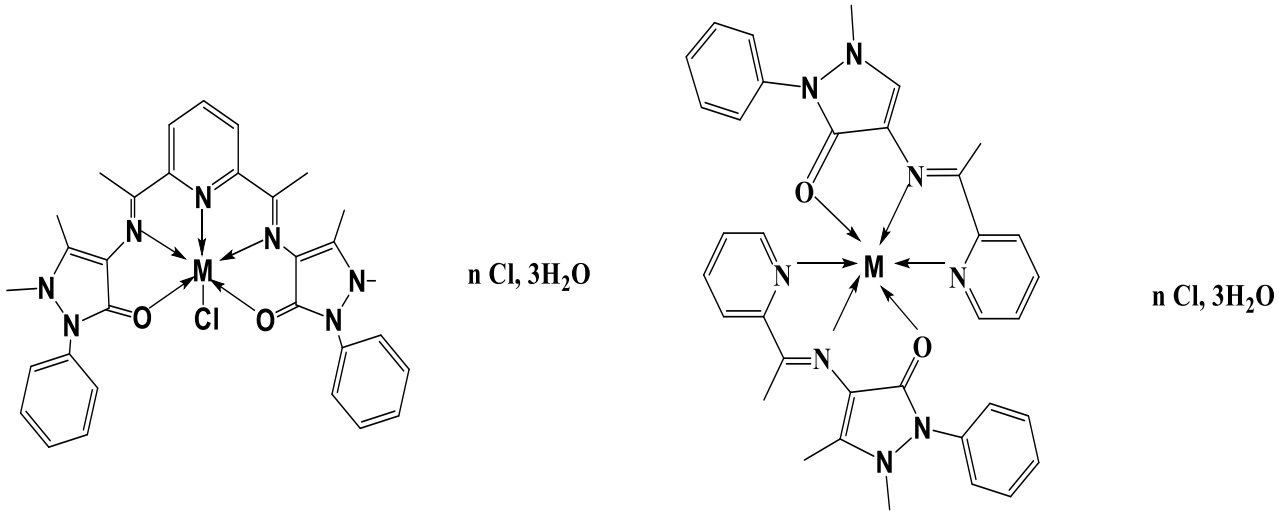
The following metal salts were used to create a novel class of physiologically active mineral compounds by Maged S. Al-Fakeh 1,2 et al: "Using contemporary densitometry, describe the complexes of $MnCl_2$ $4H_2O$, $CoCl_2$ $6H_2O$, $CuCl_2$ $2H_2O$, $CrCl_3$ $6H_2O$, and $PdCl_2$ with 2-amino-4,6-dimethyl pyrimidine (ADMPY) and Schiff's result from the reaction of benzaldehyde condensation with p-phenylene-diamine and 2-hydroxy-1-naphthaldehyde, respectively" scheme (3). The structures and frontier molecular orbitals (HOMO and LUMO) were studied using DFT/B3LYP densitometry.

Free radical tests using 2,2-diphenyl-1-picrylhydrazyl (DPPH) were used to study the complexes' antioxidant properties.Two cancer cell lines, A-549 and MRC-5, were used to assess the anticancer effects of the mineral complexes in vitro. The cytotoxic impact of the complexes was similar to that of other pharmaceuticals based on platinum. Fungi and bacteria were both decisively defeated by the complexes. Analyzed were the antioxidant, anticancer, antibacterial, antifungal, and Cr(III)/Pd(II) complexes that had been previously documented. Ovarian cancer cells (A-549 and MRC-5) were somewhat affected by all of the metal compounds that were produced, regardless of whether DMSO was included in the cell media. This is rather near to the cisplatin scheme's action [46].



Scheme (3). Synthesis [Cr(HL)(ADMPY)(H2O)Cl2] H2O

" The antibacterial and antifungal activities of complexes involving the Schiff bases of 2,6-diacetylpyridine and 2-pyridine carboxaldehyde with 4-amino-2,3-dimethyl-1-phenyl-3-pyrozolin-5-one and (E)-1,5-dimethyl-2-phenyl-4-(1-(pyridin-2-yl)ethylideneamino)-1H-pyrazol3(2H) one , as well as their Co (II), Cu (II), Ni (II), Mn (II), and Cr (III) complexes" scheme (4) , were investigated by Ispir et al. The compounds shown antibacterial and antifungal properties against E. coli, Staphylococcus aureus, Klebsiella pneumoniae, Mycobacterium smegmatis, P. aeruginosa, Enterobacter cloacae, and Micrococcus leteus [47].



n= 2 Cr(III) complexes
n= 1 for other metal complexes

n= 3 Cr(III) complexes
n= 2 for other metal complexes

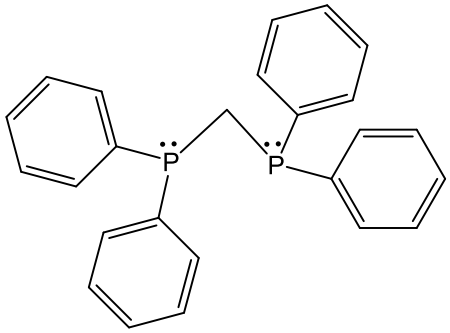
Scheme (4) The proposed structure of metal complexes

M: Co(II), Cr(III), Cu(II),Mn(II), Ni(II) with Schiff bases

"In a methanolic environment, Schiff base ligand is produced by complexing 1,4-dicarbonyl-phenyl-dihydrazide and chromium-2,3 dione with metal salts Cr(III), Mn(III), and Fe(III). Antimicrobial testing revealed that the complexes were more effective against Aspergillussp. than Rhizoctonia sp. The effectiveness of Cr(III) and Fe(III) complexes against Penicillium sp. Was higher than that of the conventional treatment. Depending on the kind of metal ion, the activity of these complexes is ranked as follows: Cr > Fe > Mn".[48].

This research primarily utilizes Bis(diphenylphosphino)methane as its major ligand. Its distinctive structure, as shown in (Fig.5)[38, 49] .

Consists of four phenyl rings connected by two bridge phosphorus atoms.



(Fig . 5) Structural formula of 1,1-bis(diphenylphospino)methane (dppm)

1,1-Bis (diphenylphosphino)methane, commonly referred to as dppm, is a fascinating organophosphorus compound characterized by the formula $CH_2(PPh_2)_2$. This remarkable substance presents itself as a white, crystalline powder, boasting a range of valuable applications in the realms of inorganic and organometallic chemistry. In particular, dppm serves as a highly effective ligand, playing a crucial role in facilitating chemical reactions and interactions. What's more, dppm is classified as a chelating ligand, owing to its exceptional ability to bond with metals via two phosphorus donor atoms, thereby forming a stable and robust complex. This unique property is attributed to its natural bite angle, which measures approximately 73 degrees, allowing it to efficiently coordinate with metal centers and influence their chemical behavior [50, 51].

Bis (diphenylphosphino)methane was first prepared by the reaction of sodium diphenylphosphide (Ph_2PNa) with dichloromethane Scheme(5) [52].

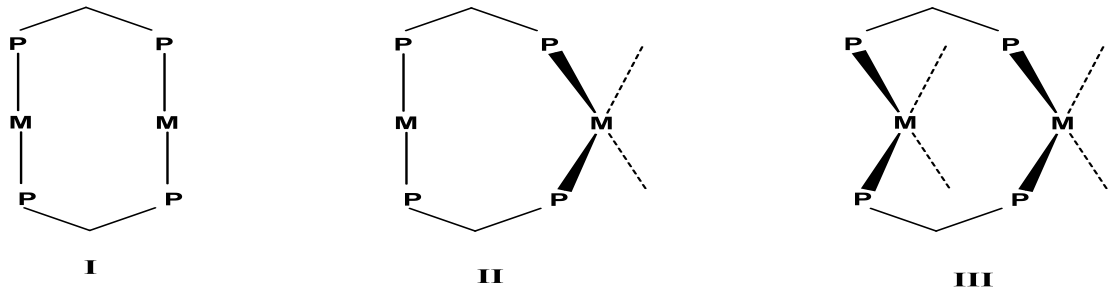
$$2NaPPh + CH_2Cl_2 \longrightarrow Ph_2PCH_2PPh_2 + 2NaCl$$

Scheme (5) Synthesis of diphenylphosphino)methane

Because they create very stable compounds with transformation, binary phosphenes are intriguing. A four-membered ring comprising MP_2C components is formed using methane-1,1-bis(diphenylphos-phoino) as a chelating link. Bimetallic compounds with five-membered M_2P_2C rings are enhanced by the ligand. This is how dppm facilitates the creation of complexes involving two metals. For instance, $Pd_2Cl_2(dppm)_2$ is an example of palladium dichloride. The Pd centers in this compound have an oxidation state of I. The A-frame complexes are a class of coordination chemicals that are generated from diphenylphospinoethane [51].

The intrinsic M2(dpm) framework is a crucial component of dinuclear bis(diphenylphosphino)methane (dpm) complexes, which are important in their chemistry. Typically, this has included dpm ligands that are trans-bound and bridged to form a planar M2P4 core structure (I) with tightly bound metal atoms. In the homobimetallic dpm complex [Mnz- (dpm),(CO)1], for instance, the unique p2-91,92 bridge-binding (u, a) mode for carbon monoxide was first found.53 and [53, 54].

" A small number of compounds, such [M2(dpm)2(p-CO)X2](M = Pd, Pt; X = C1, Br, I)[54-57]. Exhibit the unusual "unsupported" bridging CO linkage, meaning that it does not occur in conjunction with M-M bonding. Additionally, reports have been made on the bridging CO ligands in the later species.Alternate forms of the M,(dpm) structure in bis(diphenylphosphino)methane molecules are likewise rather rare, although they have been isolated and studied lately. One example is the presence of cis-bound phosphorus donor atoms in $[Pt_2(dpm)_2(CH_3)_3]^+$, which gives rise to structural type II, and $[Pt_2(dpm)_2(CH_3)_4]^+$, which gives rise to structural type III, respectively" (Fig .6) [54, 58].



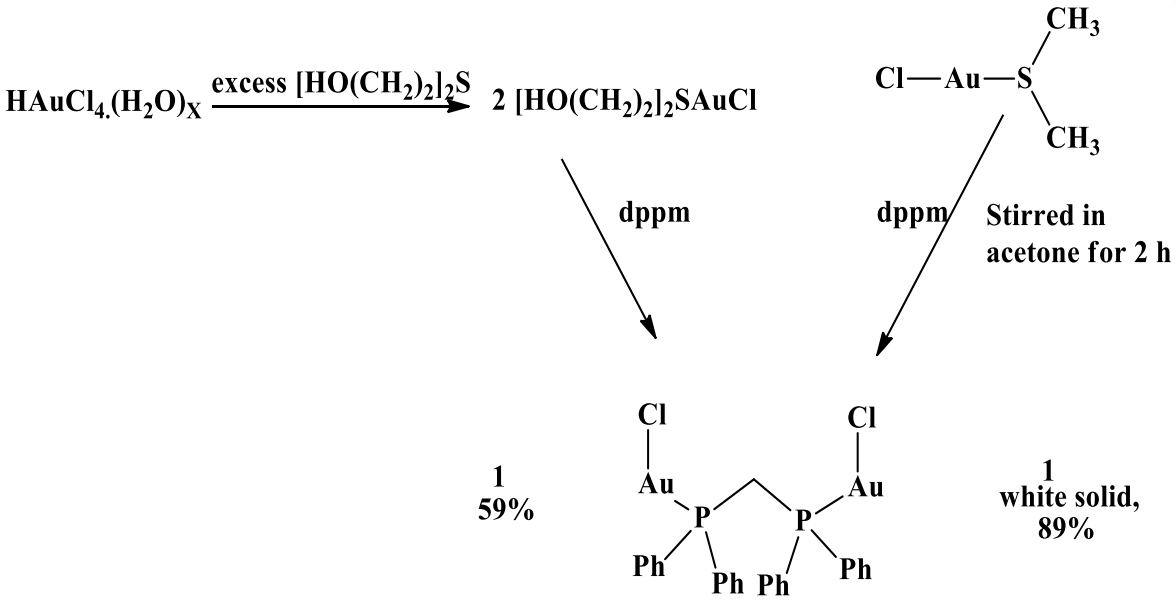
(Fig.6) Structure planar of M_2P_4(I) and cis $M_2(dpm)_2$ (II) (III)

Represent the first reported study on the anticancer activity of homobimetallic complexes bridged by dppm [56,60]. "The 1987 paper focused on the synthesis and biological study of various Au(I) 1,2-bis(diphenylphosphino)ethane (dppe) complexes

and related compounds. It reported a single Au(I) dppm complex [ClAu(m dppm)AuCl] 1, which was synthesized by the stoichiometric addition of dppm to [HO(CH$_2$)$_2$]2SAuCl, accessed through 0°C"(Scheme 6: A). The reduction of chloroauric acid in water with excess thiodiglycol was part of the synthetic process described in the paper (Scheme 6: A)[60]. The study by Tian et al. (2011) "focused on a series of Au(I)-phosphine compounds and evaluated their ability to induce autophagy in cancer cells. They found that complex 1, specifically, exhibited strong autophagy-inducing activity. The researchers further elucidated the underlying molecular mechanisms by which complex 1 induced autophagy".,[59, 60].

The complex was prepared effi- ciently according to more recent literature, which employed a reaction between chloro(dimethyl sulphide)gold(I) and dppm, and reported a yield of 89% (Scheme 6: B) [60, 61] with the researchers elucidating the underlying molecular mechanisms. Notably, complex 1, the sole bimetallic complex of the series, displayed the most potent cytotoxicity when tested against a panel of human cancer cell lines, with IC50 values comparable to or well below those of cisplatin. This research contributes significantly to our understanding of the potential of bimetallic complexes in cancer treatment" [60, 62].

A. B.



Scheme (6. A.B) synthesis of [ClAu(m dppm)AuCl] by reported by Mirabelli et al and Tian et al.

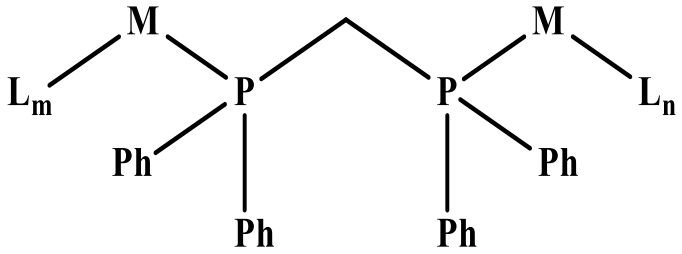
In the early 1980s, researchers undertook a series of groundbreaking studies that yielded several remarkable findings. One notable discovery was the potential anticancer

properties of auranofin and other antirheumatic agents. This breakthrough sparked widespread interest, prompting further research into the use of gold complexes as potent anticancer agents. The ultimate goal of these studies was to uncover novel and innovative strategies to combat cancer, a debilitating disease with devastating consequences. [60, 63].

Since then, numerous studies have concentrated on gold complexes featuring phosphine, carbene, and dicarbamate bonding systems [60, 65]. The metal-phosphorus bonds are typically strong, which is why the employment of bridging diphosphine ligands in binuclear transition metal complexes guarantees a robust linkage of two metal centers, thereby preventing their dissociation into mononuclear entities. [64]. Metal length of dppm ensures that the metal centres of a bimetallic system are in close proximity, potentially promoting synergistic effects[60, 64].

The discussion is divided into homobimetallic dppm-bridged complexes and heterobimetallicdppm-bridged complexes. Different metals feature distinctly different physiological activities[60, 65]. A plethora of bimetallic systems bridged by dppm have been reported in literature[60, 66, 67].

Burgert Blom A and colleagues "elaborate on the Creation of an m2-dppm bridge for homo- and hetero-metal systems within the realm of Anticancer applications, starting from the initial documented utilization of bimetallic in 1987 until of 2020. Focused on the synthesis, structure, cytotoxicity and other biological activities of these complexes in a comparative manner. Only systems that work The discussed M e M bonds do not hold, as every metal center can Potentially working independently and synergistically" (Fig .7)[60].

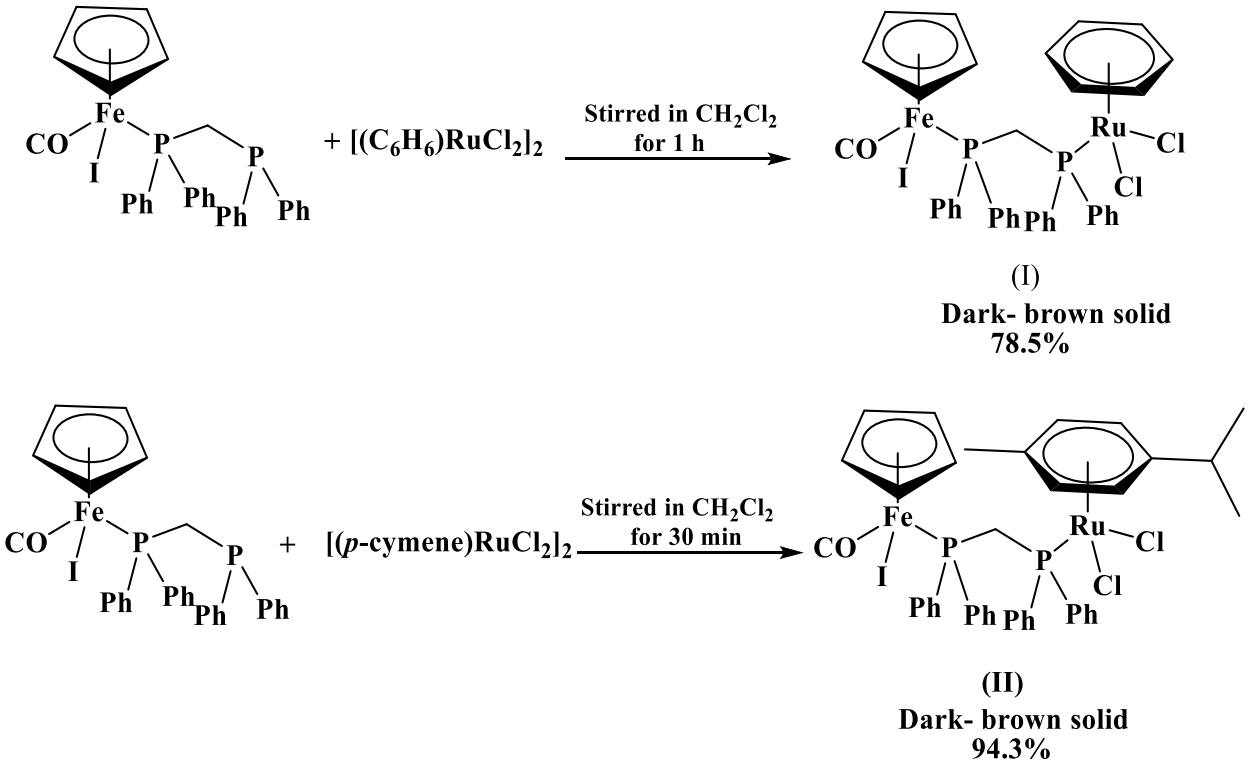


(Fig .7) General structure of reviewed complexes, where M and M¢ are transition metals which may be different or the same and Ln,m are co-ligand spheres at each metal

The most recent instance of heterobime tallic complexes bridged by dppm was documented by Herry et al[59, 60]. "They outlined the synthesis, characterization, and

anticancer activity of three novel bimetallic systems, two of which were heterobimetallic, featuring ruthenium and iron centers The two complexes presented in their findings are denoted as [(μ_6-C_6H_6)$RuCl_2$(μ-dppm)Fe(CO)I(μ_5-C_5H_5)] (I) and

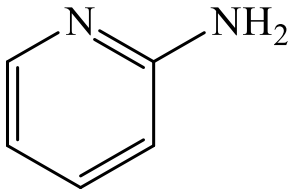
[(μ_6-p-cymene)$RuCl_2$(μ-dppm)-Fe(CO)I(h_5-C_5H_5)] (II)" in scheme (7)[68].



Scheme(7). Synthesis of [(μ^6-C_6H_6)$RuCl_2$(μ-dppm)Fe(CO)I(μ^5-C_5H_5)] (I) [(μ^6-p-cymene)$RuCl_2$(μ-dppm)Fe(CO)I(h_5-C_5H_5)](II)

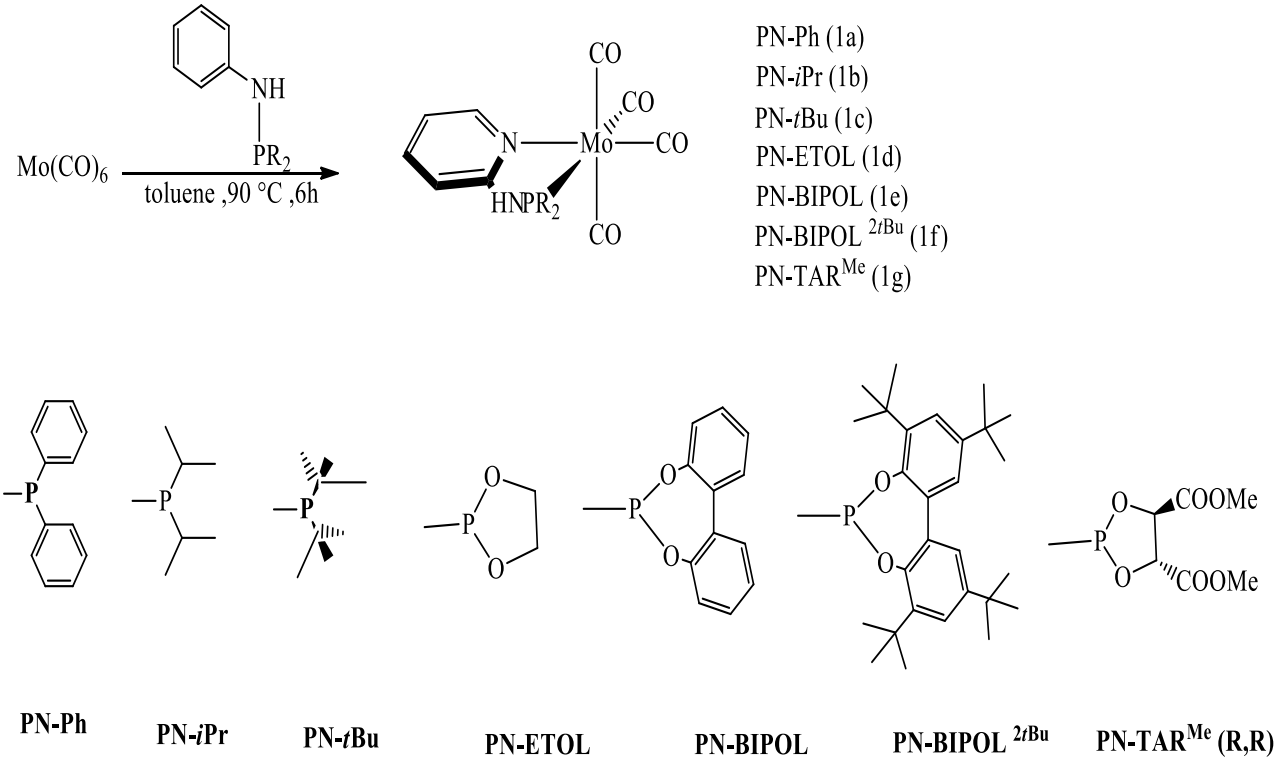
2-Aminopyridines have gained significant prominence in coordination chemistry due to their accessibility and versatility, often serving as substitutes for cyclopentadienyl bonds. In the past two decades, there has been substantial interest in the chemistry of aminopyridinato mineralogy. This ligand class exhibits a rich coordination chemistry, demonstrating coordination capabilities in both chelating (common) and bridging coordination modes.

The chemistry of cobalt(II) complexes with O- and N-donor ligands has undergone extensive investigation, revealing diverse properties [69]. Additionally, these complexes have demonstrated antimicrobial activity against resistant microbial strains(Fig . 8)[70]



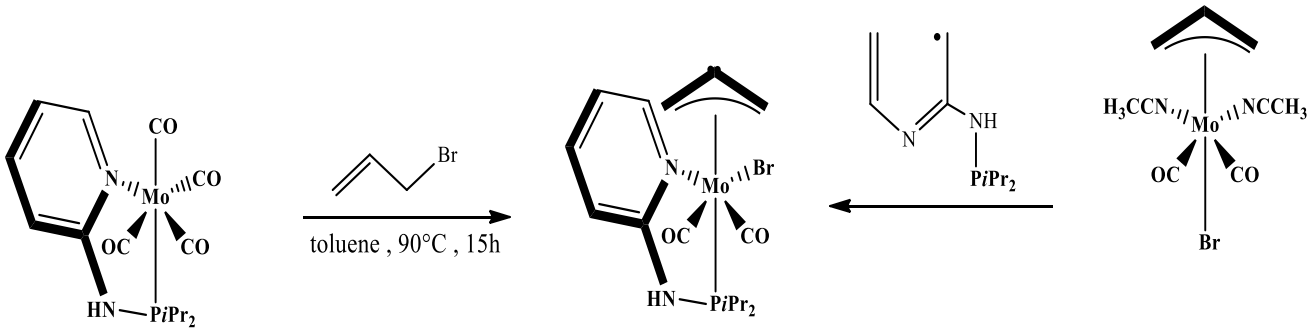
(Fig .8) Structure of 2-Aminopyridine

Kirchner and colleagues extend "their study on PN compounds based on 2-aminopyridine and prepare a series of molybdenum tetracarbons from the general formula. [Mo(PN)$(CO)_4$] The oxidative addition of allyl bromide to [Mo(PN)$(CO)_4$] was studied using PN=N-(diisopropylphosphanyl)-2-aminopyridine (PN-iPr). The X-ray structures of representative compounds were determined. The mechanism of oxidative addition of allyl bromide to [Mo(PN-iPr)$(CO)_4$]was analyzed by DFT/B3LYP calculations. The new PN linkers PN-tBu, PN-ETOL and PN-BIPOL2tBu were prepared by treating 2-aminopyridine with 1 eq., of chlorophosphane or chlorophosphite In the presence of the base (NET3 and/or nBuLi)" Scheme (8)[71]



Scheme (8) Synthesis of Mo(PN)(CO)4 where PN = N-(diisopropylphosphanyl)-2-aminopyridine (PN-iPr)(PN-Ph, PN-iPr,PN-BIPOL, and PN-TARMe)

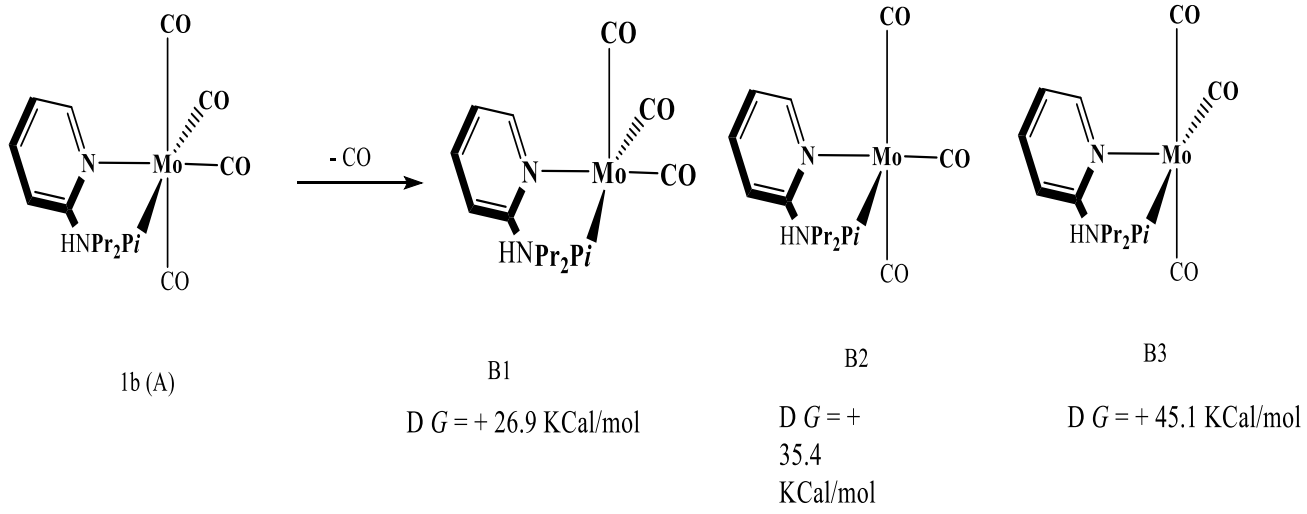
The study described by Christina Maria Standqvist-Hauser "on the reaction of molybdenum-PN complexes with allyl bromide, with the aim of producing η3-allyl complexes of a certain type. The chosen model compound, 1b, reacts with allyl bromide to produce the seven-coordinate η3-allyl compound Mo-(PN-iPr)(η^3-CH_2CHCH_2)$(CO)_2Br$ (2), and the same compound can be obtained at room temperature in high yield. By treating $Mo(\eta^3\text{-}CH_2CHCH_2)(CO)_2$- $(CH_3CN)_2Br$ with 1 eq. of PN-iPr in CH_2Cl_2. The identity of 2 was confirmed using different analytical techniques such as 1H, 13C{1H}, 31P{1H} NMR, infrared spectroscopy, and elemental analysis" (Scheme (9)[71].



1b 2

Scheme (9) Synthesis of Mo-(PN-iPr)(η3-CH2CHCH2)(CO)2Br (2)

Since CO has a higher trans influence and trans effect than phosphanes and pyridine, dissociation of one of the two CO ligands which are coordinated trans to one another is strongly favored. This is also in line with DFT calculations showing that the formation of square pyramidal intermediate B1 is strongly favored over B2 and B3(Scheme10) [71]



1b (A)

B1

D *G* = + 26.9 KCal/mol

B2

D *G* = + 35.4 KCal/mol

B3

D *G* = + 45.1 KCal/mol

Scheme (10) Synthesis of Mo(PN-iPr)(CO)4(1b),

Uma Shanker and his group "successfully used a green route to synthesize iron oxide nanoparticles[(α-FeOOH, β-FeOOH and α-Fe_2O_3)]. This approach involves the use of Sapindus mukorossi (raw reetha) as a surfactant and water as a solvent. It must be emphasized here that during the nanoparticle synthesis,This approach uses Sapindus mukorossi, which is a natural product with properties Surface tension.

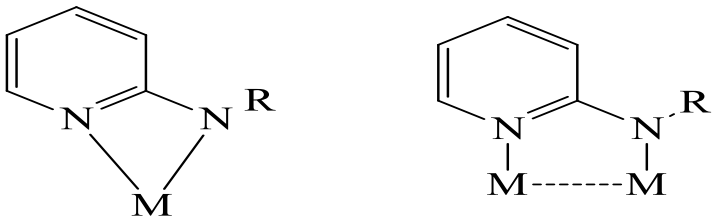
The synthesized nanoparticles were characterized by powder X-ray diffraction (PXRD), field-emission scanning Electron microscopy (FE-SEM) and transmission electron microscopy (TEM). This is done through the reaction of 2, 3, and 4-aminopyridines. α-FeOOH was found to be the most efficient catalyst for Aminopyridine adsorption, possibly due to its higher surface area among other iron oxides used" [70].

A novel one-dimensional coordination polymer synthesized by Amah Colette Benedicta Yuoh and her colleagues From " (2-aminopyridine)-μ bis(decyanamido)-cobaltate(II) was created. In this complex, the Co(II) ion is linked to two axial 2-aminopyridine bonds, two N-atom pyridine bonds, and four equatorial cyanamide bonds, resulting in a slightly distorted octahedral coordination environment (CoN_6) around the metal ion. The N amino atom within the chain participates in hydrogen bonding. Analyses through elemental, infrared, and ultraviolet-visible spectroscopy methods were used to characterize the new complexes, and the structure was determined using single crystal X-ray diffraction. Evaluation of the compound's antimicrobial

activity against eight pathogenic microorganisms (four bacteria and four fungi) derived from humans revealed that it exhibits moderate activity " [72].

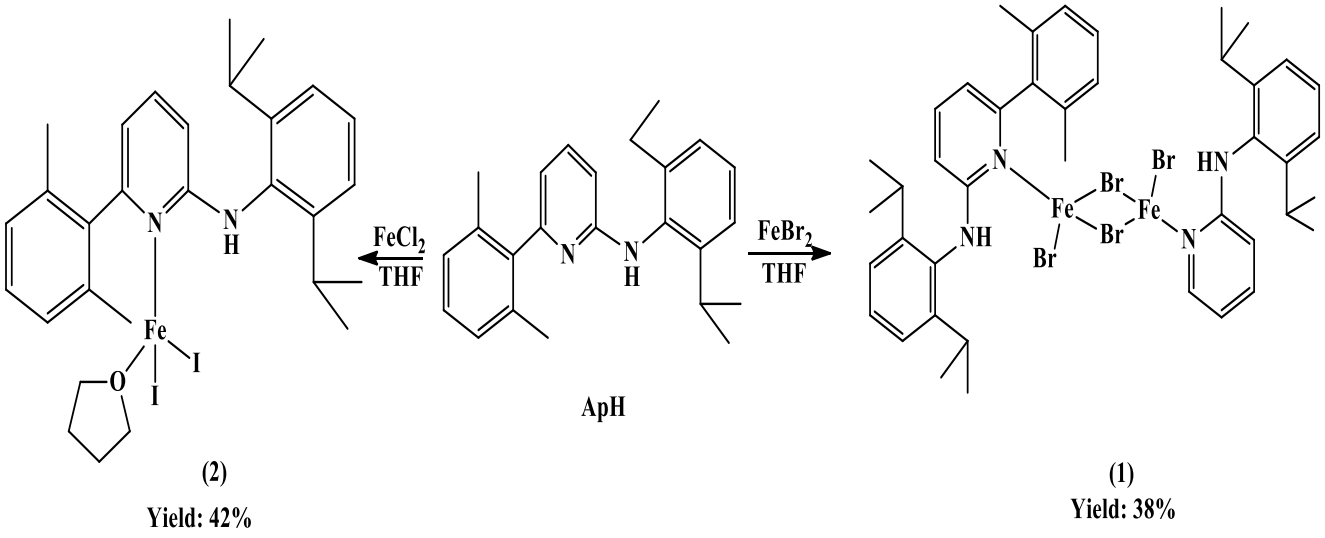
The coordination chemistry of 2-aminopyridines has emerged as a highly popular and thoroughly investigated area of research in the field of chemistry, by the fact that these compounds can be readily synthesized and are easily accessible, in addition to exhibiting a high degree of steric and electronic versatility, which allows them to form a vast array of complexes with various metals and exhibit a wide range of properties and applications. [73, 74].

The ligand class exhibits diverse coordination chemistry, primarily involving chelating and bridging coordination modes. However, monodentate coordination to metals is infrequent. In specific cases, h1-coordination via the pyridine nitrogen occurs when the metal fragment hesitates to accept six electrons due to π coordination [75, 76]



(Fig . 9). Chelating and bridging coordination modes of aminopyridinato ligands (R= alkyl,aryl or silyl: M= transition metal)

The diverse coordination chemistry of iron across various oxidation states, involving a range of chelating bonds, remains intriguing. here, with the first examples reported by Awal Noor of "structurally distinct iron complexes with saturated 2-aminopyridine. Iron (II) complexes $[ApHFeBr(-Br)]_2$(1) and $[ApHFeI_2(thf)]$(2), prepared with one equivalent reaction of N-(2,6-diisopropylphenyl)-[6-(2,4,6-triisopropylphenyl)-pyridine-2-yl]-amine (ApH) with anhydrous $FeBr_2$ and FeI_2, respectively in THF orange crystals of magnetite 1 and 2 after 2 days of toluene solution at room temperature". (Scheme 11) [76].



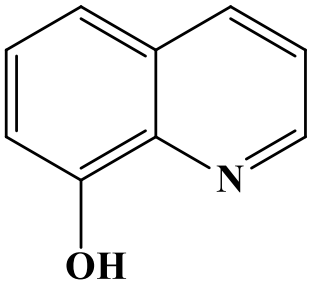
Scheme (11). Synthesis of aminopyridine Fe complexes .

I Wayan Dasna1, et al. "successfully synthesized the complex of Co(II) with 2-aminopyridine and SCN-ligands using retrograde techniques. This preliminary study of the complex structure indicated that the N-pyridine and SCN-ion are coordinated with the central cobalt (II) ion. The combined compound is an antibacterial agent against S. aureus and S. typhi" [77].

8-Hydroxyquinoline (8HQ) (Fig.10), is an organic compound with the atomic formula C_9H_7NO. This compound is derived from the quinoline heterocycle by substituting an OH group on carbon number 8. This light yellow compound is widely used commercially, but under different names.

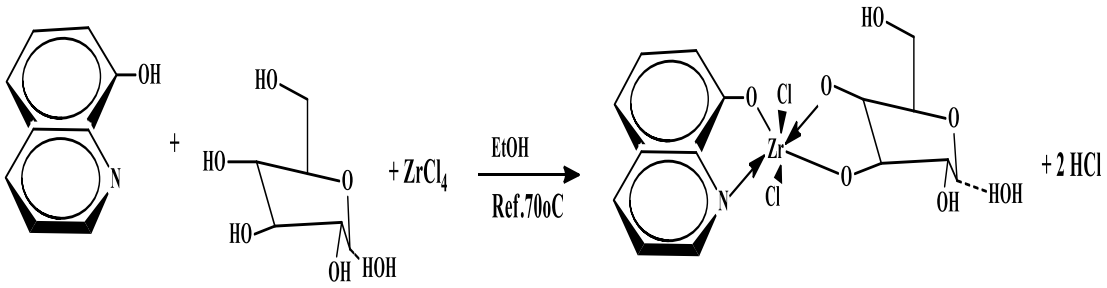
The compound is primarily synthesized from quinoline-8-sulfuric acid and through the Skraup synthesis of 2-aminophenol.The complexes of this compound as well as the heterocycle itself show antiseptic, sterilizing and insecticidal properties [78]. As they act as transcription inhibitors. His alcohol solution is used as a liquid bandage. It was previously of great importance as an anti-cancer [79].

8-Hydroxyquinoline inhibits the growth of B16 cells as well as human melanoma cell lines[79, 80].Mannich bases of 8-hydroxyquinoline have also been synthesized using pyrrolidino, piperidino, and diethylamino groups. These combinations showed high activity against p-388 leukemia and EMT 6 tumor. [79, 81].

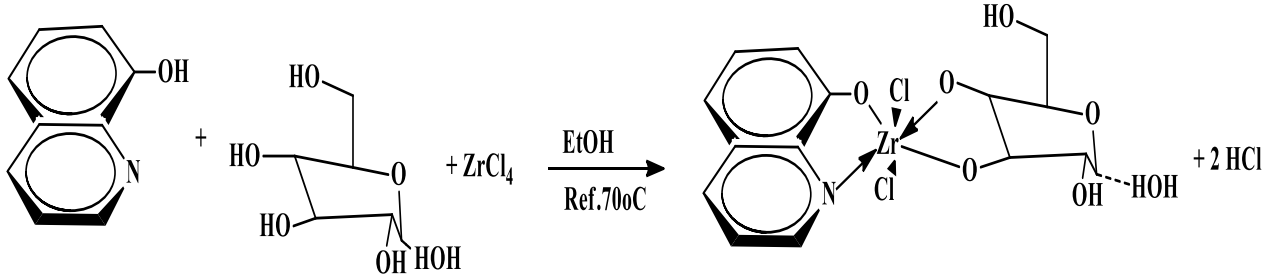


(Fig. 10) Structure of 8-Hydroxyquinoline (8HQ)

A group of zirconium complexes was prepared by Salem El-tuhami Ashoor1 and his group by "reaction with an equal amount of 8-hydroxyquinoline and sugars as secondary ligands.[Zr(QH)(Glu)Cl_2] and [Zr(QH)(Fru)Cl_2)], where (QH) 8-hydroxyquinoline, glucose (Glu) and fructos(Fru) e. They were characterized using Fourier transform infrared (FT-IR) and UV-visible spectroscopy. A study of the changing temperatures of these complexes was also completed by using visible and ultraviolet spectroscopy to monitor electronic transitions under temperature control. A DFT study has also been performed on these Pools across information from FT-IR and UV-Visible spectroscopy, then computes the topmost lowest occupied molecular orbital (HOMO) and lowest unoccupied molecular orbital (LUMO). Zirconium(IV) complexes have been found to have biological activities. Biological antibacterial" schem (12) [82]

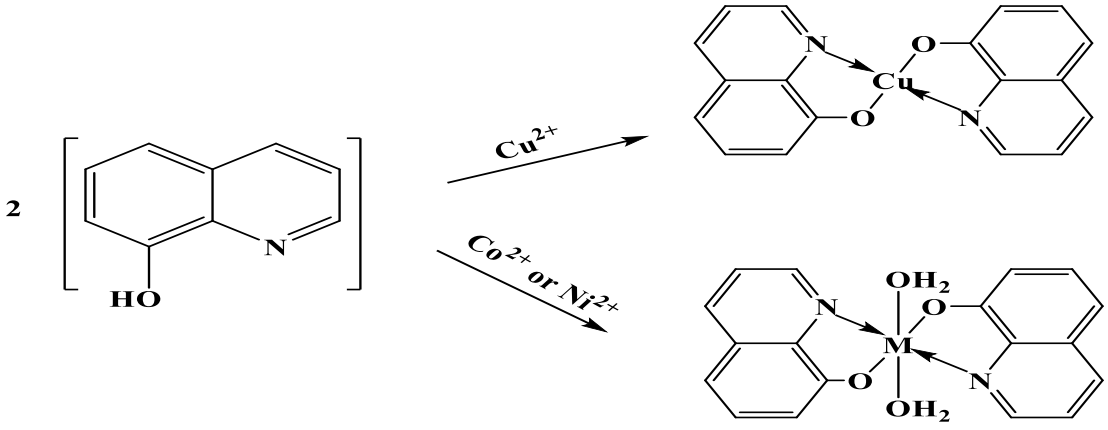


Scheme 12.1: Preparation of [Zr(HQ)(Glu)$(Cl)_2$] [1].



Scheme 12.2: Preparation of [Zr(HQ)(Fru)(Cl)2] [2].

Amira Cipurković1orcid and co-workers " synthesized three complexes of (Cu, Ni, Co) containing 8-hydroxyquinoline (8-HQ) (scheme 13). spectrophotometrically analyzed and the antimicrobial effect examined in vitro. The stoichiometric ratio of the compound was determined by conductivity and spectrophotometry. FTIR and UV/VIS spectroscopy were used for structural characterization. Antimicrobial activity was examined by diffusion technique on selected Gram-positive and Gram-negative bacteria and C. albicans. . Based on the spectral data, it was concluded that the oxygen and nitrogen atoms of 8-HQ participate in the formation of the complex. The antimicrobial activity of the complexes is high, with zones of inhibition in the range of 15–28 mm. 8-HQ has been shown to have a significantly higher ability to inhibit the growth of the tested" [83].



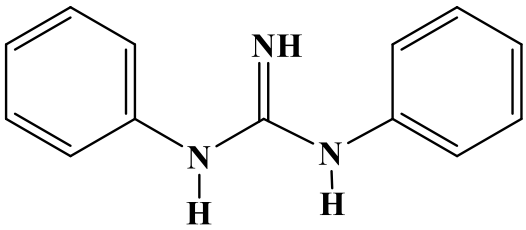
scheme (13). Reaction scheme and proposed structure of the complexes by Amira Cipurković1orcid

Additionally, Amira Cipurković and co-workers "have reported that metal complexes of mixed ligands of 8HQ-uracils exhibit significant cytotoxicity against various human cancer cells, including HepG2, A549, HuCCA-1, and MOLT-3, making them potential anticancer drugs. These metal complexes reversibly bind to DNA through non-covalent interactions, such as electrostatic bonding, groove binding, and intercalation" [84, 85].

Intercalation between metal complexes and DNA bases is considered to be the most important binding mode giving rise to antitumor activity [86, 87].

Guanidine is the compound with the formula $HNC(NH_2)_2$ Fig (11) It is a colourless solid that dissolves in polar solvents. It is a strong base that is used in the production of plastics and explosives. It is found in urine predominantly in patients

experiencing renal failure A guanidine moiety also appears in larger organic molecules, including on the side chain of arginine**[88]** .



(Fig . 11) Structural formula DPG

The structure and crystallographic analysis are characterized for Guanidine as follows:

1. Structure:

- Guanidine can be considered a nitrogenous analogue of carbonic acid.
- In carbonic acid (H_2CO_3), the C=O group is replaced by a C=NH group in guanidine.
- Additionally, each OH group in carbonic acid is replaced by an NH_2 group in guanidine.
- Isobutene serves as a carbon analogue in a similar manner [89].

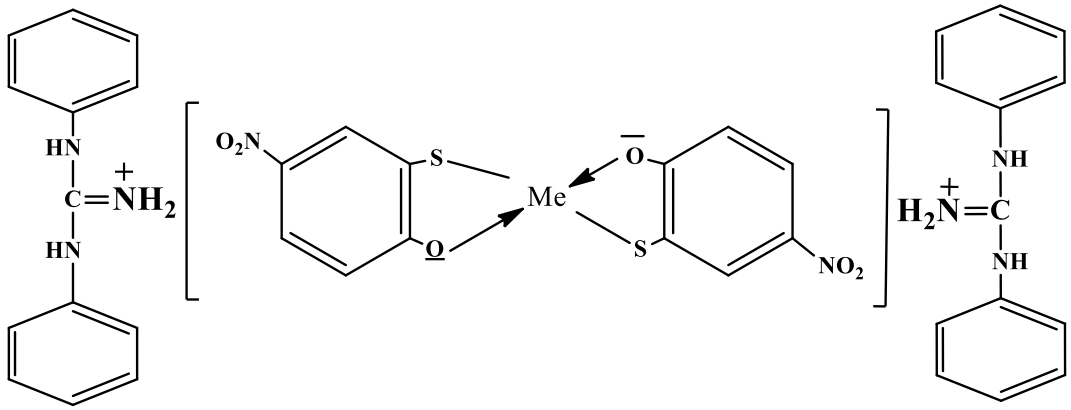
2. Crystallographic Analysis:

- Despite its apparent simplicity, guanidine's detailed crystallographic analysis was elucidated 148 years after its initial synthesis. [90].
- In 2013, single-crystal neutron diffraction accurately determined the positions of hydrogen atoms and their displacement parameters in guanidine. guanidine's nitrogenous structure and its intriguing properties continue to captivate researchers So far [91].

S.G. Aliyev1 and colleagues “found that cobalt (II) and nickel (II) react with 2-hydroxy-5-nitrothiophenol (HNTPh) and diphenylguanidine (DPG) to produce mixed chloroform-derived complexes (MLC) with specific ratios. They also determined the conditions for photoextraction of cobalt (II) and nickel (II) and the properties of MLC in a weakly acidic medium. All studies were performed with $CHCl_3$. The absorption spectrum of the nickel-cobalt(II)(II) MLC was diagnosed, and various chemical analytical parameters were calculated. HNTPh exhibits reducing properties in acidic

media, leading to the formation of a ternary compound with the formula $[Me(HNTPh)_2](DPGH)_2$" scheme (14) [92].

$$(C_6H_5NH)_2\,C = NH + H^+ \rightleftharpoons (C_6H_5NH)_2{=}NH_2^+$$



Scheme (14) Formation of a complex of cobalt(II) and nickel(II) with 2-hydroxy-5-nitrothiophenol and diphenylguanidine

Microwave technology The establishment of microwave technology dates back to just before World War II, since 1970 microwaves have been used in the food industry.In the eighties of the last century, research in laboratory and industrial fields began to appear. Where he published the first chemical reaction in the field of organic synthesis in . 1986 It is noteworthy that the first case of the use of microwaves in the synthesis of organic compounds and that the tools that were used for these purposes have certain standards for the use of electromagnetic radiation, however, they are not suitable for conducting chemical reactions according to the requirements good laboratory. The field in which microwave waves were used in chemical laboratories is microwave-assisted extraction in the subjects of organic pollutants and the isolation and preparation of natural materials. This method has become an alternative to the traditional extraction using the (Soxhlet) device. It usually needs a long time and large quantities of solvents, and one of the improvements of this method is the high temperature of the solvent used in the extraction due to the increase in pressure[93]. Microwave radiation is one of the unusual sources of energy, as the use of microwave radiation is considered one of the most practical and effective methods in organic synthesis, as it increases the

effectiveness of many chemical reactions Microwave chemistry is considered one of the most important fields of photochemistry that has attracted the attention of researchers in recent years. superlicating, endothermic reactions, and recoiribination reactions (mediated by free radicals) [94].

CHAPTER TWO
EXPERIMENTAL AND METHODE

2.1. General Procedures:

2.1.1 Reagents and Materials

All solvents (THF, Ethanol pure 99 %) were purchased from Alfa-Aesar ,Carlo-Erba , Scharlau , Romil-Pure , company and dispensed from graduated bottle. Molybdenum(0) hexa carbonyl [Mo $(CO)_6$ 98%], Chromium (0) hexacarbonyl [Cr $(CO)_6$ 98%], were purchased from Sigma-Aldrich, and 2-aminopyridin ,diphenylguaidine (98%) and 8-Hydroxy-chinolin (99%) were purchased from Alfa – Aesar and Ried de haen that used bidentate ligands.

2.1.2 Spectroscopic Techniques

The ultraviolet - visible spectra (UV-Vis) was acquired at this university on Cary 60 UV-Visible spectrophotometer (Agilent Technologies) in range 200 to 800 nm and operating at Excel software. Diamond FT-IR- Spectrometer Frontier was acquired at this university on FT – IR Spectrometer Frontier (Perkin Elmer) in range 4000 to 600 cm^{-1} and results of the infrared spectrum were recorded jpg formatted.

Mass spectrum was carried out on Direct Inlet part to mass analyzer in Thermo Scientific GCMS model ISQ at the Regional Center for Mycology and Biotechnology (RCMB), Al- Azhar University, Nasr City, Cairo. The Mass spectroscopy system was used to confirm the purity of the compounds as well as explore the characteristic fragmentation and the expected molecular weight. Mass Spectrometry (MS) under model of 689N network (Agilent Technologies), in range 200 to 600 m/s. ^1H NMR analyses were carried out by burket nmr, Al- Azhar University, Nasr City, Cairo.

Elemental analyses were carried out by Mikroan alytisches Labor Pascher of Remagen-Bandorf, Germany .

2. 1.3 Theoretical calculations

Crystal structural determinations were carried out under Gaussian 09 [46]. And output files were visualizer under Gauss View 6.0 [65] on personal computer (Ubuntu core i7) by Prof. Dr. Salem El- tuhami Ashoor. Structures in the text throughout are drawn as Chemcraft [66].

Representations derived from data imported into ‘Chem craft and Chem Draw Professional 15 for Windows, converted to tagged image finally formatted as jpg images in ‘Paint shop Pro’. Thermal ellipsoids are set at 50% unless otherwise stated.

2.1.4 Microwave instrument

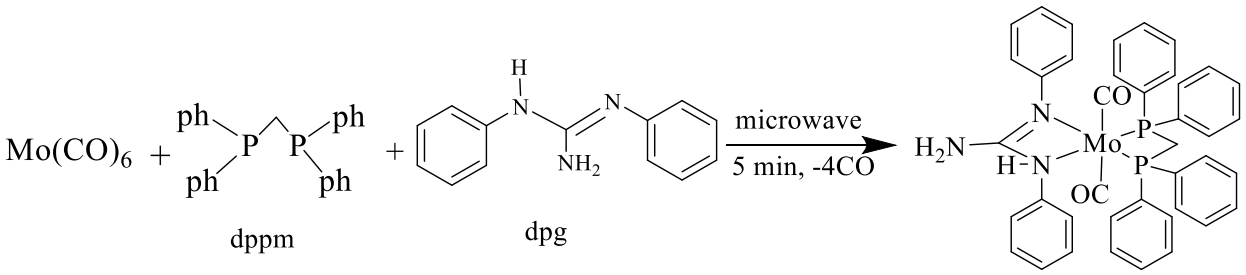
Microwave instrument with a power of 2000 W and 220 Ev from Hommer company was used for the synthesis of all complexes.

2.2 Experimental

2.2.1 Method of preparation and work steps:

2.2.2 Synthesis of $[Mo(CO)_2$ (dpg)(dppm)](F 1)

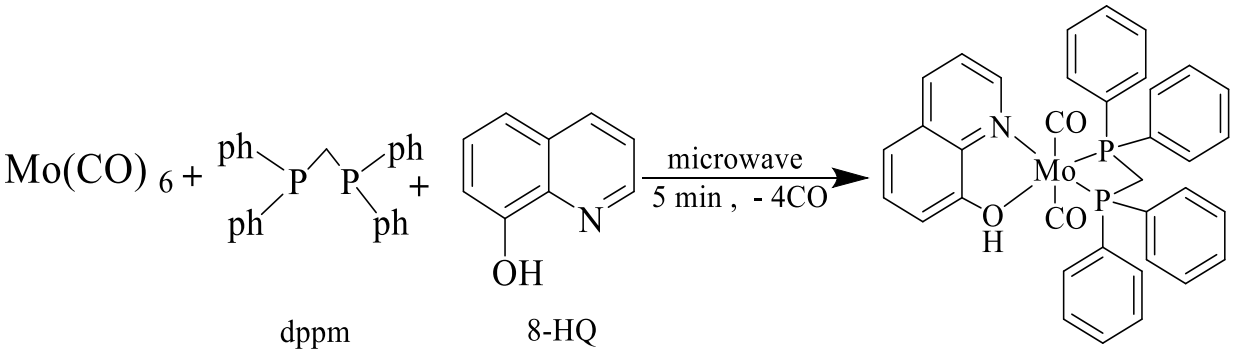
Complex was synthesized by grinding [Mo $(CO)_6$] (0.15g, 0.56818 mmol) with two ligands, bis(diphenylphosphino)-methane (dppm) (0.21815g) , 0.5681 mmol) and diphenylguanidine (DPG) (0.120g , 0.5680 mmol), the mixture was grinded well and then placed in a small tube in the microwave for 5 minutes. White solid of the product washed several times with THF scheme (15). To give (0. 42428g) white solid and recrystallization from THF. the product (44.899 %) and the melting point for this complex is (116 - 120 ˚C) .



Scheme (15) Synthesis of $[Mo(CO)_2$(dppm) (dpg)] (F 1)

2.2.3 -Synthesis of $[Mo(CO)_2$ (dppm) (8-HQ)] (F 2)

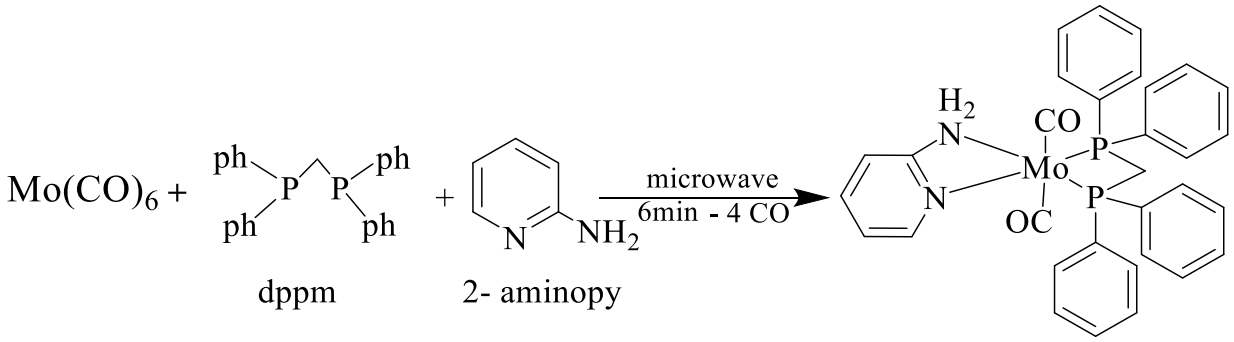
The synthesis of was achieved by grinded [Mo (CO_6)] (0.15 g ,0.56818 mmol) and well mixed with (0.21815 g ,0.56818 mmol) of dppm and (0.082386 g, 0.0005681 mmol) of 8-HQ in a small sample tube and left in a microwave oven for about 5 minutes. The solid product was washed with a small amount of dry THF at room temperature and recrystallization the solid in hot THF. The resulting solid was air sensitive and gave (0.2777g) of the product (71.77%). Melting point for this complex is (122 - 126 ˚C). Scheme (16)



Scheme (16) Synthesis of [Mo(CO)$_2$ (dppm)(8-HQ)] (F 2)

2.2.4 -Synthesis of [Mo(CO)$_2$ (dppm) (2-aminopy)](F 3)

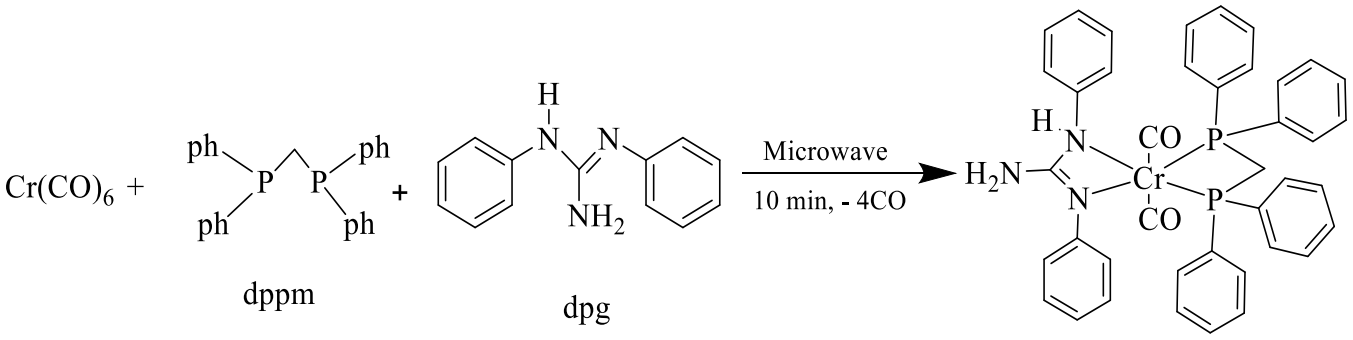
Complex was Synthesized by grinding[Mo(CO)$_6$](0.15g , 0. 568mmol) with two ligands, bis (diphenylphosphino)-methane (dppm) (0.21815g, 0.56818mmol) and 2amino-pyridine (2-aminopy) (0. 053409g, 0.56818 mmol), the mixture was grinded well and then placed in a small tube in the microwave for 6 minutes. White solid of the washed several times with THF. The recrystallization of solid in hot THF gave 0.1952 g of the product (54.53 %) and the melting point for the complex is (122-129 ˚C). Scheme (17).



Scheme(17) Synthesis of [Mo(CO)$_2$ (dppm) (2-aminopy)] (F 3)

2.2.5 Synthesis of [Cr (CO)$_2$ (dppm) (DPG)](F 4)

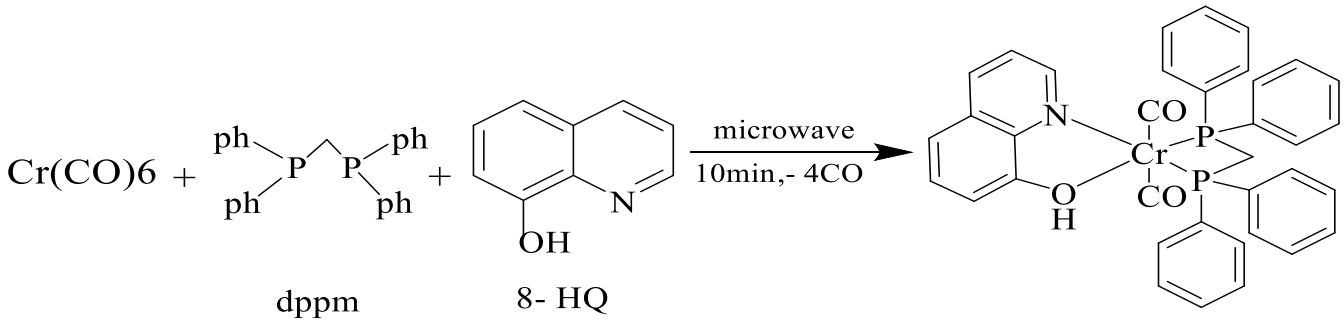
Synthesis of complex was by grinding [Cr (CO)$_6$] (0.15 g, 0.0006818 mmol) with (diphenylguanidine) (DPG) (0.144g,0.0006818 mmol) and bis(diphenylphosphino)-methane (dppm) (0.26177g , 0. 0006818 mmol), grinding well and then placing them in a small tube in the microwave for 10 minutes. White solid of the product washed several times with THF. The recrystallization of solid in hot THF gave (0.47929) g of the product (52.91%)and the melting point (116-120 ˚C). Scheme (18).



Scheme (18) Synthesis of [Cr $(CO)_2$ (dppm) (DPG)](F 4)

2.2.6- Synthesis of [Cr $(CO)_2$ (dppm) (8-HQ)](F 5)

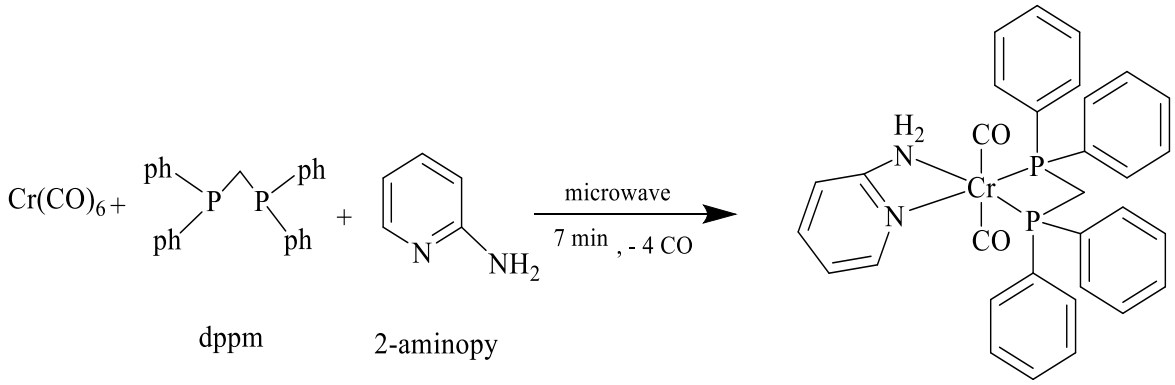
Synthesis of complex was by grinding [Cr $(CO)_6$] (0.15 g , 0. 0006818 mol) with two ligands bis (di phenyl phosphino)-methane (dppm) (0.2617 g, 0.006818mmol) and 8-hydroxyquonuline(8-HQ) (0. 09892 g, 0.0006818 mmol), grinding well and then placing them in a small tube in the microwave for 10 minutes. White solid of the product washed several times with THF. The recrystallization of solid in hot THF gave (0.2778) g of the product (63.97%) and the melting point for the complex is (112-123 °C). Scheme (19)



Scheme (19) Synthesis of [Cr $(CO)_2$ (dppm) (8-HQ)] (F 5)

2.2.7- Synthesis of [Cr $(CO)_2$ (dppm) (2-aminopy)] (F 6)

Synthesis of complex was by grinding [Cr $(CO)_6$] (0.15 g, 0.00068181 mmol) with two ligands bis(diphenylphosphino)-methane (dppm) (0.26177 g, 0.00068181 mmol) and 2-aminopyridine(2-aminopy) (0. 06417g, 0.00068181 mmol), grinding well and then placing them in a small tube in the microwave for 7 minutes. White solid of the product washed several times with THF. The recrystallization of solid in hot THF gave 0.3995 g of the product (49. 33%) and the melting point for this complex is (121-127 °C). Scheme (20)



Scheme (20) Synthesis of [Cr $(CO)_2$ (dppm) (2-aminopy)] (F 6)

Materials and Method.

2.3 Determination of potential cytotoxicity of novel Chromium molybdenum complexes with DPPM ligand.

2.3.1 Principle:

The sensitivity of the to Cr(0), Mo(0) complexes was determined by sulphorhodamine-B (SRB) assay, which provides a sensitive index of cellular protein content. SRB is a bright pink aminoxanthene dye with two sulphonic groups that stains protein by binding to the amino groups of intracellular protein HEPG-2 under mild acidic conditions [99]

2.3.2 Reagents and buffers:

1. Acetic acid: 1% concentration was used for dissolving the unbound SRB dye.
2. SRB: 0.4% SRB dissolved in 1% acetic acid was used as protein dye in cytotoxicity assay.
3. TCA: A stock solution of TCA (50%) was prepared and stored at 4◦C in the refrigerator. Fifty µl of the stock were added to 200 µl RPMI-1640 medium/well to yield a final concentration of 10% for protein precipitation.
4. Tris base: It was used for SRB dye solubility at a concentration of 10 mM and pH of 10.5 (adjusted by 2 M HCl)

2.4 Measurement Of Biological Activity :

2.4.1 Procedure:

1. Cells were used when 70% confluence was reached in T75flasks. The adherent cell line was harvested with 0.025% trypsin. Viability was determined by trypan blue exclusion using the inverted microscope.

2. Cells were seeded in 96-well plate microtiter plates at a concentration of 3×103 cells/well in fresh medium and left to attach to the plates for 24 hours.
3. After 24 hours, cells were incubated with four concentrations of Cr(0) , Mo(0) complexes (62.5-5, 125, 250, 500 µg/ml) for HEPG-2 cell line. Wells were completed to 200 µl volume/well using fresh medium and incubation was continued for 48hours. Control cells were treated with vehicle alone. For each drug concentration, 4 wells were used, and the experiment was repeated 3 times each.
4. Following treatment, the cells were fixed with 50 µl cold 50% TCA for 1 hour at 4◦C. Wells were then washed once with distilled water and stained for 30 minutes at room temperature with 50 µl of 0.4% SRB dissolved in 1% acetic acid.
5. The wells were then washed once with 1% acetic acid and the plates were air dried and the dye was solubilized with 10 mM of tris base (pH 10.5, 100µl/well) for 5minutes on a shaker (Orbital shaker OS 20, Boeco, Germany).
6. The optical density (O.D.) of each well was measured spectrophotometrically at 570 nm with amicroplate reader (Tecan SunriseTM, Germany). The mean values for each drug concentration were calculated.

2.4.2. Calculation:

The percentage of cell survival was calculated as follows: Survival fraction= O.D. (treated cells)/ O.D. (control cells). The concentrations of Cr(0) and Mo (0)complexes with DPPM ligand required to produce 50% inhibition of cell growth (IC50values) were calculated using dose response curve-fitting models (GraphPad Prizm software, version 5).

Table (1) The elemental analysis data of molybdenum complexes

Complexes	Colour	M.Wt Found	Elemental analysis						M.P	Yield %
			%C		%H		%N			
			Calc.	Found	Calc.	Found	Calc.	Found		
[Mo(Co)$_2$ (dppm) (DPG)](F1)	white	746.95	64.26	64.51	4.71	4.85	5.62	5.89	116 -124	44.899 %
[Mo(Co)$_2$)(dppm) (8-HQ)](F2)	purple	680.95	63.44	63.70	4.28	4.39	2.055	2.21	122 -126	71.77 %
[Mo(Co)$_2$)(dppm)(2-minopy](F3)	white	629.96	60.95	60.71	4.47	4.32	4.44	4.68	122-129	54.53 %

Table (2) The elemental analysis of chromium complexes

Complexes	Colour	M.Wt Found	Elemental analysis						M.P	Yield
			C %		H%		N%			
			Calc.	Found	Calc.	Found	Calc.	Found		
[Cr (Co)$_2$ (dppm) (dPG)] F 4	White	702.99	68.27	68.45	5.01	5.09	5.97	6.13	116-120	52.91 %
[Cr (Co)$_2$)(dppm) (8-HQ)] F 5	White	636.80	67.81	68.58	4.58	4.69	2.19	2.33	112- 117	64.14 %
[Cr(Co)$_2$)(dppm)(2-aminpy)] F 6	White	585.00	65.53	65.47	4.77	4.85	4.77	4.19	121- 124	49.33 %

CHAPTER THREE

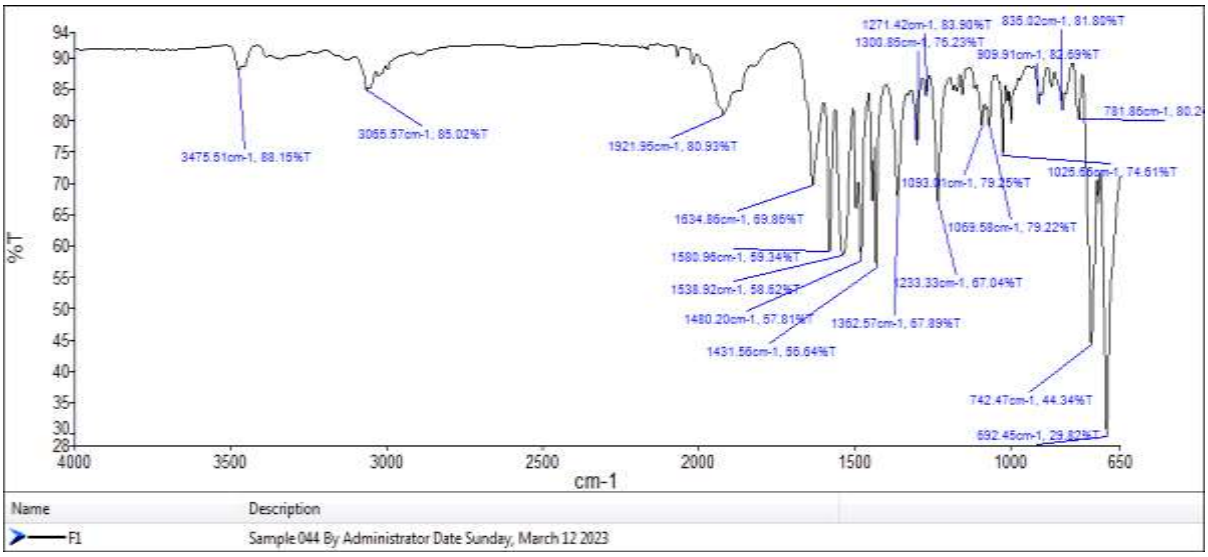
Results and Discussion

3.1. Spectroscopic Studies Of Molybdenum (0) complexes

The first complex **[Mo $(CO)_2$(dppm)(DPG)]F1 (Fig.12)** was tested under infrared spectrum When measuring the infrared spectrum of these complexes, the absorption bands of the clusters appeared at lower frequencies compared to the free state, which confirms the binding of the metal to the linker. where the bonding spectrum showed two weak absorption bands at (and 3065 cm-1) due to tensile vibrations of the (C-H)Ar [95] aromatic bond. Similarly (3475 cm^{-1}) belongs to (N-H) from[96, 97] . The infrared spectrum of compound 1 shows intense bands from (1634, 1538, 1480, 1431 cm^{-1}). These frequencies correspond well to ν (C = N) and ν (C = C) [97]. It can be classified according to what was mentioned in the references due to the appearance of an average absorption (1634, 1580, 1538 cm -1) due to the (C = N) bond belonging to the linker [96, 98]. as it shifted to low frequencies, which confirms its stability with respect to the metal. For (C=C)Ar, its absorption range at (1480-1431 cm-1) [95] .was shown as its rate. It is converted to lower frequencies than in the free state. The displacement of the (C - N) bond from (DPG) to a lower frequency as it appeared at (1362 - 1233 cm^{1})[99], which indicates its involvement in coordination with the metal. It has been reported that the infrared bands of $Mo(CO)_6$ appearing at 2004cm^{-1}(C=O) in the free state where partial substitution (CO) leads to an increase in the extent of the back metallic dp donation of the remaining CO groups; Thus, it is expected that the order of the Mo-CO bond will increase, and the order of the C=O bond of the remaining carbonyl bonds is expected to decrease. absorption appeared at (1976 cm^{-1}) (7) as well as weak at (1872 cm^{-1})[100]. It was also observed that new absorptions appeared in the infrared spectrum at (743 cm^{-1}) from the expansion vibration of the (Mo-N) bond and (692 cm^{-1}) from the (Mo-P)[99, 101].

Table (3) Absorbed vibrational frequencies of molybdenum complexes $Mo(CO)_2(dppm)(dpg)$

Assignments2+	IR (cm^{-1}) Experimental (cm^{-1})
Complex $Mo(CO)_2(dppm)(dpg)$	
N-H (dpg)	3475 cm^{-1}
C-H Ar	3065 cm^{-1}
C=O	1976 cm^{-1} & 1872 cm^{-1}
C=N(dpg)	1580 cm^{-1} - 1538 cm^{-1}
C=C	1480 cm^{-1}-1431 cm^{-1}
Mo-N	743 cm^{-1}
Mo-P	692 cm^{-1}



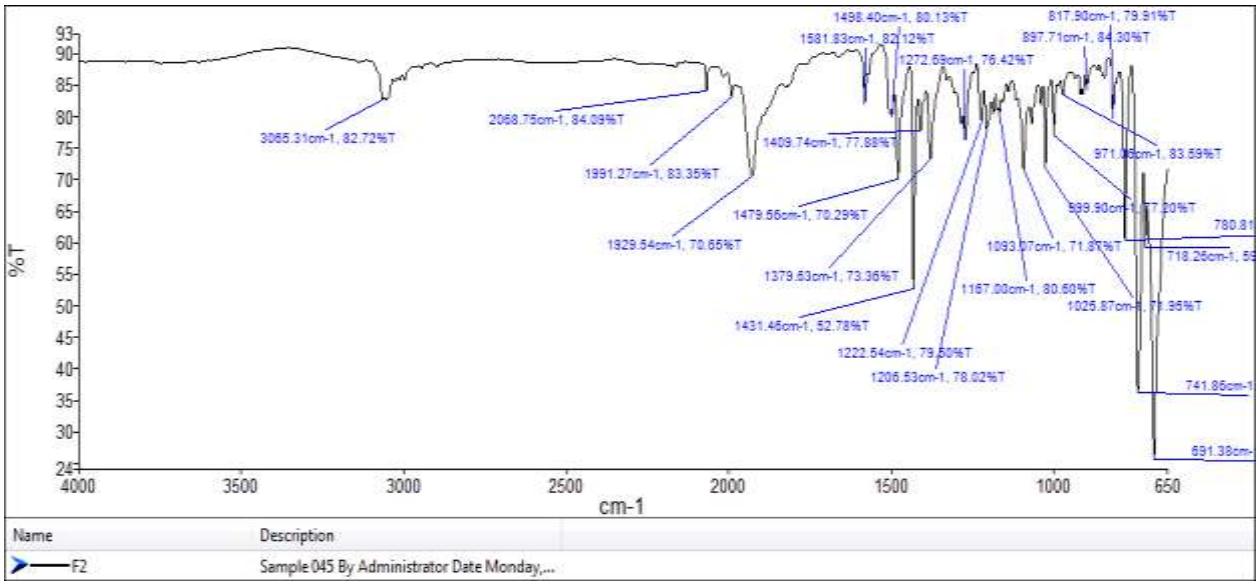
(Fig .12)Infrared spectrum of [Mo $(CO)_2$(dppm)(DPG)](F1)

The infrared spectrum of the **$[Mo(CO)_2(dppm)(8HQ)]$ F2 (Fig.13)** displays a noticeable shift of most bands to lower frequencies relative to the free ligands, confirming successful coordination to the molybdenum center. A weak absorption band appears at (3065 cm^{-1}), attributed to the aromatic (C–H)_Ar stretching vibrations [95], The N-H stretching vibration around(3475 cm^{-1}) is absent. This disappearance indicates that the N-H group is involved in coordination with the central metal. The carbonyl region exhibits two characteristic bands at (1991 cm^{-1} and 1929 cm^{-1}),

indicating the presence of two CO groups in a cis configuration around the metal center. An additional band at (2058 cm^{-1}) is assigned to the asymmetric CO stretching mode, appearing at a higher frequency due to reduced π-back bonding from Mo to CO, which strengthens the C=O bond and increases its vibrational energy. The region between (1581–1498 cm^{-1}) exhibits the typical C=N stretching bands of the 8-hydroxyquinoline ligand (8-HQ) [103], with a noticeable decrease in intensity upon coordination. Aromatic C=C stretching vibrations are also observed at (1479–1431 cm^{-1}) [101]. A significant shift in the phenolic ν(C–O) stretching band to (1206–1222 cm^{-1}).The disappearance of the(O–H)stretching band confirms deprotonation and coordination through the phenolic oxygen. In the lower-frequency region, several diagnostic metal–ligand vibrations are identified: the Mo–O stretching band at (853 cm^{-1}) [103] , the Mo–N band at (741 cm^{-1}) , and the Mo–P band of the dppm ligand at (691 cm^{-1}) [44, 103] . Collectively, these spectral features confirm bidentate coordination of (8-HQ) through its nitrogen and phenolic oxygen atoms, chelation of dppm through both phosphorus donor atoms, and the presence of two cis-CO ligands, thereby verifying the successful formation of the proposed molybdenum complex

Table (4) Absorbed vibrational frequencies of molybdenum complexes $[Mo(CO)_2(dppm)(8\text{- HQ})]$.

Assignments	IR (cm^{-1}) Experimental (cm^{-1})
Complex $Mo(CO)_2$(dppm)(8- HQ)	
C-H (Ar)	3065 cm^{-1}
C=O	1991& 1929 cm^{-1}
C=N(8-HQ)	1581 - 1498 cm^{-1}
C=C (Ar)	1479 -1431 cm^{-1}
C-O (8 –HQ)	1222-1206 cm^{-1}
Mo-O	853 cm^{-1}
Mo – N	741 cm^{-1}
Mo – P	691 cm^{-1}

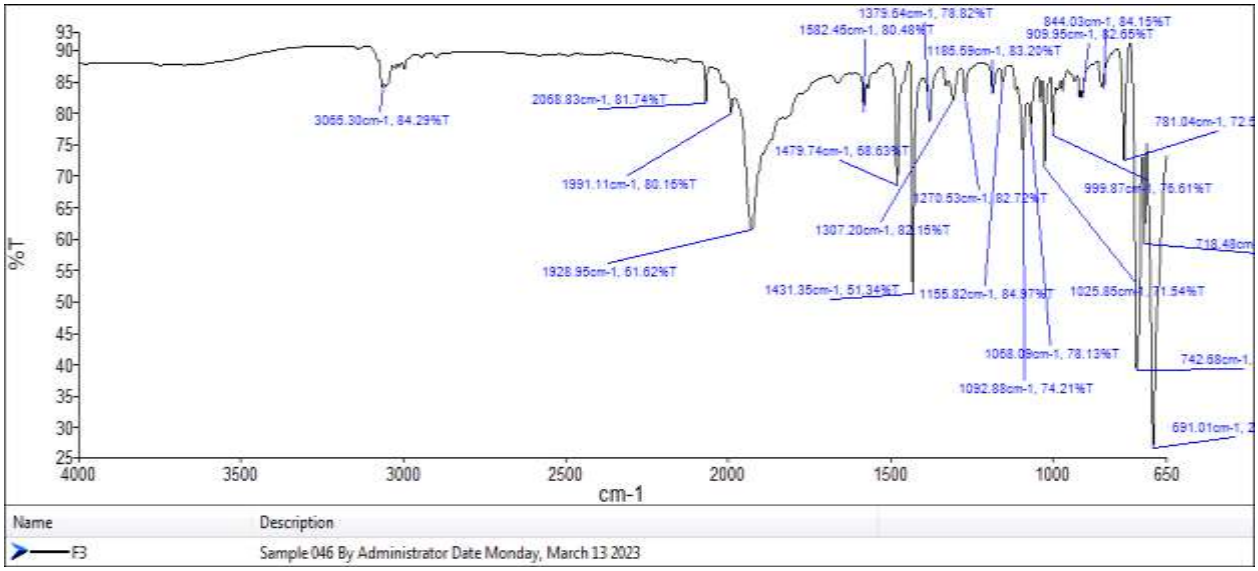


(Fig. 13) Infrared spectrum of [Mo $(CO)_2$(dppm)(8HQ)] (F 2)

The infrared spectrum of the molybdenum complex **[$Mo(CO)_2$(dppm)(2-aminopy)]F3 (Fig. 14)** shows a clear absorption band at (3065 cm^{-1}) attributed to the aromatic (Ar–H) stretching of both dppm and 2-aminopy. Two sharp and intense bands at (1991 cm^{-1} and 1928 cm^{-1}) correspond to the terminal carbonyl groups, consistent with the cis-arrangement of coordinated CO ligands [104]. In addition to these two expected carbonyl absorptions, a weak extra band was observed at(2068 cm^{-1}). This band is most reasonably assigned to a trace carbonyl-containing impurity or a residual precursor species, as its higher wavenumber indicates a CO group in a more electron-withdrawing environment than the coordinated carbonyls of the final complex. The spectrum also displays several characteristic absorptions of the co-ligands; bands at (1431, 1479, 1582, and 1379 cm^{-1}) arise from (Ar C=C), (C=N), and (C–N) stretching vibrations, which are typical for the pyridine ring[44, 46], in addition to (C=C) modes associated with dppm[101]. Notably, the disappearance of the band at (3452 cm^{-1}), corresponding to the asymmetric and symmetric stretching vibrations of the free ($–NH_2$) group in (2-aminopyridine) , indicates coordination through the pyridine nitrogen atom [105,106]. Furthermore, the appearance of characteristic metal–ligand vibrations supports the proposed coordination mode: the Mo–N stretching at (742 cm^{-1}), Mo–P at (692 cm^{-1}) , and Mo–C at (853 cm^{-1}) are all consistent with the formation of the target complex [103] . These spectral features collectively confirm the successful coordination of dppm and 2-aminopy to the molybdenum center and support the proposed structure of the complex.

Table (5) Absorbed vibrational frequencies of molybdenum complexes [$Mo(CO)_2$(dppm)(2- aminopy)].

Assignments	IR (cm^{-1}) Experimental (cm^{-1})
Complex $Mo(CO)_2$(dppm)(2- amino py)	
C-H Ar(dppm & 2-aminopy**)**	3065 cm^{-1}
C=O	1991& 1928 cm^{-1}
C=N (2-aminopy**)**	1582 cm^{-1}
C=C (Ar)	1479 -1431 cm^{-1}
C-N **(**2-aminopy**)**	1307-1270 cm^{-1}
Mo-C	781 cm^{-1}
Mo-N (2-aminopy)	742cm^{-1}
Mo-p(dppm))	691 cm^{-1}



(Fig .14) Infrared spectrum of [Mo $(CO)_2$(dppm) (2-aminopy)] (F 3)

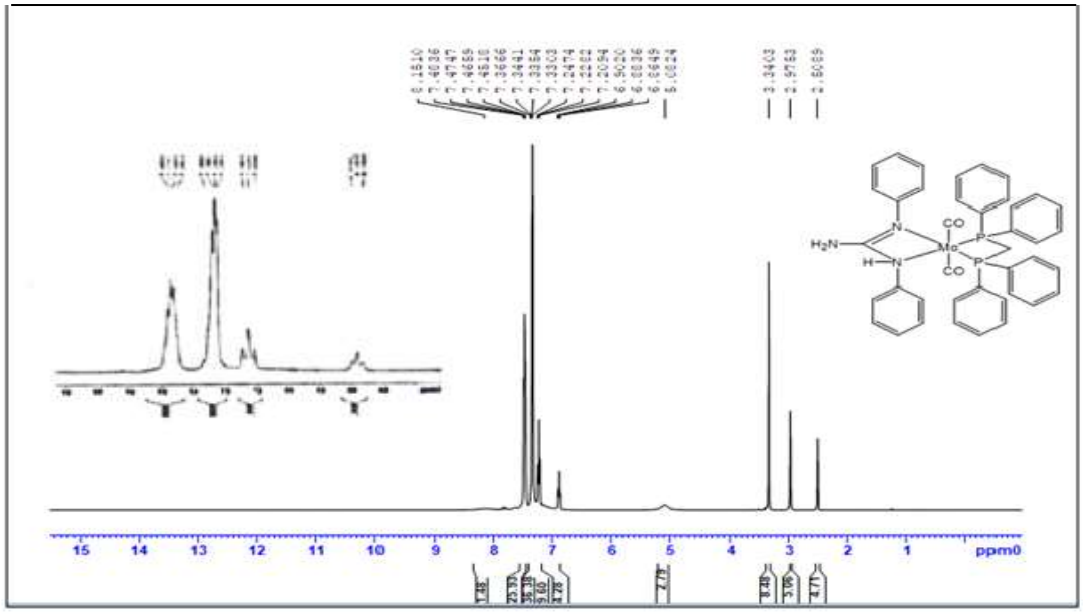
The ^{1}HNMR spectrum of d^6-DMSO shows an important role in the characterization of molybdenum complexes(Fig.15.16.17). The bonds show two sets of peaks due to the presence of two chemically different types of protons. The first set of peaks in the three complexes appears between (δ=6.9 – 6.8 ppm)

[54]. Which corresponds to the aromatic protons of the vinyl groups in (dppm) (m, 5H, CHPh). The second peak appears at (δ = 3.34 ppm), corresponds to the

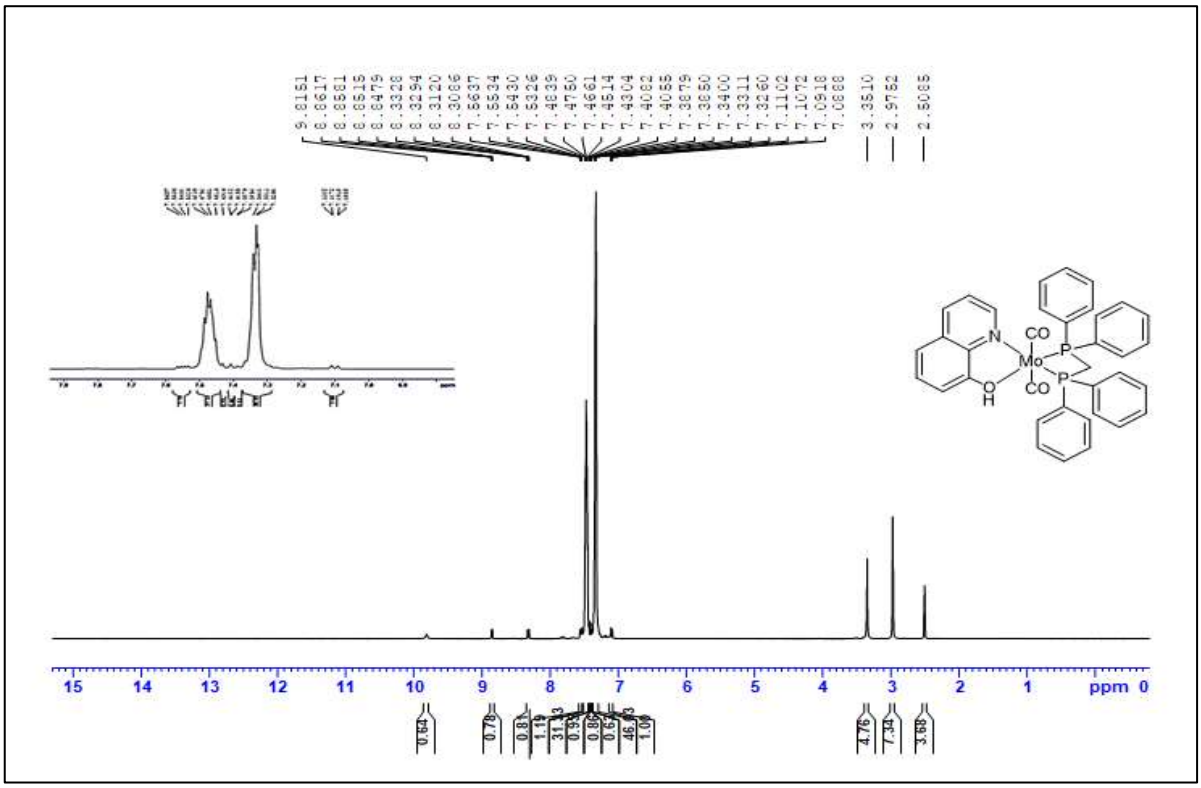
methylene protons (-CH_2-) adjacent to the phosphorus atoms[95]. The complexes also show an absorption number traced to the ^{1}H NMR spectrum of (DPG) for **[Mo $(CO)_2$(dppm) (DPG)]** chemical shifts and multiple protonation signals of the aromatic protonswere observed at (δ = 7.90 – 6.90) compared to those observed in the free DPG spectrum. Which was from (δ = 7.2 - 11). The ^{1}H NMR of **[Mo $(CO)_2$(dppm) (DPG)]**F1 (Fig 18) is also characterized by a peak at which it returns to (δ = 8.99 (s, 1H, NH), 7.17 d, 5 H, Ph)[96, 102]. The proton nuclear magnetic resonance (^{1}HNMR) spectrum of **[Mo $(CO)_2$(dppm) (8-HQ)]**F2 (Fig.19) is shown, revealing the proton peaks in the aromatic ring of the 8-hydroxyquinoline bond. Specifically, the spectrum shows peaks at(δ = 7.56 to 7.32 ppm, 8.48 ppm)[99, 103] . and (δ = 9.8 ppm), which correspond to the protons in the aromatic ring and the proton peak in the (-OH) group, respectively. This information helps determine and understand the structure of the

[Mo $(CO)_2$(dppm) (8-HQ)] complex. Four aromatic protons of (dppm) are degradable and can be seen in the region (δ = 7.11 ,7.10 ,7.09 ,7.08). The proton ring of tetraphenyl(Ph) groups (m, 5H,CHPh) and the singlet peak arising from methylene (-CH_2-) at (δ = 3.34 ppm) are coordinated with the chromium center and (δ = 2.50 ppm) of the THF solvent due to the non-driing complexes[54,82]. The ^{1}HNMR spectrum of **[Mo $(CO)_2$(dppm) (2- aminopy)] F 3 (Fig.20)** shows four DPPM peaks of aromatic ring protons in the 7 ppm region. The absorption at (δ = 25 -7.35 ppm), which belongs to the proton ring of the tetraphenyl (Ph) groups (m, 5H, CHPh) and the singlet peak arising from the methylene bridge group (-CH_2-) at (δ = 2.9 ppm), and the aromatic protons on the back of the pyridine on the ring. Form multiples of the range

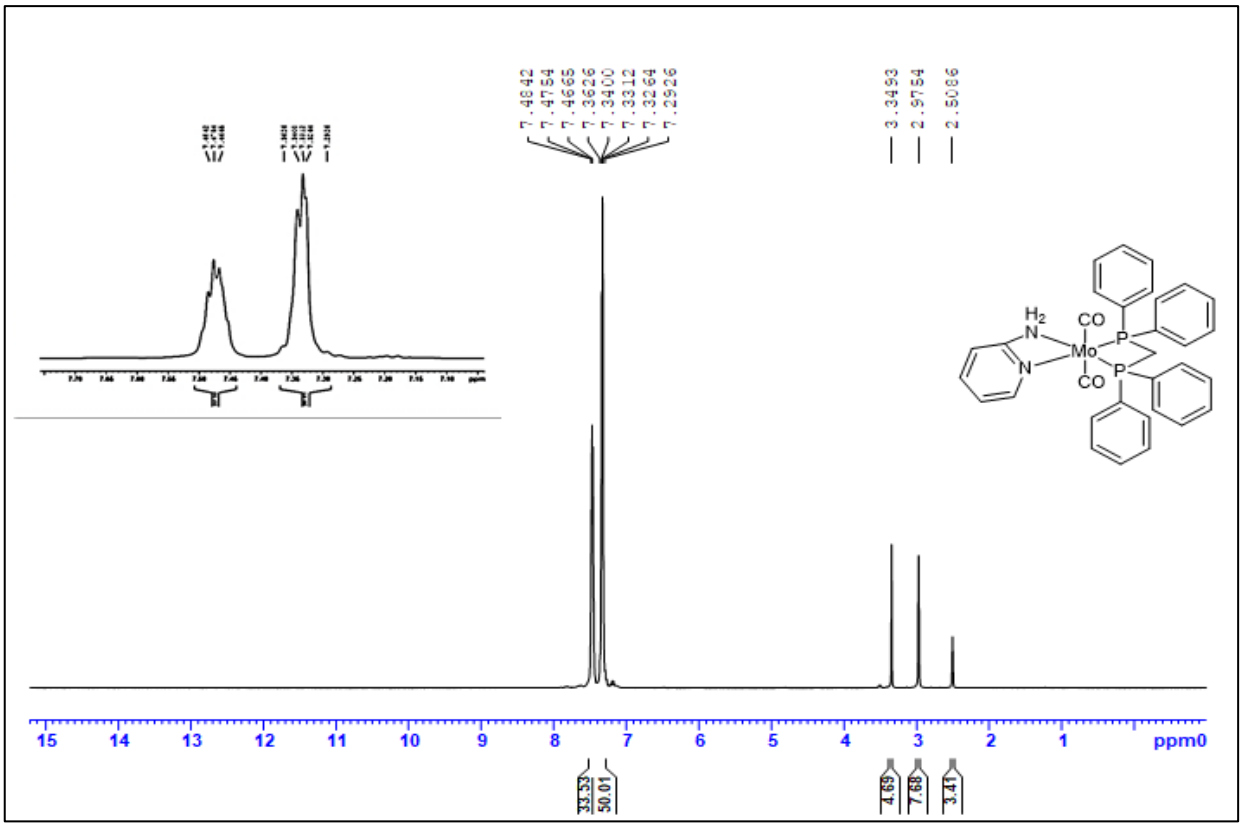
(δ =1H d 7.484 , 1H d7.4754 ,1H t 7.4665 ,1H t 7.3626 ppm) As for the amino proton: located in the amino group (-NH_2-), it appears as one piece within (δ = 2H s 3.34 ppm).



(Fig .15) ^{1}H NMR spectrum of [Mo $(CO)_2$)(dppm) (DPG)] (F 1)



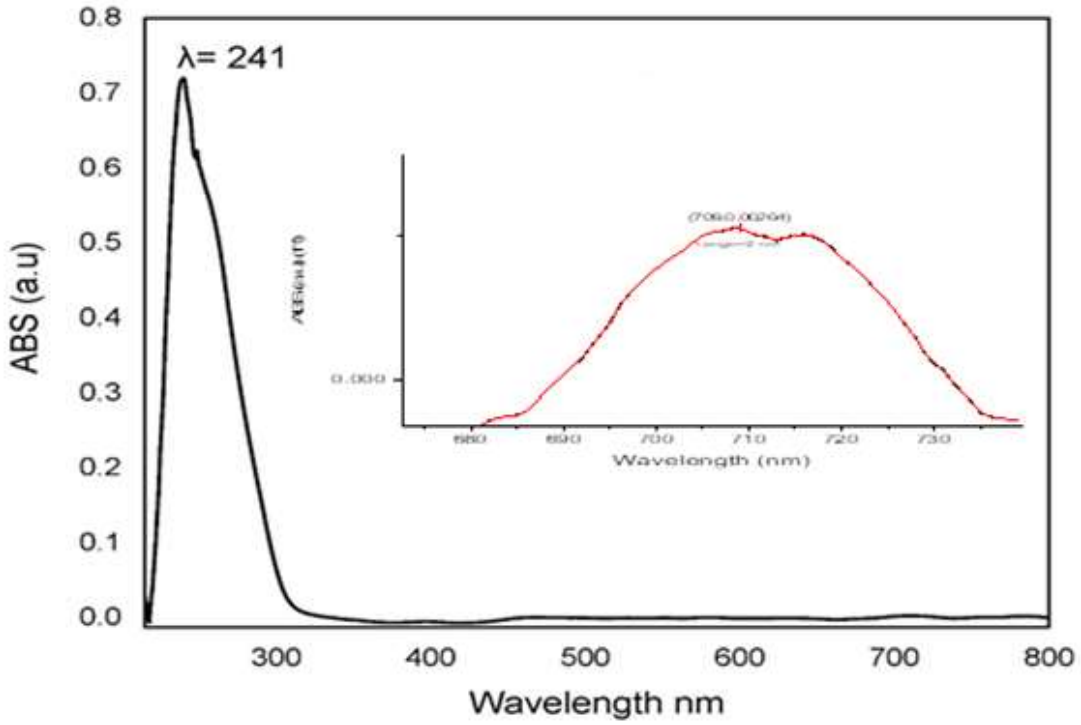
(Fig.16) ^{1}HNMR spectrum of [Mo $(CO)_2$(dppm) (8- HQ)] (F 2)



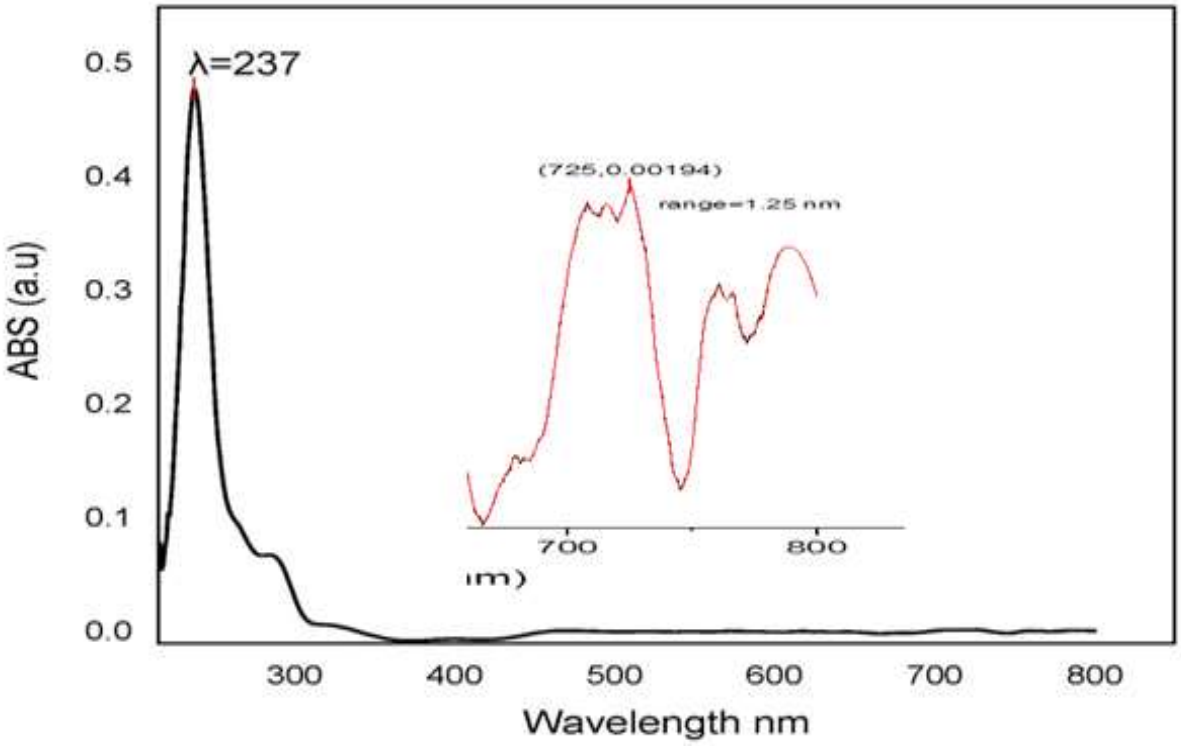
(Fig .17) ^{1}HNMR spectrum of [Mo $(CO)_2$(dppm) (2-aminopy)] (F 3)

The electron absorption spectra of the molybdenum complexes in dimethyl sulfoxide (DMSO) showed distinct peaks in the wavelength range of 200-800 nm. The complexes **[Mo(CO) $_2$ (dppm) (DPG)], [Mo$(CO)_2$)(dppm) (8-HQ)], and [Mo$(CO)_2$ (dppm) (2-Aminobi)] (Fig.18.19.20)** exhibited intrinsic π–π* bonding at approximately (241 nm, 237 nm, and 238 nm)[104] , respectively, indicating the presence of aromatic rings in these complexes.

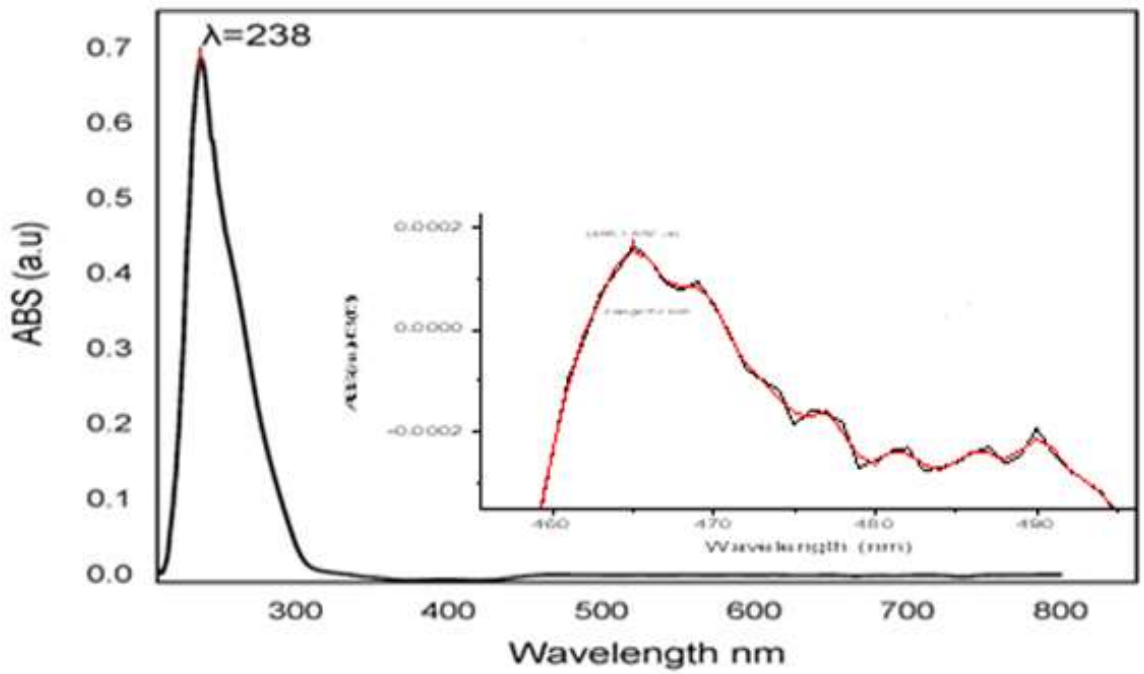
Additionally, a strong absorption band was observed at (709 nm,729nm and 765 nm) which is attributed to metal-to-ligand charge transfer (MLCT) transitions. The ligands, including CO, dppm, DPG, 8-HQ, and 2-aminopy, exhibited pronounced d-d transitions, indicating a wide range of charge transfer transitions M → L of the M (d π) → L (p π*) type , which masked the intensity of the field transition. These findings highlight the complex nature of the electron absorption spectra of molybdenum complexes in DMSO.



(Fig.18) Electronic spectrum of [Mo(Co)$_2$(dppm) (DPG)](F 1)

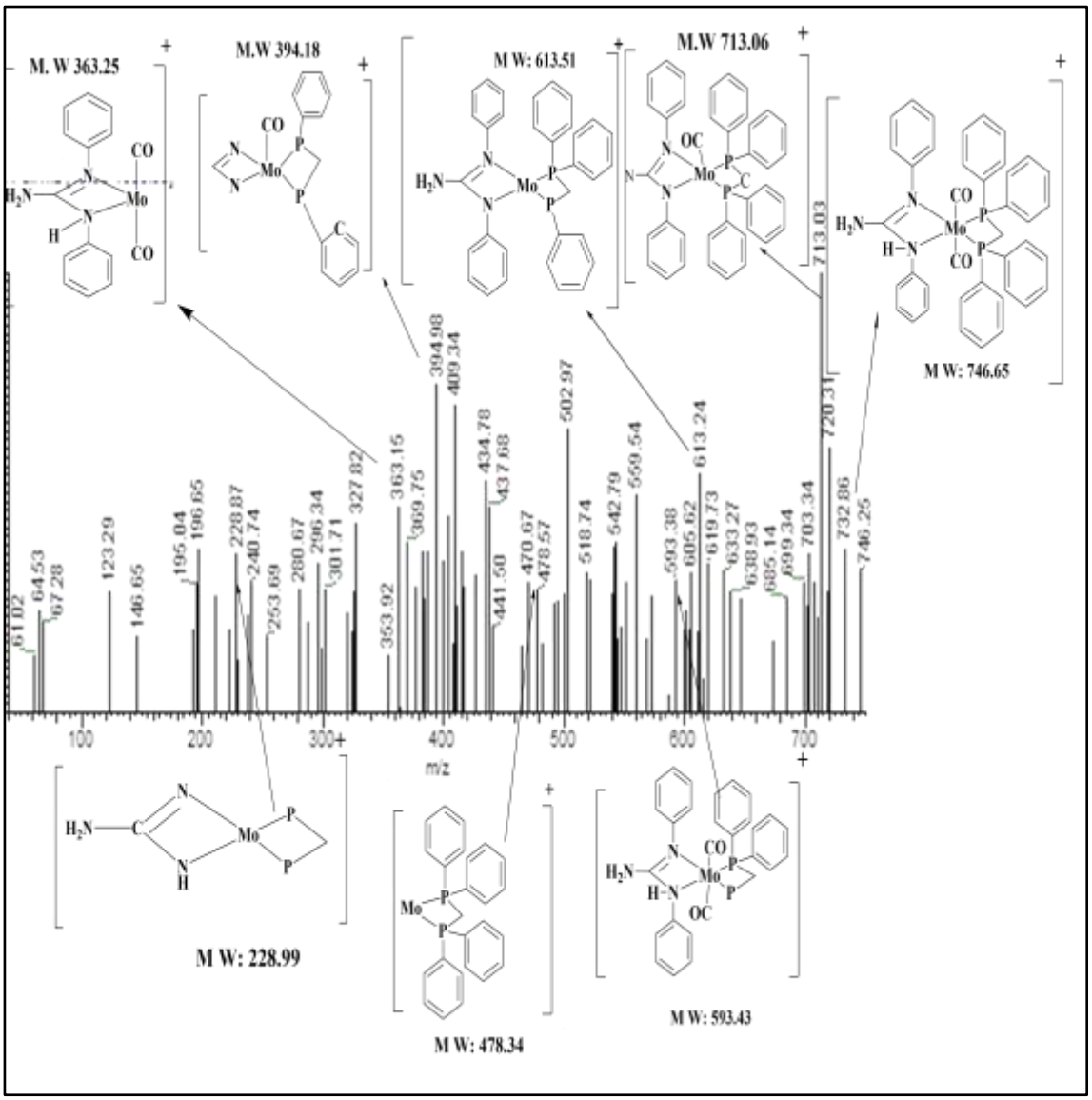


(Fig.19)Electronic spectrum of [Mo(CO)$_2$(dppm) (8-HQ)] (F 2)



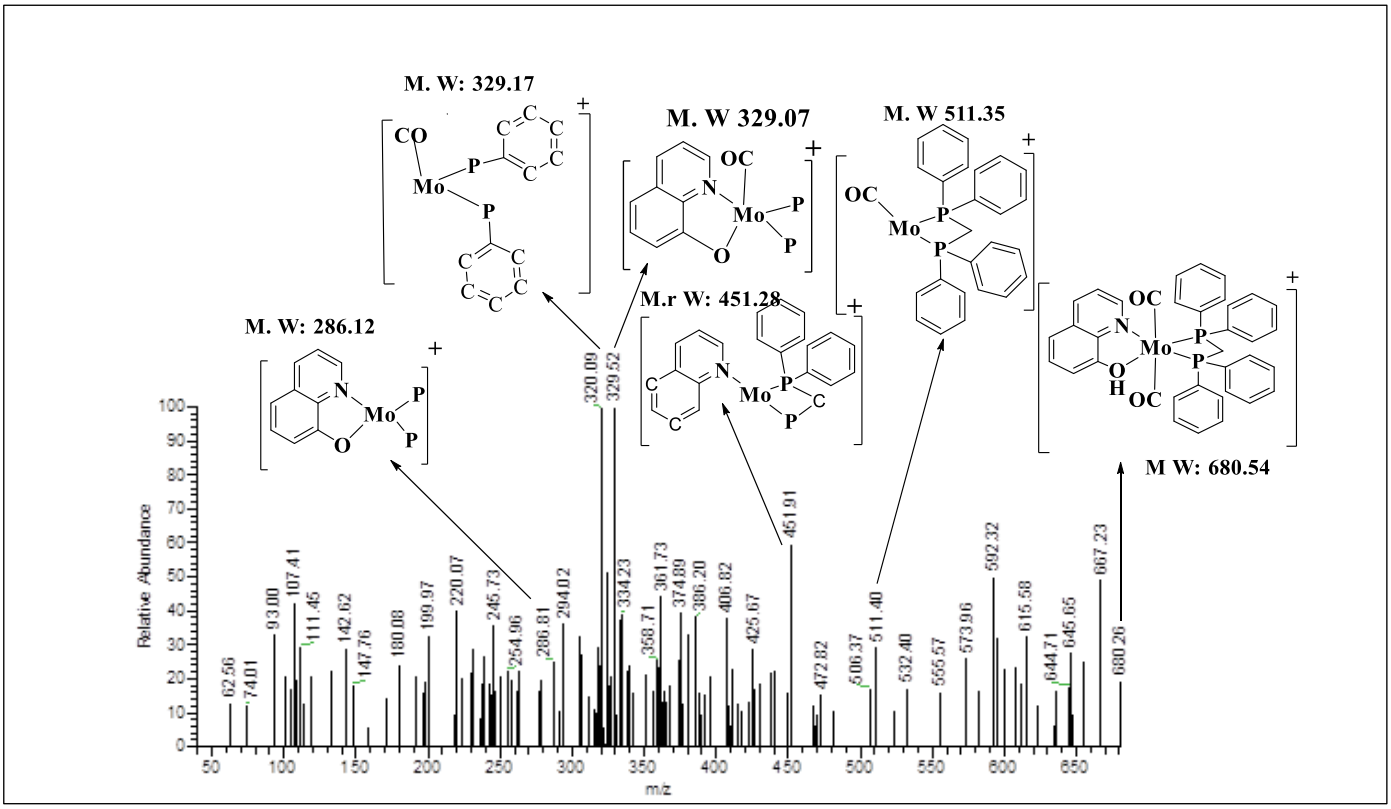
(Fig.20)Electronic spectrum of [Mo(CO)$_2$(dppm) (2-aminopy)] (F 3)

The mass spectrum of the complex [Mo(CO)$_2$(dppm)(DPG)]$^+$ (F1) (Fig.21) exhibits a molecular ion peak at m/z = 746.25 with a relative intensity of 34%, which confirms the formation of the target complex. A base peak is observed at m/z = 713.03 (100%), corresponding to the loss of CO and five hydrogen atoms from the molecular ion. A characteristic fragment appears at m/z = 613.24 (54%), which is attributed to the loss of one phenyl group (C_6H_5) and two CO units. Another fragment at m/z = 594.43 (30%) results from the elimination of two phenyl groups ($C_{12}H_{10}$). A peak at m/z = 478.57 (28%) is assigned to the loss of DPG, two CO groups, and two hydrogen atoms. A strong fragment is observed at m/z = 394.18 (76%), resulting from the cleavage and loss of four phenyl rings ($C_{24}H_{20}$) in addition to NH_3 and CO. Another significant fragment appears at m/z = 363.15 (46%), which corresponds to the fragmentation of the dppm ligand. Finally, a peak at m/z = 228.87 (36%) is attributed to the elimination of six phenyl rings ($C_{36}H_{30}$) together with two CO groups, indicating extensive breakdown of the ligand framework during ionization.



(Fig.21) Mass spectrum for [Mo $(CO)_2$ (dppm)(DPG)] (F 1)

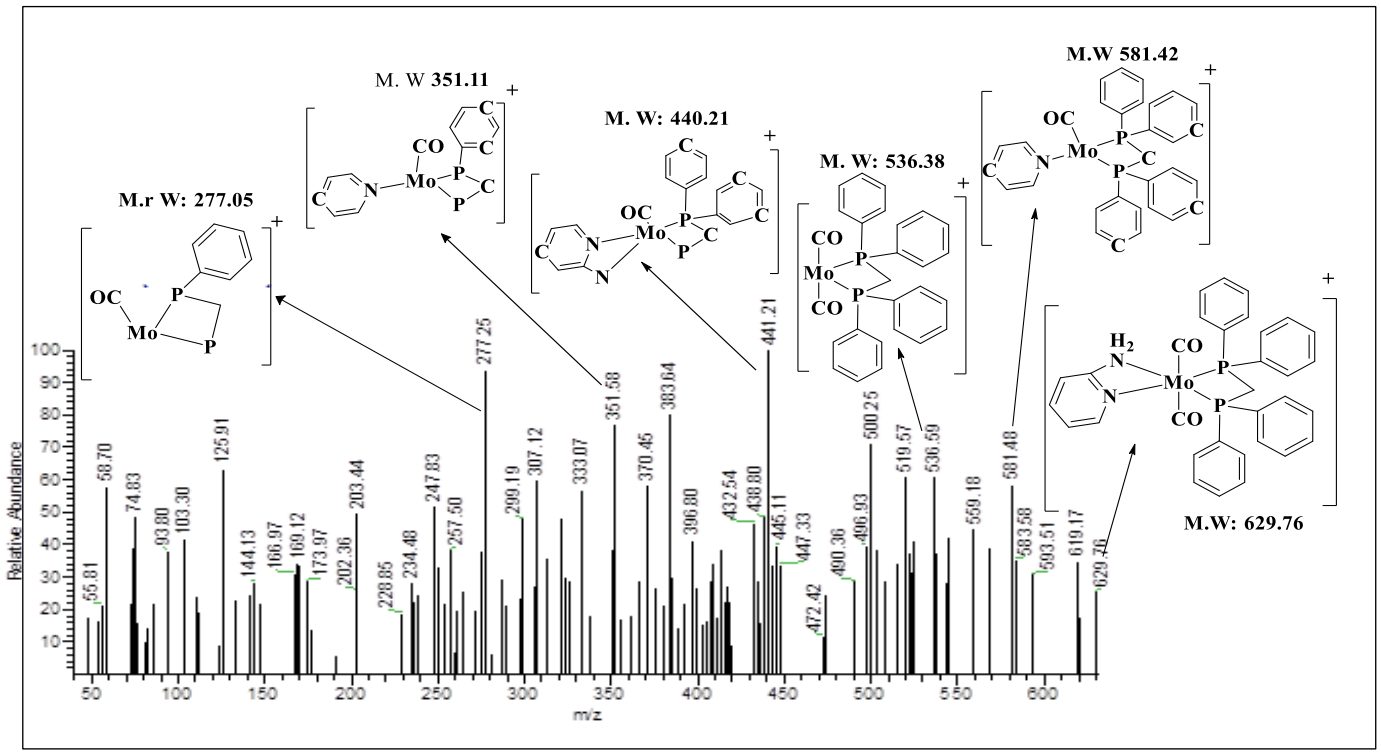
The mass spectrum of the compound $[Mo(dppm)(8\text{-}HQ)(CO)_2]^+$ (F 2)(Fig.22) shows the molecular ion (680.26 m/z) with an intensity of (20%), as shown in the spectra of the ion at (511.35 m/z) (30%) as a result of the exit of [(CO) , 8-HQ], as well as the ion at (451.67 m/z) with an intensity of (58%), which is a result of the exit of [O, H5, Ph, $(CO)_2$]. The mass spectrum also appears at (329.52) with an intensity of (100%), indicating the exit of two phenyl groups [$C_{12}H_{10}$, CO , 8-HQ , CH_2 ,10H] or the exit products of four phenyl rings + a methylene group CH_2 , CO, as well as the bands at m/z and the ion at (286.81) (20%) as a result of the exit of [four rings (phenyl) , 2(CO) , CH_3] with a number of other parts due to the cleavage of the parent compound.



(Fig.22) Mass spectrum for [Mo $(CO)_2$ (dppm)(8 -HQ)](F 2)

The mass spectrum of the compound $[Mo(CO)_2(dppm)(2\text{-aminoby})]^+$(F3)

(Fig.23) shows the molecular ion (629.76 m/z) (% 26), as observed in the spectra for the ion at (581.48 m/z) abundance rate (58%). As a result of the exit of [CO, NH_2, 6H], as well as the ion at (536 m/z), which is the result of the [(2-aminopy) exit. The m/z spectrum also appears at (441.21 m/z) (100%), which indicates the exit of two phenyl groups [(2ph), CO + NH_2 + 8 H], as observed in the spectra for the ion at (351.58 m/z) (78%) as a result of the exit of (3ph, CO, NH_2, 5H) as well as the spectral bands at (277.26 m/z) (94%) as a result of the exit of two phenyl groups and the [(2-amino py, 5H, CO, 3Ph], with a number of other parts due to the cleavage of the main compound.



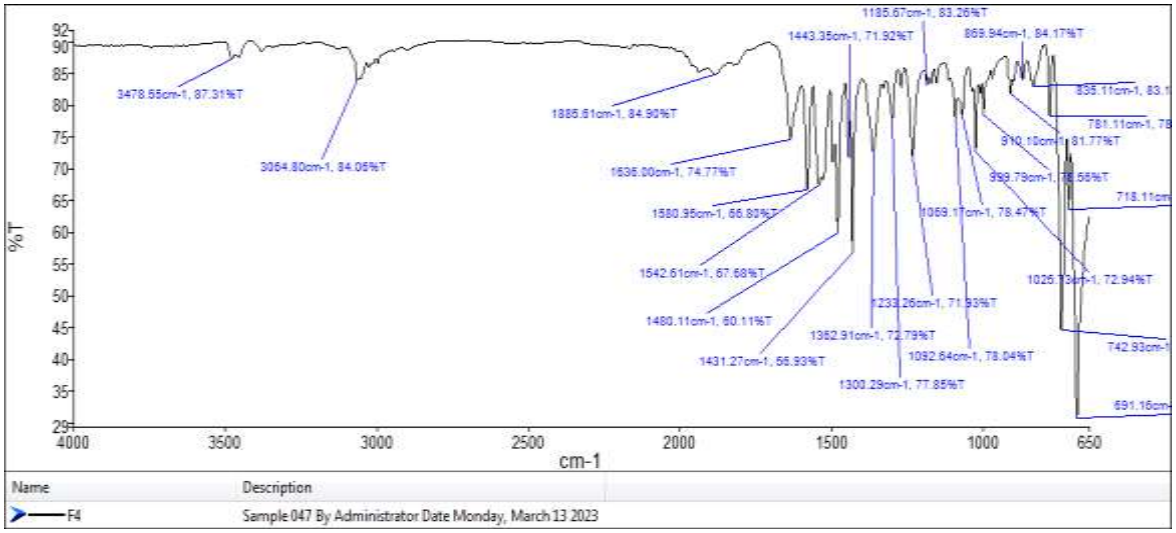
(Fig.23) Mass spectrum for [Mo $(CO)_2$ (dppm)(2-aminopy)] (F 3)

3.2. Results and diagnosis of chromium (0) complexes

The infrared spectrum of the **[Cr$(CO)_2$(dppm)(DPG)]F4** complex (Fig. 24) shows clear evidence for coordination through both the dppm and DPG ligands. A weak absorption band appears at 3064 cm^{-1}, corresponding to aromatic C–H stretching of the dppm and DPG ligands. A characteristic broad band at (3478 cm^{-1}) is assigned to the ν(N–H) vibration of the NH_2 group in DPG, confirming its presence in the coordinated ligand [98, 99] . In the carbonyl region, two distinct ν(C≡O) bands are observed at (1885 cm^{-1}) [110] and 1836 cm^{-1}, both shifted to lower frequencies compared with free $Cr(CO)_6$ (1889 and 1906 cm^{-1}), indicating a reduction in back-bonding energy upon coordination and confirming the cis-CO arrangement. The ν(C=N) vibrations of the DPG ligand also shifted markedly to lower frequencies, appearing at (1580–1542 cm^{-1}) relative to the free ligand, consistent with coordination of the imine nitrogen to chromium [79]. Furthermore, medium to sharp aromatic ν(C=C) absorptions of dppm and DPG appear at (1480–1431 cm^{-1}) [103]. In the low-frequency region, the characteristic band at (742 cm^{-1}) corresponds to ν(Cr–N) stretching of coordinated DPG, while the band at (691 cm^{-1}) is attributed to ν(Cr–P) stretching of the dppm ligand [111] , confirming bidentate coordination through phosphorus and nitrogen atoms.

Table (6) Absorbed vibrational frequencies of chromium complexes [Cr $(CO)_2$(dppm)(dpg]

Assignments	IR (cm^{-1}) Experimental (cm^{-1})
Complex $Cr(CO)_2$(dppm)(DPG)	
N-H_2(DPG)	3478 cm^{-1}
C-H Ar(dppm & DPG)	3065 cm^{-1}
C=O	1912 cm^{-1}& 1889 cm^{-1}
C=N (DPG**)**	1580 & 1542 cm^{-1}
C=C (Ar)	1480 &1431 cm^{-1}
C-N (DPG)	1362&1300 cm^{-1}
Cr-P	691 cm^{-1}
Cr- N	742 cm^{-1}



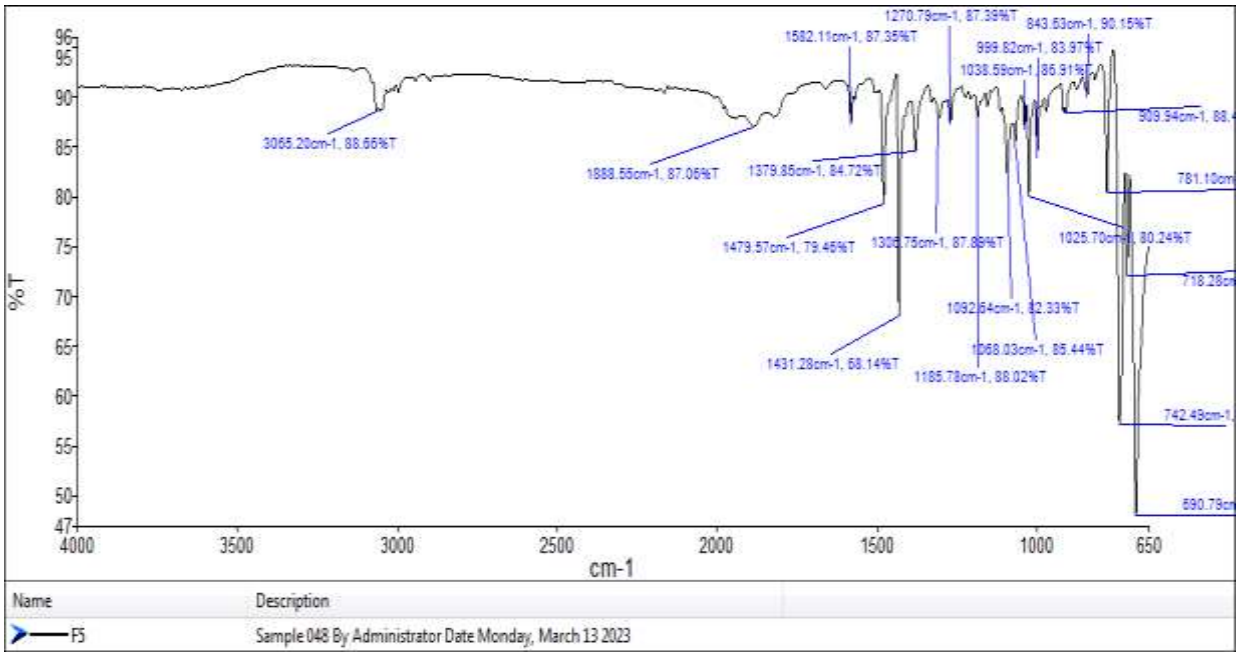
(Fig.24) Infrared spectrum of [$Cr(CO)_2$(DPG)(dppm)] (F 4)

infrared spectral analysis of the **[$Cr(CO)_2$(dppm)(8-HQ)]F5** complex (Fig. 25) provides clear evidence for the successful coordination of the ligands to the chromium center and reveals systematic shifts in the characteristic vibrational bands of the free ligands upon complex formation. The aromatic stretching vibration ν(Ar–H) is observed as a weak band at 3065 cm^{-1}, corresponding to the aromatic environments of both dppm and 8-HQ. Notably, the broad ν(O–H) absorption band of free 8-hydroxyquinoline at 3400 cm^{-1} disappears upon complexation, confirming deprotonation and subsequent coordination through the phenolic oxygen. This coordination mode is further supported by the emergence of the phenolic ν(C–O) stretching band at 1310 cm^{-1} [112], in

addition to other C–O absorptions in the 1379–1306 cm^{-1} region. The complex exhibits distinct ν(C≡O) stretching bands between 1991–1888 cm^{-1}, consistent with the presence of cis-terminal carbonyl groups, with the weaker band at 1888 cm^{-1} assigned to the carbonyl stretching vibration. The ν(C=N) stretching frequency of the 8-HQ ligand appears as a weak band at 1582 cm^{-1} , shifted to lower wavenumbers due to coordination with the metal center. Furthermore, sharp to moderately intense absorption bands at 1479 cm^{-1} and 1431 cm^{-1} are attributed to aromatic ν(C=C) vibrations arising from both dppm and 8-HQ [111] [111]. The fingerprint region displays additional characteristic vibrations of the coordinated phosphine, including the P–Ph bands at 1334 cm^{-1} and 694 cm^{-1} [111]. New diagnostic metal–ligand vibrations appear at lower frequencies, specifically the ν(Cr–N) band at 742 cm^{-1} and the ν(Cr–P) band at 690 cm^{-1} , confirming chelation of the 8-HQ ligand in its (N,O) bidentate mode along with coordination of the dppm ligand. Collectively, these spectral features strongly support the formation of the proposed [$Cr(CO)_2$(dppm)(8-HQ)] complex, characterized by cis-carbonyl geometry and complete coordination of both ligands

Table (7) Absorbed vibrational frequencies of chromium complexes Cr $(CO)_2$(dppm)(8- HQ).

Assignments	IR (cm^{-1}) Experimental (cm^{-1})
Complex Cr $(CO)_2$(dppm)(8- HQ)	
C-H (Ar)	3065 cm^{-1}
C=O	1920 cm^{-1}&1846 cm^{-1}
C=N(8-HQ)	1582 cm^{-1}
C=C (Ar)	1479 -1431 cm^{-1}
C-N (Ar)	1379-1306 cm^{-1}
C-O (8 –HQ)	1270- 1185 cm^{-1}
Cr-N	742 cm^{-1}
Cr-P	690 cm^{-1}



(Fig .25) Infrared spectrum of [Cr(CO)$_2$(dppm)(8-HQ)] (F 5)

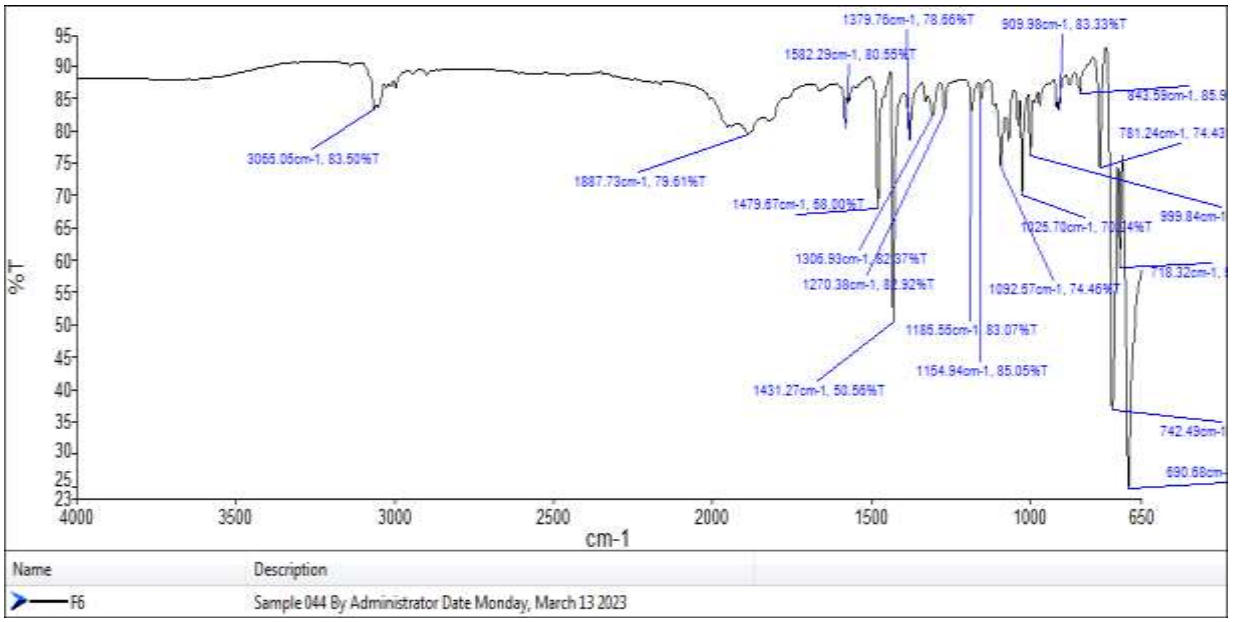
The infrared spectrum of the **[Cr(CO)$_2$(dppm)(2-aminopy)]**F6 complex (Fig. 26) reveals a weak absorption at $\mathcal{V}$(w, 3065 cm^{-1}), characteristic of the aromatic (C–H) stretching vibrations arising from both the dppm ligand and the 2-aminopy moiety. A weak carbonyl-related absorption is also observed at 1987 cm^{-1} [73], which fits within the expected range for ν(w.CO) absorptions of the cis-dicarbonyl chromium environment. A defining feature of the complex is indeed the presence of two distinct ν (CO) absorptions within $\mathcal{V}$ (w.1985–1910 cm^{-1}), typically centered near 1990 cm^{-1} and 1930 cm^{-1} .

This pattern is fully consistent with a cis-dicarbonyl geometry around the chromium center. The observation of only two carbonyl bands reflects the reduced symmetry of the coordination environment and rules out the possibility of a trans arrangement. The marked lowering of ν(CO) relative to free CO ligands signifies appreciable π-back-donation from chromium d-orbitals into the π* orbitals of the carbonyl groups, an effect further enhanced by the strong σ-donor capacity of the dppm ligand. Furthermore, the C=N stretching vibration associated with the coordinated 2-aminopy ligand appears as a weak band at ν (1582 cm^{-1}) [103], indicating retention of the heteroaromatic framework upon coordination. Additional well-defined absorptions at ν (m 1479 cm^{-1} and 1431 cm^{-1}) correspond to aromatic (C=C) stretching modes of both ligands, while the region ν (m 1379–1306 cm^{-1}) is attributed to C–N stretching

frequencies. In the lower-frequency region, newly emerging diagnostic absorptions at ν (s 742 cm^{-1} and 690 cm^{-1}) are assigned to ν(Cr–N) and ν(Cr–P), respectively, substantiating the establishment of a mixed (P,N) chelation mode. Notably, the disappearance of the NH_2 stretching band—present in the free ligand—provides compelling evidence for the direct involvement of the amino group in coordination to the chromium center [46] [46]. Collectively, these spectral features conclusively affirm the successful formation and structural integrity of the mixed-ligand complex [$Cr(CO)_2$(dppm)(2-aminopy)].

Table (8) Absorbed vibrational frequencies of chromium complexes Cr $(CO)_2$(dppm)(2-aminopy).

Assignments	**IR (cm^{-1}) Experimental (cm^{-1})**
Complex [$Cr(CO)_2$(dppm)(2-aminopy)]	
C-H (Ar)	3065 cm^{-1}
C=O	1910 cm^{-1} & 1985 cm^{-1}
C=N(8-HQ)	1582 cm^{-1}
C=C (Ar)	1479 cm^{-1} - 1431 cm^{-1}
C-N (Ar)	1379 cm^{-1} - 1306 cm^{-1}
Cr-N	742 cm^{-1}
Cr-P	690 cm^{-1}

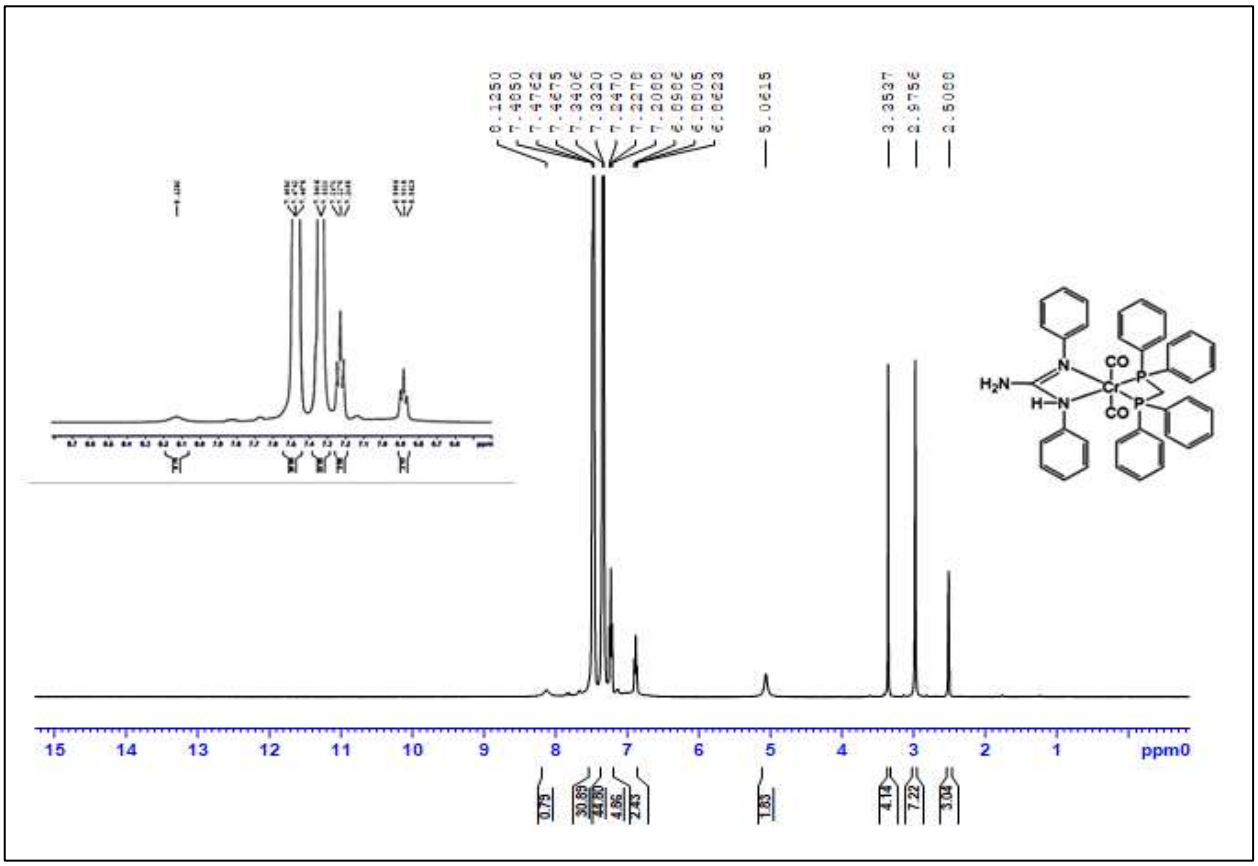


(Fig .26) Infrared spectrum of [Cr $(CO)_2$(dppm)(2-aminopy)](F6)

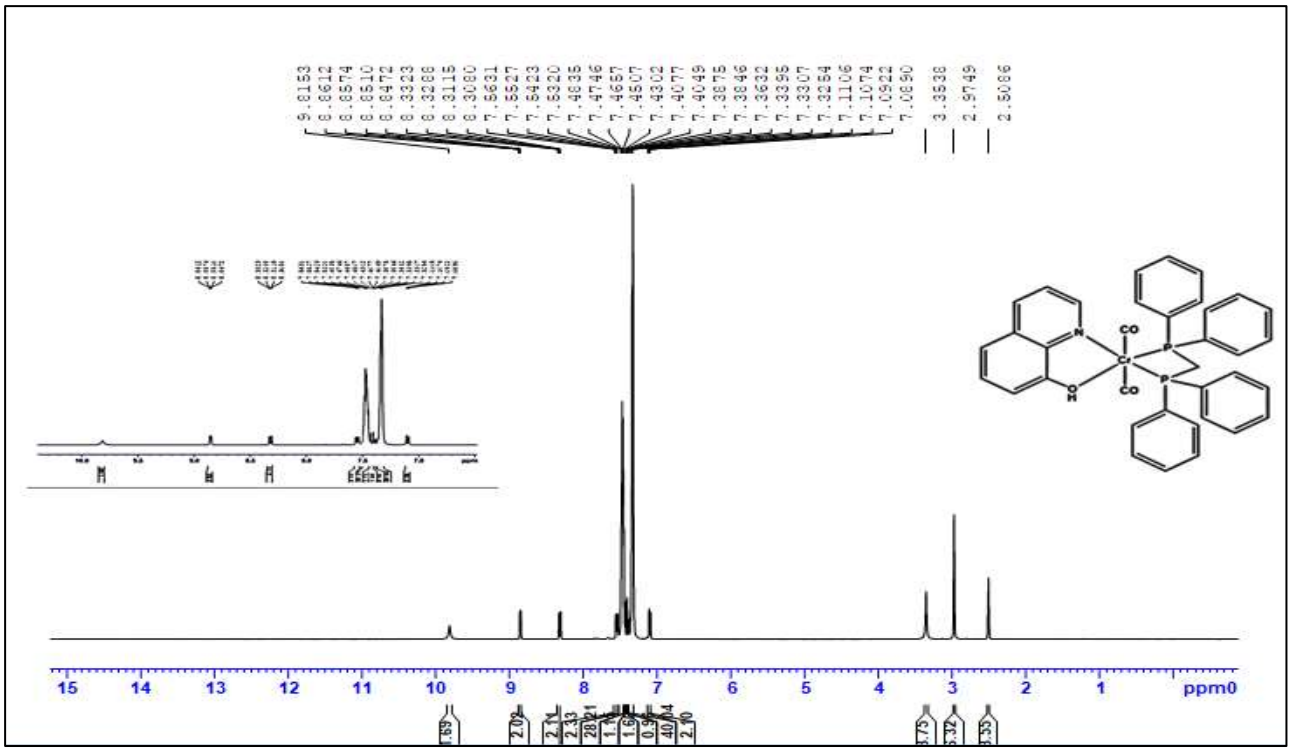
The ^{1}H NMR spectrum of **[Cr$(CO)_2$(dppm)(DPG)] (F4)** (Fig.27)in DMSO-d_6 confirms the coordination of both dppm and DPG ligands to the chromium center. The methyl protons of the phosphine groups appear as a singlet at δ 3.35 ppm (s, 2H, -CH_2-), while the aromatic protons of the DPPM phenyl rings resonate as multiplets at δ 6.86–6.89 ppm (m, 5H, Ph), reflecting their coordinated environment. Signals corresponding to the DPG ligand include the amino protons at δ 5.06 ppm (s, 2H, NH_2), the secondary amine proton at δ 8.12 ppm (s, 1H, NH), and aromatic protons at δ 7.48–7.46 ppm (t, 4H, Ph), δ 7.34–7.33 ppm (d, 4H, Ph), and δ 7.24–7.20 ppm (t, 4H, Ph), consistent with the ligand's aromatic pattern [98]. The observed chemical shifts and multiplicities unambiguously support the successful formation of the chromium(0) complex. [98]. (^{1}HNMR) spectrum of **[Cr$(CO)_2$(dppm)(8-HQ)] F5** (Fig. 28) is shown, revealing the proton peaks in the aromatic ring of the 8-hydroxyquinoline bond. Specifically, the spectrum shows peaks at δ(7.56 to 7.32 ppm, 8.48 ppm and 8.8 ppm) [101], which correspond to the protons in the aromatic ring for (8-HQ). At δ (s 9.8 ppm), a broad signal with an integral of one proton is observed, attributed to the proton of the OH group in 8-HQ. This signal may vanish during the D_2O exchange experiment, co and despite its low intensity (<10%), it indicates coordination of the phenol group to the chromium center in the F5 complex. nfirming it is due to an exchangeable proton. Fourtic protons of (dppm) are degradable and can be seen in the region δ (7.11, 7.10, 7.09, 7.08 aroma). The proton ring of tetraphenyl (Ph) groups (m, 5H, CHPh) and the

singlet peak arising from methylene (CH_2) at (δ = 3.34 ppm) are coordinated with the chromium center and (δ = 2.50 ppm) of the THF solvent due to the non-drying complexes [54, 84]. The ^{1}H NMR spectrum of the **[Cr(CO)$_2$(dppm)(2-aminopy)] (F6)** complex (Fig.29)was recorded in (DMSO-d$_6$, specify frequency). The aromatic region shows multiple signals in the range δ 7.32–7.48 ppm, corresponding to the phenyl protons of the dppm ligand together with the pyridyl protons of the coordinated 2-aminopyridine. The observed multiplicities (d, t) and the chemical shift distribution are consistent with the H3–H6 protons of the pyridine ring after coordination to the chromium center.

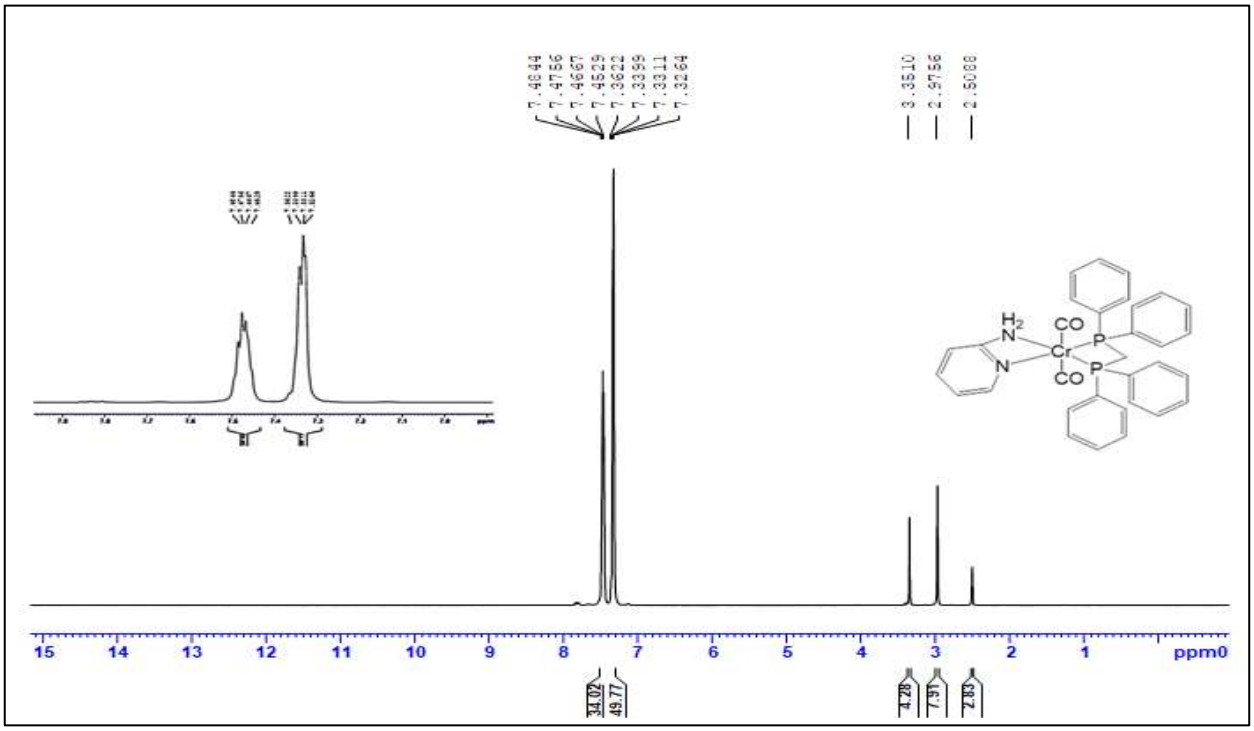
The methylene bridge of the dppm ligand (–CH_2–) appears at δ 2.98 ppm (≈ 2H), . A signal at δ 3.35 ppm (≈ 2H, broad) is assigned to the amino protons –NH_2,. The residual solvent peak of DMSO-d$_6$ appears at δ 2.50 ppm. Overall, the chemical shift changes and splitting patterns, when compared with the free ligands, support the successful coordination of both dppm and 2-aminopyridine to the chromium metal center.



(Fig .27) ^{1}HNMR spectrum of [Cr(CO)$_2$(dppm) (DPG)] (F 4)



(Fig.28) ^{1}HNMR spectrum of [Cr(CO)$_2$)(dppm) (8- HQ)] (F 5)



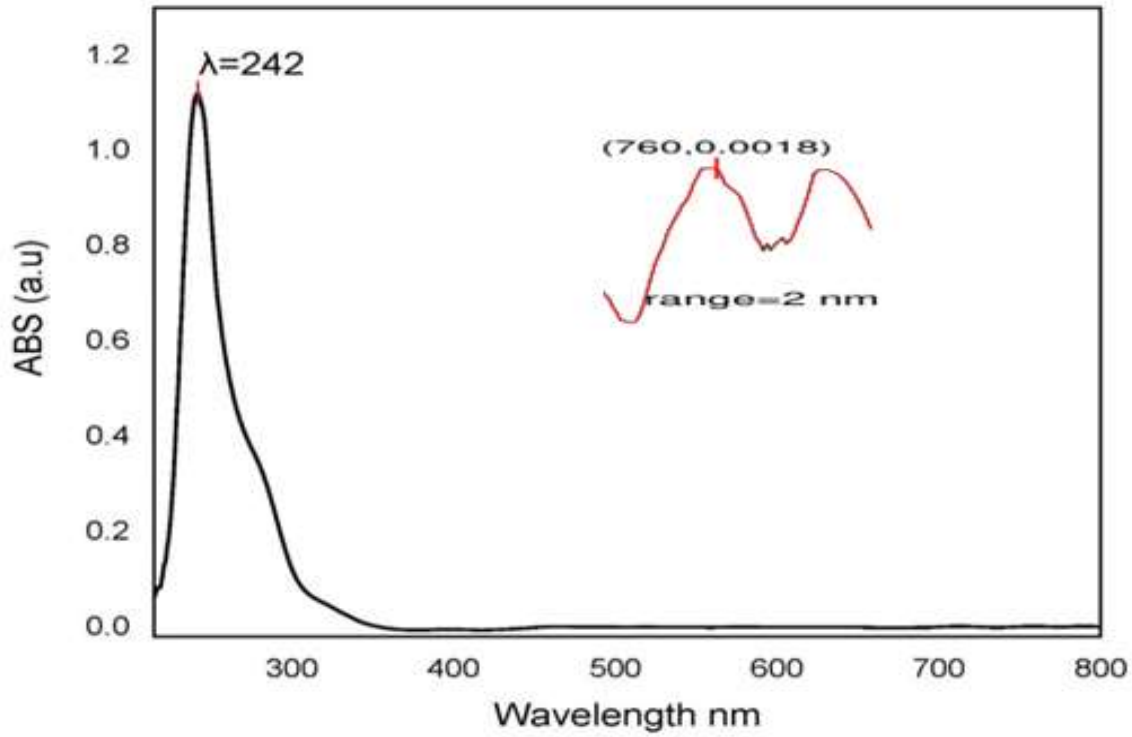
(Fig .29) H^{1} NMR spectrum of [Cr(CO)$_2$(dppm) (2-aminopy)] (F 6)

The electron absorption spectra of the molybdenum complexes in dimethyl sulfoxide (DMSO) showed distinct peaks in the wavelength range of 200-800 nm. The complexes [Cr(CO)$_2$(DPG)(dppm)], [Cr(CO)$_2$(8-HQ)(dppm)], and [Cr(CO)$_2$(2-

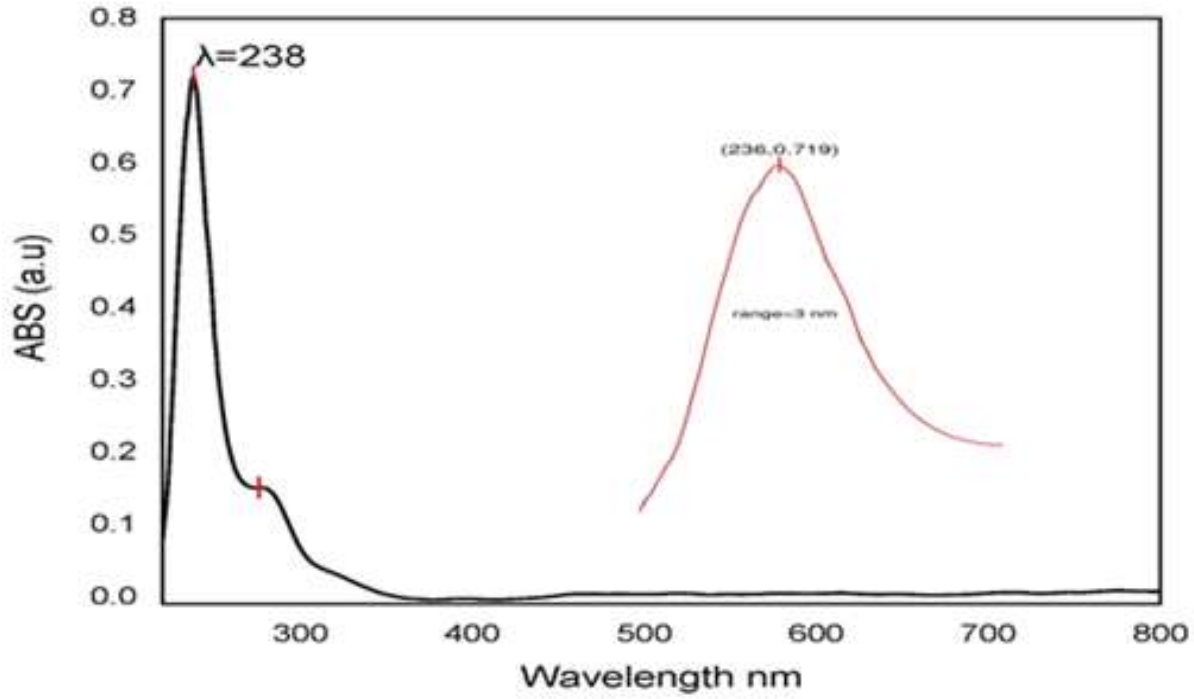
Aminoby(dppm)] (Figs.30.31.32) exhibited intrinsic π–π* bonding at approximately(242 nm, 238nm, and 242 nm), respectively, indicating the presence of aromatic rings in these complexes.Additionally, a strong absorption band was observed at (760 nm, 776 nm and 582nm) which is attributed to metal-to-ligand charge transfer (MLCT) transitions. The ligands, including CO, dppm, DPG, 8-HQ, and 2-aminopy, exhibited pronounced

d-d transitions, indicating a wide range of charge transfer transitions

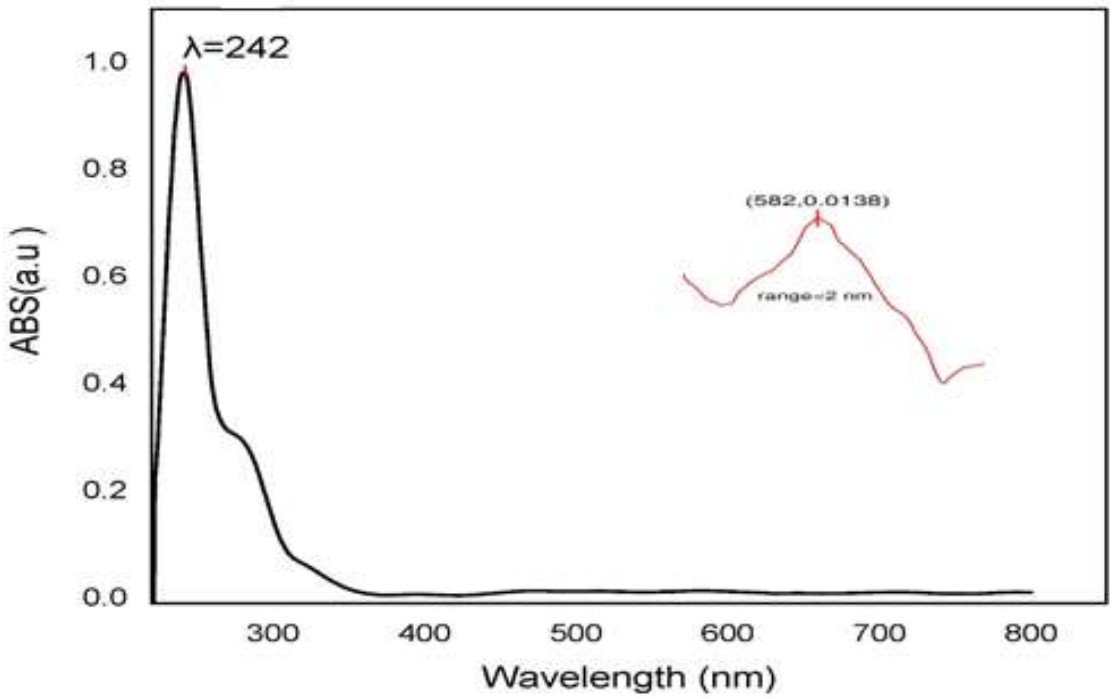
M → L of the M (d π) → L (p π*) type , which masked the intensity of the field transition. These findings highlight the complex nature of the electron absorption spectra of molybdenum complexes in DMSO.



(Fig.30) Electronic spectrum of [Cr $(Co)_2$ (dppm) (DPG)] (F 4)

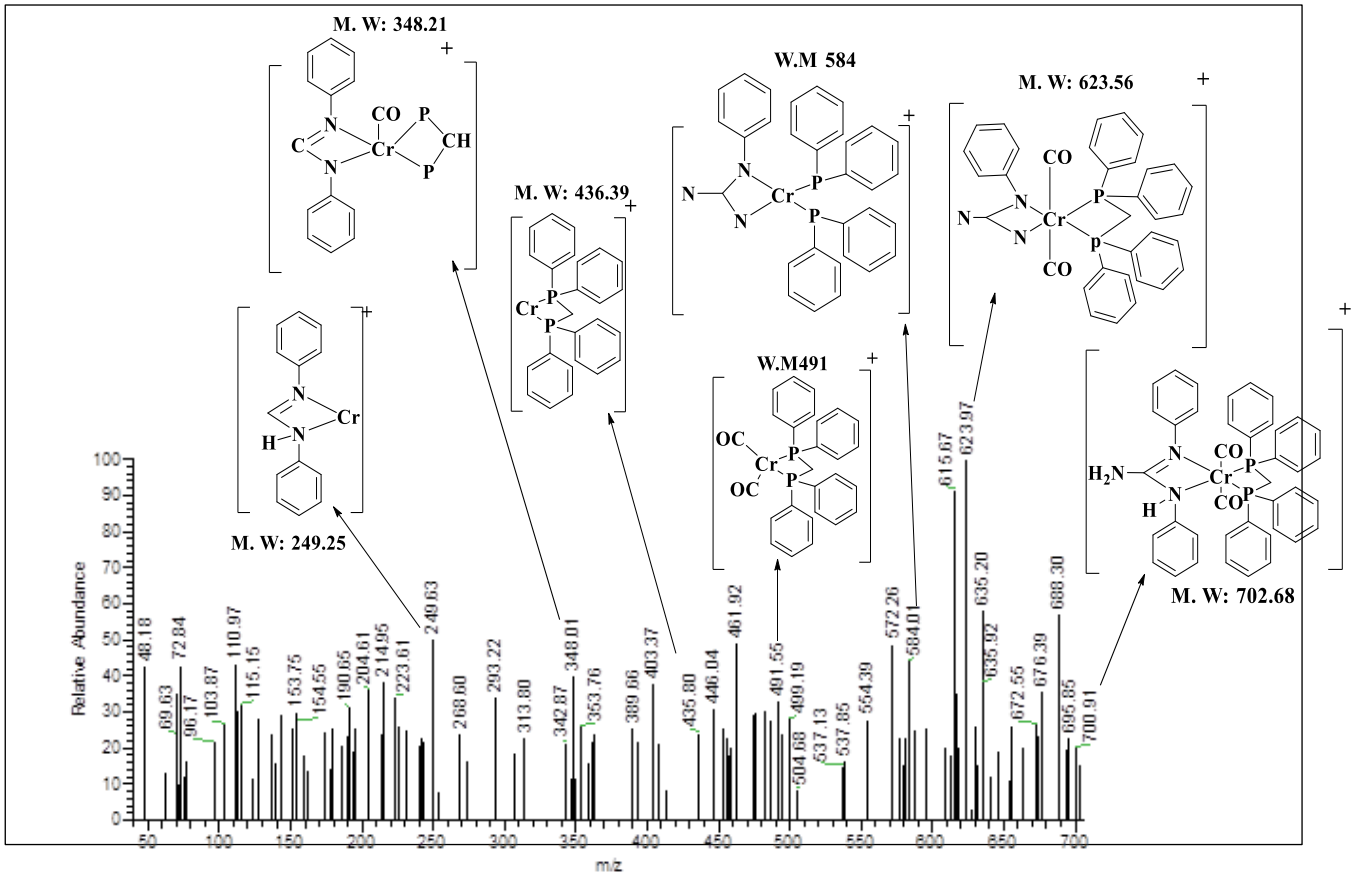


(Fig.31) Electronic spectrum of [Cr $(Co)_2$(dppm) (8-HQ)] ***(F 5)***



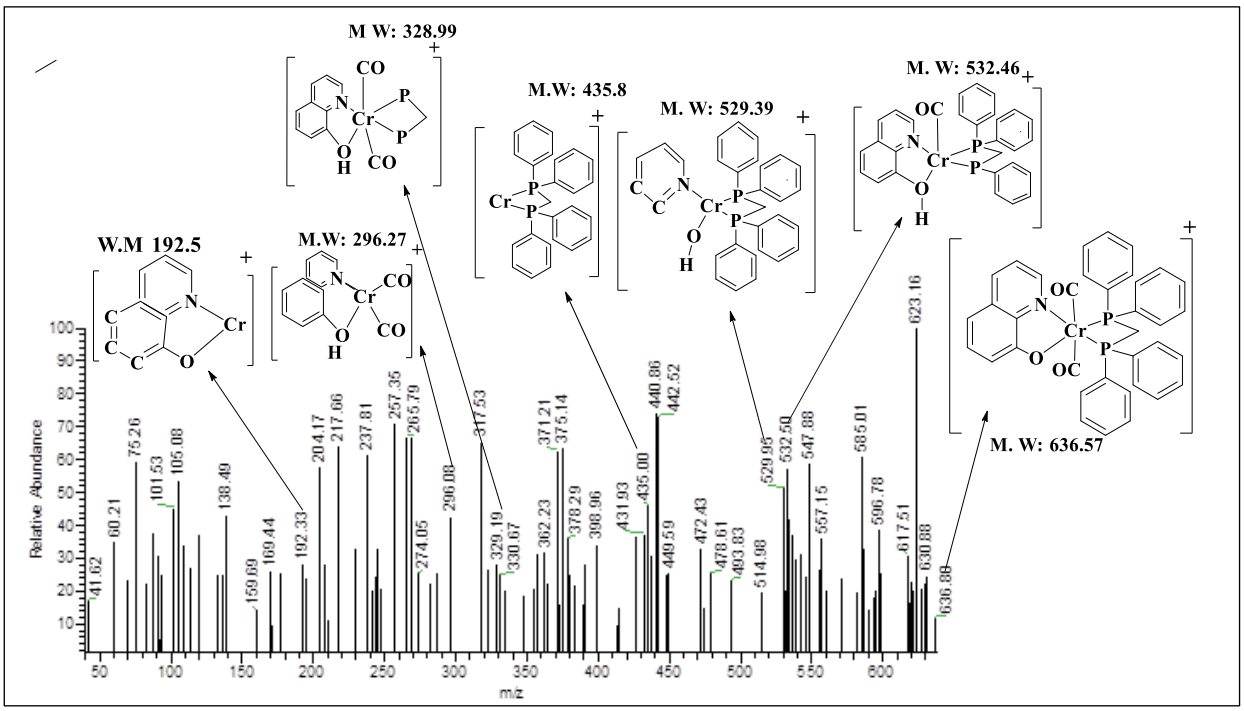
(Fig.32) Electronic spectrum of [Cr$(Co)_2$(dppm) (2-aminopy)] ***(F 6)***

The mass spectrum of the compound $[Cr(dppm)(dpg)(CO)_2]^+$ (Fig.33) shows the molecular ion, (700.91 m/z), as observed in the spectra of the ion at (623.97 m/z). The exit result of (C_6H_8) as well as the ions at (584 m/z) which is the result of the exit of $[(C_6H_8)(CO)_2]$. The m/z spectrum is also shown at (491m/z), indicating the exit of (DPG) as well as the spectral bands at (436 m/z)as a result of the exit $[(dpg)(CO)_2]$, an ion at(349 m / z) as a result of the exit of four phenyls,[2 (CO) (NH_4)], as well as a spectrum at (249) of the exit of [NH_2 $(DPPM)_2$ (CO)] with a number of fragments the other due to the cleavage of the main parent compound



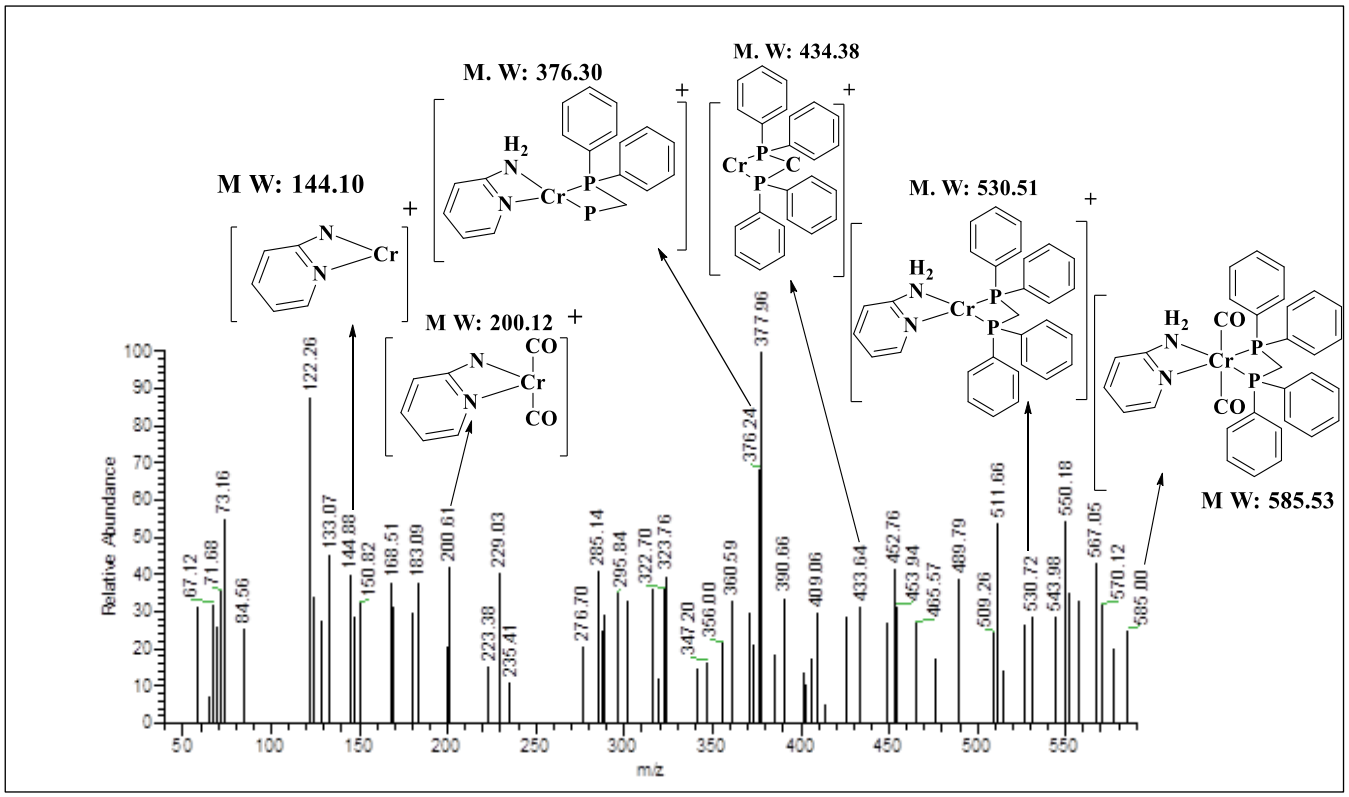
(Fig. 33) Mass spectrum for $[Cr(CO)_2$ (dppm)(DPG)] (F 4)

The mass spectrum of the compound $[Cr(dppm)(8\text{-}HQ)(CO)_2]^+$ (Fig.34) shows the molecular ion,(636.80 m/z), as observed in the spectra of the ion at (532.50 m/z). The exit result of (CO) as well as ions at(529.50 m/z) which is the result of the exit of $[(C_4H_3)(CO)_2]$. The m/z spectrum also appears at (435.8 m/z), which indicates the exit of [(8- HQ (CO)$_2$] , as well as the spectral bands at(328.19 m/z) due to the exit of four phenyl rings, the ion at (296.80 m/z) due to the exit of (dppm), as well as the spectrum at(192.33 m/z) of the exit of [(DPPM) $(CO)_2$ (H_4)] with A number of other parts due to the split of the main original are grouped together.



(Fig .34) Mass spectrum for [Cr(CO)$_2$ (dppm)(8 -HQ)] (F 5)

The mass spectrum of the compound $[Cr(dppm)(2\text{-aminopy})(CO)_2]^+$ (Fig.35) shows the molecular ion, (585.00m/z), as observed in the spectra of the ion at (530.51 m/z). The result of the exit of $(CO)_2$ and ions at (433.64 m/z) which is the result of the exit of [$(CO)_2$, H_2 , 2- aminopy]. The m/z spectrum also appears at (376.24 m/z), indicating the exit of the $(CO)_2$, two rings phenyl [$C_{12}H_{10}$] as well as spectral bands at (200 m/z) due to the exit of the (dppm), ion at (144.88 m/z). due to the exit of [(dppm) (H_2) $(CO)_2$] with a number of other parts due to the splitting of the principal asset are grouped together



(Fig.35) Mass spectrum for [Cr(CO)$_2$ (dppm)(2-aminopy)] (F 6)

Results and discussion.

3.3. Biological activity.

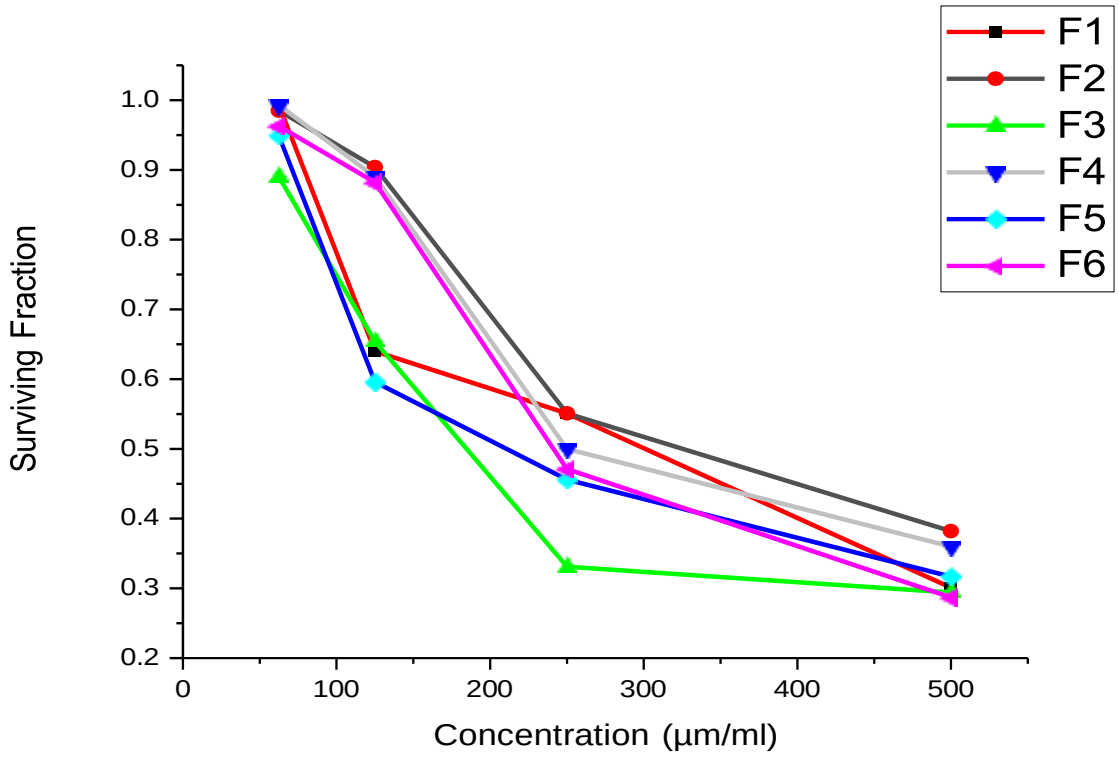
3.3.1 In vitro results

Cytotoxicity of Chromium-Molybdenum complexes with DPPM ligand on cancer cell line (HEPG-2):

We studied the relationship between structure and activity to impact a series of six inorganic complexes of chromium and molybdenum with DPPM in inhibiting the cancer cell line of liver cells. These complexes showed a clear effect in inhibiting the growth of cancer cells (HEPG-2) outside the living organism (in the laboratory). The anti-proliferative activities of the compounds were quantitatively evaluated by calculating their average growth-inhibitory concentrations (IC_{50} values). Low IC_{50} values correlated with increased cellular toxicity at low doses. It is worth noting that compounds F3 and F5 showed the most effective activities with IC_{50} values of 183 and 207 micrograms/ml, respectively, resulting in significantly less suppression of cancer cell growth at less than 200 micrograms/ml. In contrast, F1 and F2 had relatively weak effects, with IC_{50} exceeding 295 micrograms/ml. The results we have obtained provide promising early threads for further anti-cancer improvement with a focus on the importance of wise molecular modification to achieve a balance between efficacy and safety. The results shown in Table (9) and Figure (36) illustrate the effect of four different concentrations of chromium and molybdenum complexes (F1-F6) (62.5, 125, 250, 500 micrometers) on the remaining part of (HEPG-) 2) cell line after 48 hours of treatment**.**

Table (9). Effect of different concentration of Chromium-Molybdenum complexes with DPPM ligand on surviving fraction of (HEPG-2) cell line following 48 hours of treatment and IC_{50}.

Concentration µm/ml	Surviving fraction HEPG2					
	F1	F2	F3	F4	F5	F6
62.500	0.993	0.985	0.890	0.993	0.949	0.963
125.000	0.640	0.904	0.654	0.890	0.596	0.882
250.000	0.551	0.551	0.331	0.500	0.456	0.471
500.000	0.301	0.382	0.294	0.360	0.317	0.287
IC_{50}	295 µg/ml	324 µg/ml	180 µg/ml	249 µg/ml	207 µg/ml	240 µg/ml



(Fig.36.) Shows Surviving fraction and IC_{50} of HEPG-2 cells treated with Chromium-Molybdenum with DPPMligand for 48 hours.

3.4 Molecular docking studies

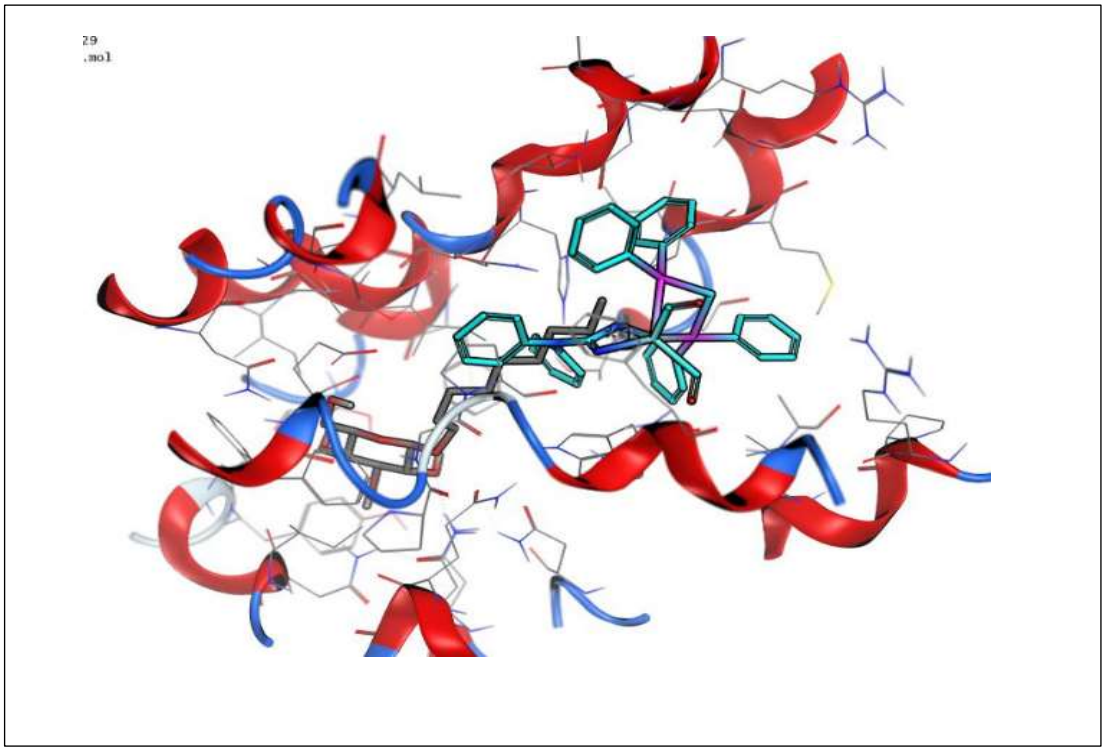
Molecular docking analysis was performed to identify the optimal binding modes and docked ligand binding energies of various chromium-molybdenum complexes with the Human liver cancer cell line type topo HEPG-2 protein. The study calculated binding parameters, including association strength based on minimum binding energy and scoring function, and employed an active site target binding approach to assess target protein specificity at a structural level. Atomic affinity potentials were used to evaluate the interaction energy between the complexes and the protein (PDB ID: 1ZXM). The lowest binding energies indicated successful docking of target proteins with the complexes.

The best binding mode of the docked ligands simulations of various ligands of Prepared complexes ([Mo(Co)2(DPG)(dppm)], [Mo(Co)2(8-HQ)(dppm)], [Mo(Co)2(2-aminopy)(dppm)], [Cr(Co)2(DPG)(dppm)], [Cr(Co)2(8-HQ)(dppm)], and [Cr(Co)2(2-aminopy)(dppm)]) (F1, F2, F3, F4, F5, and F6) with the Estrogen Receptor Alpha Ligand Binding Domain (PDB ID: 4PYP) is outlined in (Table 10 and Figures37 – 38) The molecular docking study identified various interaction types, including H-bonding,

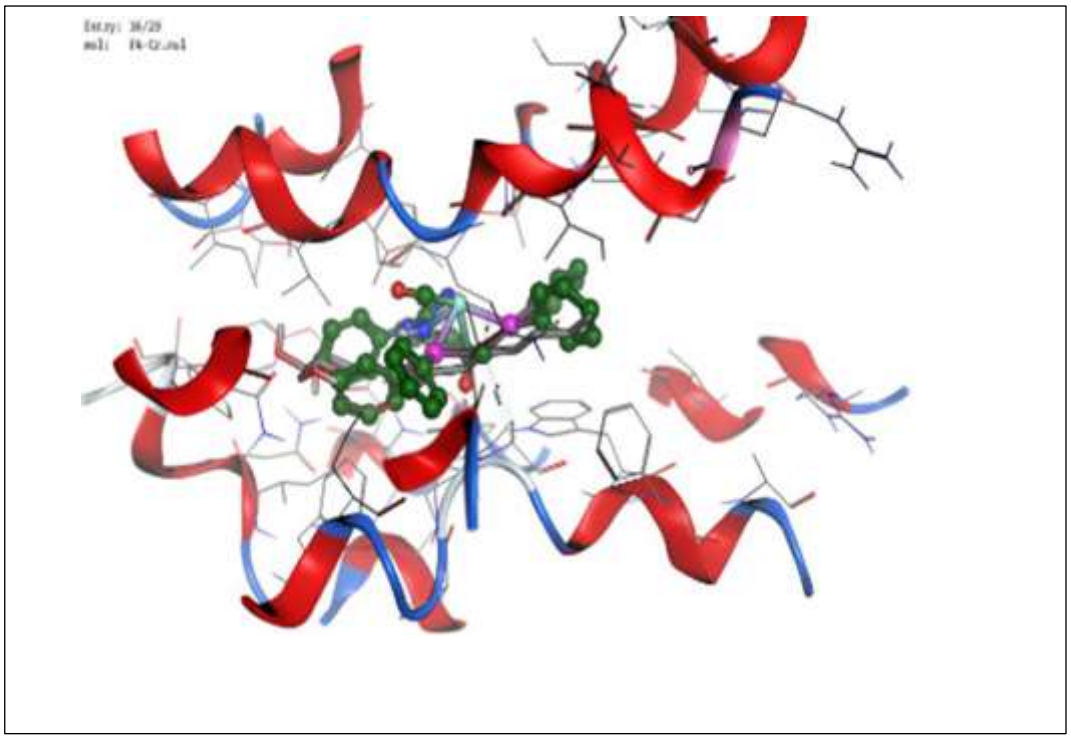
hydrophobic, and electrostatic interactions. Notably, F1, F4, and F6 exhibited deeper penetration into the active site of 4PYP, while F3 interacted with two amino acids. The binding energies of the molybdenum and chromium complexes were -8.8526, -8.5405, and -8.4329 kcal/mol for F6, F4, and F1, respectively. In contrast, F2, F3, and F5 had weaker interactions with 4PYP, with binding energies of -7.3878, -6.7793, and -7.1327 kcal/mol, respectively. The analysis indicated that F1, F4, and F6 exhibited stronger binding than F2, F3, and F5 with the Receptor Alpha Ligand Binding Domain 4PYP, with a negligible difference in binding free energy of 0.00 kcal/mol.

Table 10. Energy values were obtained during docking analysis of compounds as ligand molecules against 4PYP as target molecules.

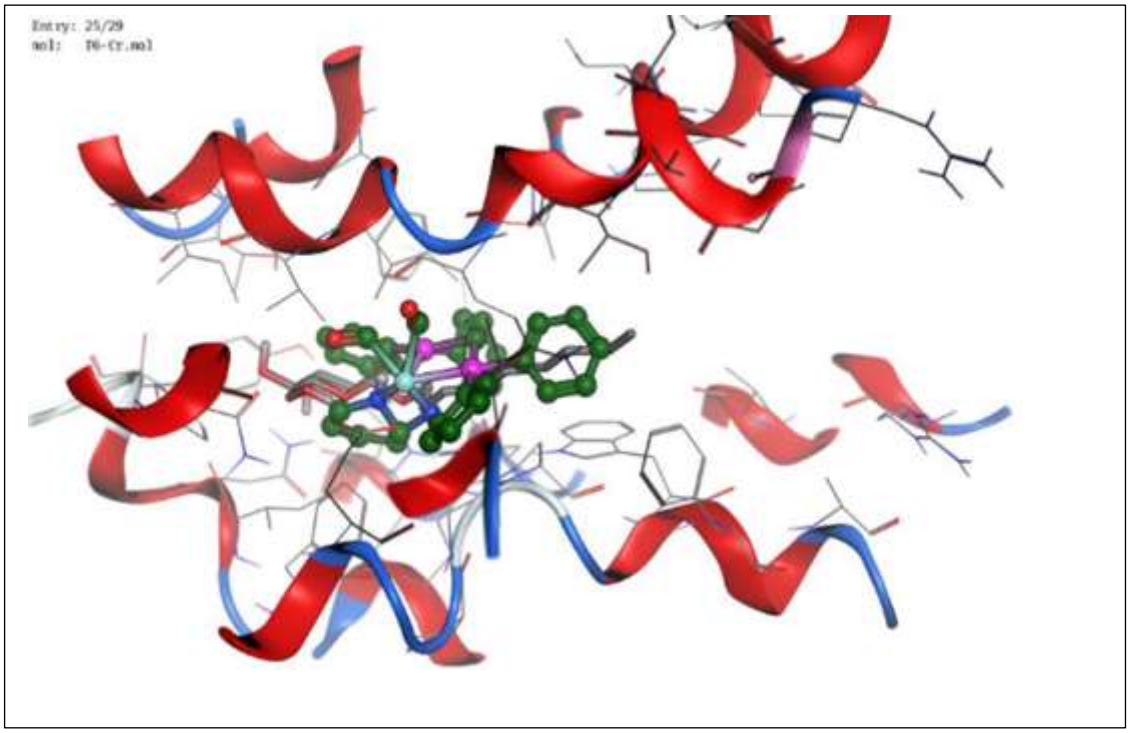
Compound	Comp. 1	Comp. 2	Comp. 3	Comp. 4	Comp. 5	Comp. 6
Rseq	1	1	1	1	1	1
Mseq		2	3	4	5	6
S	- 8.4329	-7.3878	- 6.7793	- 8.5405	-7.1327	- 8.8526
rmsd-refine	3.2615	1.8958	1.9370	1.7960	2.4502	2.2537
E-conf	115.5827	42.7945	7.7899	167.8200	101.9784	46.2388
E-place	- 41.0825	-58.4418	- 65.3690	-78.4093	- 24.9463	- 52.7490
E-refine	- 46.1967	-36.1778	-31.7549	- 27.1006	-18.9927	- 43.3298
E-score 2	- 8.4329	- 7.3878	- 6.7793	- 8.5405	-7.1327	- 8.8526



F 1

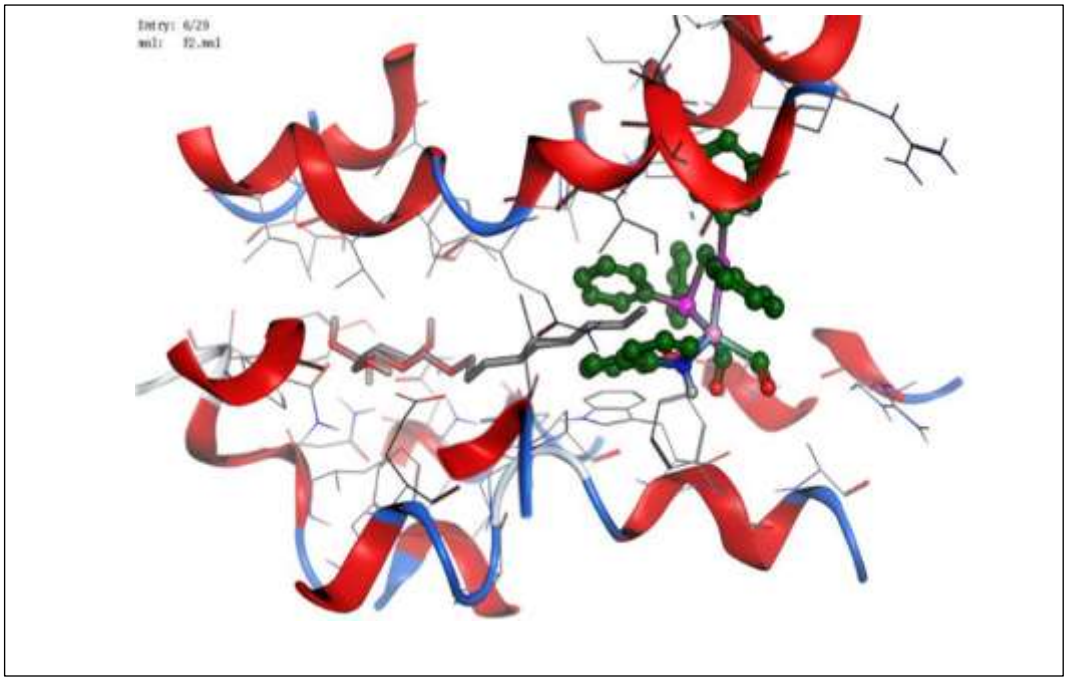


F 4

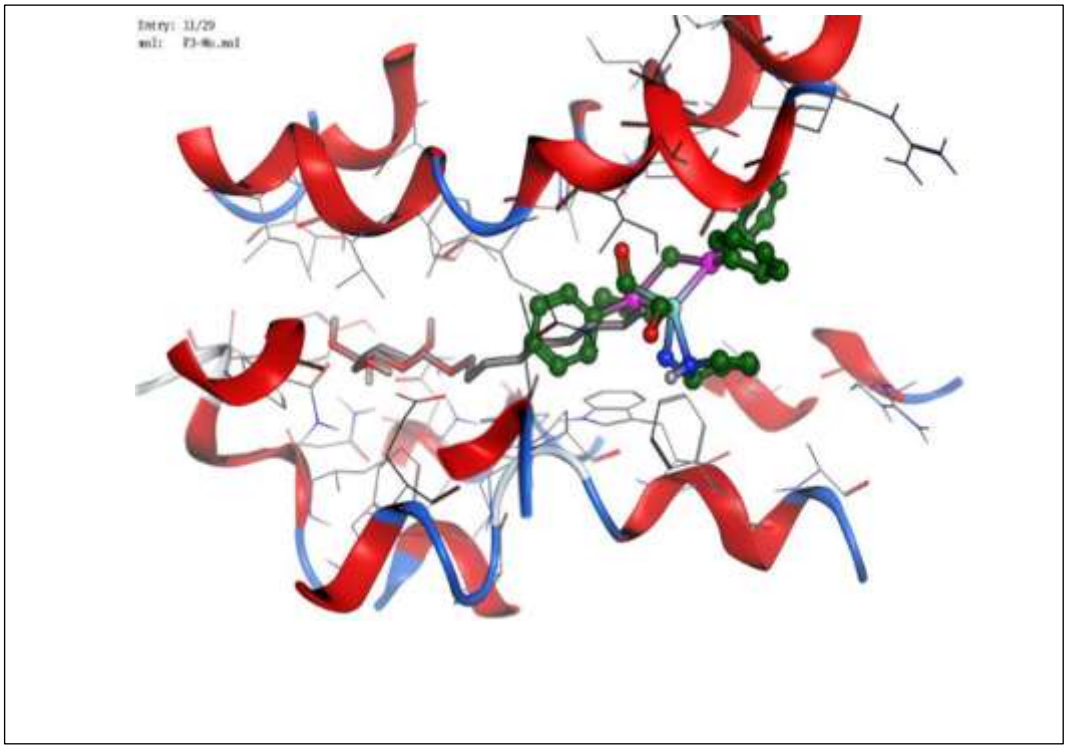


F 6

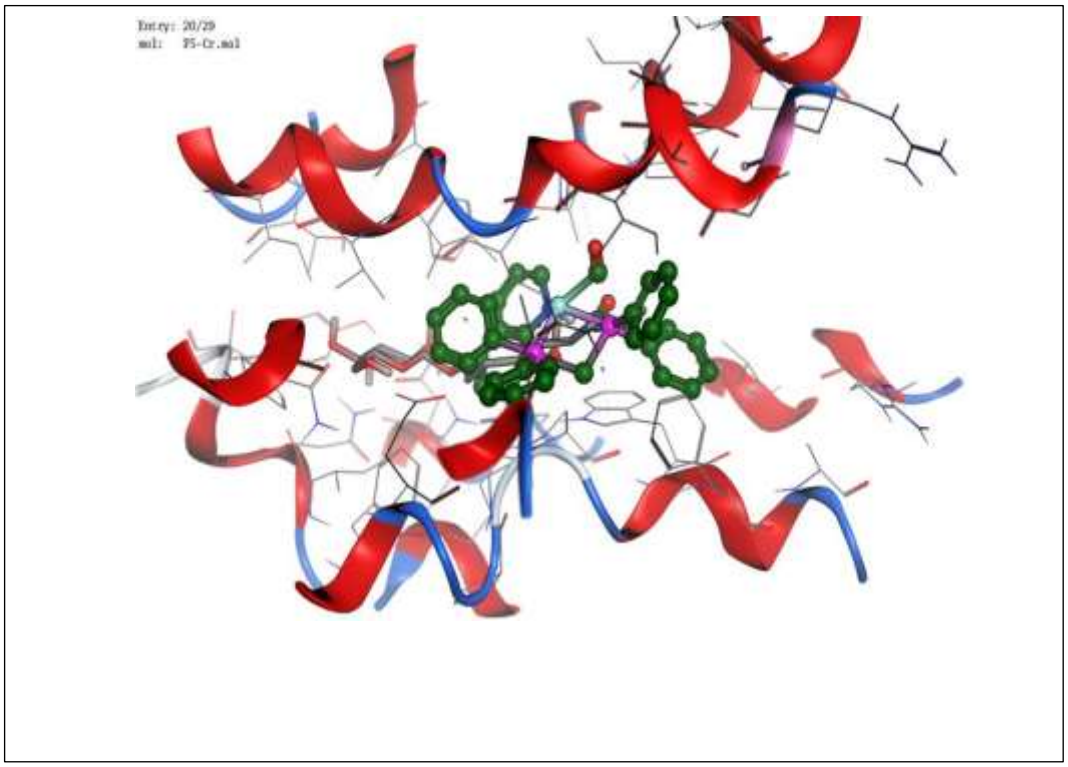
(Fig.37). Docking Interaction of amino acid residues of PDB Id: 4PYP (Green color) with F1, F4 and F6 (Brown color)



F 2



F 3



F 5

(Fig.38). Docking Interaction of amino acid residues of PDB Id: 4PYP (Green color) with F2, F3 and F5 (Brown color)

3.5 Conclusions

This study successfully synthesizes a series of molybdenum(0) carbonyl and chromium(0) carbonyl complexes featuring dimeric ligands (dppm, DPG, 8-HQ, 2-aminoPy) via an eco-friendly microwave-assisted method. Characterization by FTIR, NMR, 1H NMR, and elemental analysis (CHN) confirms their composition, suggesting an octahedral geometry with six coordination sites for both chromium and molybdenum, comprised of two C(CO) and two P(dppm), N,N' (DPG), N,O (8-HQ), or N,N' (2-aminoPy) interactions. FT-IR data indicate a cis arrangement of carbonyl groups in all chromium-molybdenum complexes.

Cytotoxicity tests against liver cancer cells (HEPG-2) show that the synthesized complexes exhibit varied levels of inhibition at different concentrations, with IC_{50} values ranging from 180 to 324 µg/ml. Complex F3 is the most potent, inhibiting hepatic carcinoma cells(HEPG-2) with an(IC_{50} of 180 µg/ml).

Molecular docking studies were also carried out by analyzing the appropriate binding modes for the Cr-Mo complexes Ligands(F1-F6) with estrogen receptor binding domain Alpha Ligand (PDB ID: 4PYP). (F1, F4, and F6) bind strongly to the active site with energy of (-8.4329, -8.5405, and -8.8526 kcal/mol), respectively. In contrast, F2, F3, and F5 are weakly bound with energies of (-7.3878, -6.7793, and -7.1327 kcal/mol), respectively. The analysis indicates that (F1, F4, and F6) are more strongly associated with(4PYP) than (F2, F3, and F5).

References

[1] R. H. Crabtree, *The organometallic chemistry of the transition metals*: John Wiley & Sons, 2009.

[2] U. Dolfus, H. Briem, and M. Rarey, "Visualizing Generic Reaction Patterns," *Journal of Chemical Information and Modeling*, vol. 62, pp. 4680-4689, 2022.

[3] M. N. Rao, R. Manne, J. M. Tanski, R. Butcher, and P. Ghosh, "One pot synthesis of propargylamines by three component amine-aldehyde-acetylene (A3) coupling catalyzed by neutral Ag (I) and Au (I) and cationic Pd (II) and Ni (II) complexes of a pincer N-heterocyclic carbene," *Molecular Catalysis*, vol. 529, p. 112515, 2022.

[4] G. Jaouen and A. Vessières, "Transition metal carbonyl oestrogen receptor assay," *Pure and applied chemistry*, vol. 57, pp. 1865-1874, 1985.

[5] S. Top, G. Jaouen, A. Vessieres, J. P. Abjean, D. Davoust, C. A. Rodger, *et al.*, "Chromium tricarbonyl complexes of estradiol derivatives: differentiation of. alpha.-and. beta.-diastereoisomers using 1-and 2-dimensional NMR spectroscopy at 500 MHz," *Organometallics*, vol. 4, pp. 2143-2150, 1985.

[6] H. Pfeiffer, "Synthesis and biological activity of molybdenum carbonyl complexes and their peptide conjugates," Universität Würzburg, 2012.

[7] E. S. Antonarakis and A. Emadi, "Ruthenium-based chemotherapeutics: are they ready for prime time?," *Cancer chemotherapy and pharmacology*, vol. 66, pp. 1-9, 2010.

[8] S. J. Dougan, A. Habtemariam, S. E. McHale, S. Parsons, and P. J. Sadler, "Catalytic organometallic anticancer complexes," *Proceedings of the National Academy of Sciences*, vol. 105, pp. 11628-11633, 2008.

[9] M. J. Abrams, A. Davison, A. G. Jones, C. E. Costello, and H. Pang, "Synthesis and characterization of hexakis (alkyl isocyanide) and hexakis (aryl isocyanide) complexes of technetium (I)," *Inorganic Chemistry*, vol. 22, pp. 2798-2800, 1983.

[10] G. Jaouen, S. Top, A. Vessières, and R. Alberto, "New paradigms for synthetic pathways inspired by bioorganometallic chemistry," *Journal of Organometallic Chemistry*, vol. 600, pp. 23-36, 2000.

[11] J. E. Clark, P. Naughton, S. Shurey, C. J. Green, T. R. Johnson, B. E. Mann, *et al.*, "Cardioprotective actions by a water-soluble carbon monoxide–releasing molecule," *Circulation research*, vol. 93, pp. e2-e8, 2003.

[12] J. Burgaud, J. Riffaud, and P. Soldato, "Nitric-oxide releasing molecules: a new class of drugs with several major indications," *Current pharmaceutical design*, vol. 8, pp. 201-213, 2002.

[13] C. E. Anson, T. J. Baldwin, C. S. Creaser, M. A. Fey, and G. R. Stephenson, "IR-active organometallic pH probes," *Organometallics*, vol. 15, pp. 1451-1456, 1996.

[14] C. S. Creaser, W. E. Hutchinson, and G. R. Stephenson, "An attenuated total reflectance optrode sensor incorporating infrared-active carbonylmetal probe groups," *Sensors and Actuators B: Chemical*, vol. 82, pp. 150-157, 2002.

[15] M. Cais, S. Dani, Y. Eden, O. Gandolfi, M. Horn, E. Isaacs, *et al.*, "Metalloimmunoassay," *Nature*, vol. 270, pp. 534-535, 1977.

[16] H. Kimura, "Hydrogen sulfide as a neuromodulator," *Molecular neurobiology*, vol. 26, pp. 13-19, 2002.

[17] R. S. Yalow and S. A. Berson, "Assay of plasma insulin in human subjects by immunological methods," *Nature*, vol. 184, pp. 1648-1649, 1959.

[18] E. Palek and M. Fojta, "Peer reviewed: detecting DNA hybridization and damage," ed: ACS Publications, 2001.

[19] T. G. Drummond, M. G. Hill, and J. K. Barton, "Electrochemical DNA sensors," *Nature biotechnology*, vol. 21, pp. 1192-1199, 2003.

[20] E. J. Lyon, S. Shima, G. Buurman, S. Chowdhuri, A. Batschauer, K. Steinbach, *et al.*, "UV-A/blue-light inactivation of the 'metal-free'hydrogenase (Hmd) from methanogenic archaea: The enzyme contains functional iron after all," *European Journal of Biochemistry*, vol. 271, pp. 195-204, 2004.

[21] S. C. Lee and R. Holm, "The clusters of nitrogenase: Synthetic methodology in the construction of weak-field clusters," *Chemical reviews*, vol. 104, pp. 1135-1158, 2004.

[22] D. J. Cram, "The design of molecular hosts, guests, and their complexes," *Science*, vol. 240, pp. 760-767, 1988.

[23] S. Komiya and A. Fukuoka, "11 Group 9 (Co, Rh, Ir) Metal Compounds," *Synthesis of Organometallic Compounds: A Practical Guide*, vol. 15, p. 219, 1997.

[24] Y. Tao, F. Ma, M. Teng, Z. Jia, and Z. Zeng, "Designed fabrication of super high hardness Ni-B-Sc nanocomposite coating for anti-wear application," *Applied Surface Science*, vol. 492, pp. 426-434, 2019.

[25] S. J. Bonyhady, D. E. DeRosha, J. Vela, D. J. Vinyard, R. E. Cowley, B. Q. Mercado, *et al.*, "Iron and Cobalt Diazoalkane Complexes Supported by β-Diketiminate Ligands: A Synthetic, Spectroscopic, and Computational Investigation," *Inorganic Chemistry*, vol. 57, pp. 5959-5972, 2018.

[26] F. Ozawa, "12 Group 10 (Ni, Pd, Pt) Metal Compounds," *Synthesis of Organometallic Compounds: A Practical Guide*, vol. 15, p. 249, 1997.

[27] G. Hogarth, S. E. Kabir, and E. Nordlander, "Cluster chemistry in the Noughties: new developments and their relationship to nanoparticles," *Dalton Transactions*, vol. 39, pp. 6153-6174, 2010.

[28] C. E. Ellul, J. P. Lowe, M. F. Mahon, P. R. Raithby, and M. K. Whittlesey, "[Ru 3 (6-NHC)(CO) 10]: synthesis, characterisation and reactivity of rare 46-electron tri-ruthenium clusters," *Dalton Transactions*, vol. 47, pp. 4518-4523, 2018.

[29] R. G. Smart, F. B. Glaser, Y. Israel, H. Kalant, R. E. Popham, W. Schmidt, *et al.*, *The pharmacology of hallucinogens*: Springer, 1983.

[30] P. G. Corrie, "Cytotoxic chemotherapy: clinical aspects," *Medicine*, vol. 36, pp. 24-28, 2008.

[31] Y. Jung and S. J. Lippard, "Direct cellular responses to platinum-induced DNA damage," *Chemical reviews*, vol. 107, pp. 1387-1407, 2007.

[32] E. Ogunniyi and H. Pienaar, "Overview of battery energy storage system advancement for renewable (photovoltaic) energy applications," in *2017 International Conference on the Domestic Use of Energy (DUE)*, 2017, pp. 233-239.

[33] M. R. N. Matos, C. C. Romao, C. C. L. Pereira, S. S. Rodrigues, M. Mora, M. J. P. Silva, *et al.*, "Compositions comprising organometallic molybdenum compounds for treating cancer," ed: Google Patents, 2008.

[34] F. TOMONOBU, S. TOSHIHARU, Y. TOSHIHIRO, and S. YOSHIKO, "Antitumor Activity of New Antitumor Substance, Polyoxomolybdate, against Several human Cancers in Athymic Nude Mice," *The Tohoku Journal of Experimental Medicine*, vol. 168, pp. 421-426, 1992.

[35] I. Berasaluce, K. Cseh, A. Roller, M. Hejl, P. Heffeter, W. Berger, *et al.*, "The First Anticancer Tris (pyrazolyl) borate Molybdenum (IV) Complexes: Tested in Vitro and in Vivo—A Comparison of O, O-, S, O-, and N, N-Chelate Effects," *Chemistry–A European Journal*, vol. 26, pp. 2211-2221, 2020.

[36] H. FUJITA, T. FUJITA, T. SAKURAI, T. YAMASE, and Y. SETO, "Antitumor activity of new antitumor substance, polyoxomolybdate, against several human cancers in athymic nude mice," *The Tohoku Journal of Experimental Medicine*, vol. 168, pp. 421-426, 1992.

[37] F. Garzon, M. Berger, and D. Schmähl, "Paradoxical effect of dichlorobis (1-phenylbutane-1, 3-dionato) molybdenum (IV),(Mo (bzac) 2Cl2 on the growth of autochthonous chemically induced colorectal tumors in SD rats," *Cancer letters*, vol. 34, pp. 325-330, 1987.

[38] A. M. Abu-Dief and I. M. Mohamed, "A review on versatile applications of transition metal complexes incorporating Schiff bases," *Beni-suef university journal of basic and applied sciences*, vol. 4, pp. 119-133, 2015.

[39] M. Baile, N. Kolhe, P. Deotarse, A. Jain, and A. Kulkarni, "Metal ion complex-potential anticancer drug-a review," *IJPRR*, vol. 4, pp. 59-66, 2015.

[40] A. T. Odularu, P. A. Ajibade, and J. Z. Mbese, "Impact of molybdenum compounds as anticancer agents," *Bioinorganic chemistry and applications*, vol. 2019, 2019.

[41] M. Nair and D. Thankaman, "Synthesis and characterisation of oxomolybdenum (V) and dioxomolybdenum (VI) complexes with Schiff base derived from isonicotinoylhydrazide," 2009.

[42] P. Martins, M. Marques, L. Coito, A. JL Pombeiro, P. Viana Baptista, and A. R Fernandes, "Organometallic compounds in cancer therapy: Past lessons and future directions," *Anti-Cancer Agents in Medicinal Chemistry (Formerly Current Medicinal Chemistry-Anti-Cancer Agents)*, vol. 14, pp. 1199-1212, 2014.

[43] J. B. Waern, C. T. Dillon, and M. M. Harding, "Organometallic anticancer agents: cellular uptake and cytotoxicity studies on thiol derivatives of the antitumor agent molybdocene dichloride," *Journal of medicinal chemistry*, vol. 48, pp. 2093-2099, 2005.

[44] J. M. Mir and R. C. Maurya, "Nitric oxide functionalized molybdenum (0) pyrazolone Schiff base complexes: thermal and biochemical study," *RSC advances*, vol. 8, pp. 35102-35130, 2018.

[45] L. K. E. Samuel and A. K. Y. Daniel, "Chalcone-ligated molybdenum carbonyl complexes: Synthesis and evaluation as quadruplex DNA binders."

[46] M. S. Al-Fakeh, M. A. Alsikhan, and J. S. Alnawmasi, "Physico-Chemical Study of Mn (II), Co (II), Cu (II), Cr (III), and Pd (II) Complexes with Schiff-Base and Aminopyrimidyl Derivatives and Anti-Cancer, Antioxidant, Antimicrobial Applications," *Molecules,* vol. 28, p. 2555, 2023.

[47] M. More, P. Joshi, Y. Mishra, and P. Khanna, "Metal complexes driven from Schiff bases and semicarbazones for biomedical and allied applications: a review," *Materials Today Chemistry,* vol. 14, p. 100195, 2019.

[48] G. Kumar, S. Devi, R. Johari, and D. Kumar, "Synthesis, spectral characterization and antimicrobial evaluation of Schiff base Cr (III), Mn (III) and Fe (III) macrocyclic complexes," *European journal of medicinal chemistry,* vol. 52, pp. 269-274, 2012.

[49] V. V. Kumar, M. P. Kumar, K. Thiruvenkadaravi, P. Baskaralingam, P. S. Kumar, and S. Sivanesan, "Preparation and characterization of porous cross linked laccase aggregates for the decolorization of triphenyl methane and reactive dyes," *Bioresource technology,* vol. 119, pp. 28-34, 2012.

[50] W. Hewertson and H. Watson, "283. The preparation of di-and tri-tertiary phosphines," *Journal of the Chemical Society (Resumed),* pp. 1490-1494, 1962.

[51] A. C. Albéniz and P. Espinet, "Palladium: Inorganic & Coordination Chemistry," *Encyclopedia of Inorganic Chemistry,* 2006.

[52] Q. Xu and O. Kwon, "1, 2-Bis (diphenylphosphino) methane," *Encyclopedia of Reagents for Organic Synthesis,* 2001.

[53] C. J. Commons and B. F. Hoskins, "A novel carbonyl bridging mode: the structure of the metal carbonyl complex [Mn2 (CO) 5 (Ph2PCH2PPh2) 2]," *Australian Journal of Chemistry,* vol. 28, pp. 1663-1672, 1975.

[54] D. M. Ho and R. Bau, "Preparation and structural characterization of [Ag2 (dpm) 2 (NO3) 2] and [Ag4 (dpm) 4 (NO3) 2] 2+[PF6] 2-: conformational flexibility in the M2P4 core structure of bis (diphenylphosphino) methane complexes," *Inorganic Chemistry,* vol. 22, pp. 4073-4079, 1983.

[55] M. P. Brown and M. RASHIDI, "SOME BINUCLEAR BIS (DIPHENYLPHOSPHINO) METHANE COMPLEXES OF PLATINUM WITH BRIDGING AND TERMINAL HYDRIDO GROUPS," 1977.

[56] L. S. Benner and A. L. Balch, "Novel reactions of metal-metal bonds. Insertion of isocyanides and carbon monoxide into the palladium-palladium bond of some

palladium (I) dimers," *Journal of the American Chemical Society,* vol. 100, pp. 6099-6106, 1978.

[57] M. Brown, "Puddephatt. RJ, Rashidi, M. and Seddon, KR," *Inorg. Chim. Acta,* vol. 23, p. L27, 1977.

[58] M. P. Brown, S. J. Cooper, A. A. Frew, L. Manojlovic-Muir, K. W. Muir, R. J. Puddephatt, *et al.*, "Synthesis, structure, and bonding in the complex cation [Pt2Me3 (. mu.-Ph2PCH2PPh2) 2]+: an example of a donor-acceptor metal-metal bond," *Inorganic Chemistry,* vol. 20, pp. 1500-1507, 1981.

[59] S. Tian, F.-M. Siu, S. C. Kui, C.-N. Lok, and C.-M. Che, "Anticancer gold (I)–phosphine complexes as potent autophagy-inducing agents," *Chemical Communications,* vol. 47, pp. 9318-9320, 2011.

[60] M. Odachowski, C. Marschner, and B. Blom, "A review on 1, 1-bis (diphenylphosphino) methane bridged homo-and heterobimetallic complexes for anticancer applications: Synthesis, structure, and cytotoxicity," *European Journal of Medicinal Chemistry,* vol. 204, p. 112613, 2020.

[61] M.-C. Brandys, M. C. Jennings, and R. J. Puddephatt, "Luminescent gold (I) macrocycles with diphosphine and 4, 4′-bipyridyl ligands," *Journal of the Chemical Society, Dalton Transactions,* pp. 4601-4606, 2000.

[62] S. Abrahamyan, Z. Ahmed, K. Allada, D. Anez, T. Averett, A. Barbieri, *et al.*, "Search for a new gauge boson in electron-nucleus fixed-target scattering by the APEX experiment," *Physical Review Letters,* vol. 107, p. 191804, 2011.

[63] M. J. McKeage, L. Maharaj, and S. J. Berners-Price, "Mechanisms of cytotoxicity and antitumor activity of gold (I) phosphine complexes: the possible role of mitochondria," *Coordination Chemistry Reviews,* vol. 232, pp. 127-135, 2002.

[64] P. C. Bruijnincx and P. J. Sadler, "Controlling platinum, ruthenium, and osmium reactivity for anticancer drug design," *Advances in inorganic chemistry,* vol. 61, pp. 1-62, 2009.

[65] W. Liu and R. Gust, "Metal N-heterocyclic carbene complexes as potential antitumor metallodrugs," *Chemical Society Reviews,* vol. 42, pp. 755-773, 2013.

[66] G. B. Kauffman, "The role of gold in alchemy. Part I," *Gold bulletin,* vol. 18, pp. 31-44, 1985.

[67] R. Koch, "Die aetiologie der tuberkulose," 2010.

[68] S. Chatterjee, S. Kundu, A. Bhattacharyya, C. G. Hartinger, and P. J. Dyson, "The ruthenium (II)–arene compound RAPTA-C induces apoptosis in EAC cells through mitochondrial and p53–JNK pathways," *JBIC Journal of Biological Inorganic Chemistry*, vol. 13, pp. 1149-1155, 2008.

[69] S. Shimizu, N. Watanabe, T. Kataoka, T. Shoji, N. Abe, S. Morishita, *et al.*, "Pyridine and pyridine derivatives," *Ullmann's Encyclopedia of Industrial Chemistry*, 2000.

[70] V. Jassal, U. Shanker, and S. Gahlot, "Green synthesis of some iron oxide nanoparticles and their interaction with 2-amino, 3-amino and 4-aminopyridines," *Materials Today: Proceedings*, vol. 3, pp. 1874-1882, 2016.

[71] C. M. Standfest-Hauser, G. Dazinger, J. Wiedermann, K. Mereiter, and K. Kirchner, "Molybdenum Carbonyl Complexes Bearing PN Ligands Based on 2-Aminopyridine," ed: Wiley Online Library, 2009.

[72] A. C. B. Yuoh, M. O. Agwara, D. M. Yufanyi, M. A. Conde, R. Jagan, and K. Oben Eyong, "Synthesis, crystal structure, and antimicrobial properties of a novel 1-D cobalt coordination polymer with dicyanamide and 2-aminopyridine," *International Journal of Inorganic Chemistry*, vol. 2015, 2015.

[73] R. Kempe, "The Strained η2-NAmido− NPyridine Coordination of Aminopyridinato Ligands," *European Journal of Inorganic Chemistry*, vol. 2003, pp. 791-803, 2003.

[74] A. Noor, "Coordination chemistry of bulky aminopryridinates with main group and transition metals," *Topics in Current Chemistry*, vol. 379, pp. 1-30, 2021.

[75] N. M. Scott, T. Schareina, O. Tok, and R. Kempe, "Lithium and potassium amides of sterically demanding aminopyridines," *European Journal of Inorganic Chemistry*, vol. 2004, pp. 3297-3304, 2004.

[76] A. Noor, "Crystallographic Evidence of η 1-Coordination of Bulky Aminopyridine in Halide-Containing Iron (II) Complexes," *Crystals*, vol. 12, p. 697, 2022.

[77] A. Munadhiroh, H. W. Wijaya, N. Farida, S. Golhen, and I. Wayan, "Synthesis, Characterization, and Preliminary Study of [Co (2-aminopyridine) 2 (NCS) 2] or bis (2-aminopyridine) dithiocyanato cobalt (II) as An Antibacterial," *Jurnal Kimia Valensi*, vol. 8, pp. 23-29, 2022.

[78] J. Phillips, "The reactions of 8-quinolinol," *Chemical Reviews*, vol. 56, pp. 271-297, 1956.

[79] A. Y. SHEN, S. N. WU, and C. T. CHIU, "Synthesis and cytotoxicity evaluation of some 8-hydroxyquinoline derivatives," *Journal of pharmacy and pharmacology,* vol. 51, pp. 543-548, 1999.

[80] J. Nordenberg, A. Novogrodsky, E. Beery, M. Patia, L. Wasserman, and A. Warshawsky, "Anti-proliferative effects and phenotypic alterations induced by 8-hydroxyquinoline in melanoma cell lines," *European Journal of Cancer and Clinical Oncology,* vol. 26, pp. 905-907, 1990.

[81] J. Dimmock, E. Erciyas, S. Raghavan, and D. Kirkpatrick, "Evaluation of the cytotoxicity of some Mannich bases of acetophenone against the EMT6 tumour," *Die Pharmazie,* vol. 45, pp. 755-757, 1990.

[82] S. E.-t. Ashoor, R. A. Abokhater, and N. B. Treina, "Synthesis, DFT Study and the Biological Activity of 8-Hydroxyquinoline Zirconium (IV) Complexes," *European Journal of Applied Sciences,* vol. 10, pp. 726-737, 2022.

[83] A. Cipurković, E. Horozić, S. Marić, L. Mekić, and H. Junuzović, "Metal complexes with 8-hydroxyquinoline: synthesis and in vitro antimicrobial activity," *Open Journal of Applied Sciences,* vol. 11, p. 1, 2021.

[84] S. Mathur and S. Tabassum, "New homodi-and heterotrinuclear metal complexes of Schiff base compartmental ligand: Interaction studies of copper complexes with calf thymus DNA," *Central European Journal of Chemistry,* vol. 4, pp. 502-522, 2006.

[85] J. A. Cowan, "Chemical nucleases," *Current opinion in chemical biology,* vol. 5, pp. 634-642, 2001.

[86] R. B. Dixit, T. S. Patel, S. F. Vanparia, A. P. Kunjadiya, H. R. Keharia, and B. C. Dixit, "DNA-binding interaction studies of microwave assisted synthesized sulfonamide substituted 8-hydroxyquinoline derivatives," *Scientia pharmaceutica,* vol. 79, pp. 293-308, 2011.

[87] V. Prachayasittikul, S. Prachayasittikul, S. Ruchirawat, and V. Prachayasittikul, "8-Hydroxyquinolines: a review of their metal chelating properties and medicinal applications," *Drug design, development and therapy,* pp. 1157-1178, 2013.

[88] J. Sawynok and J.-K. Dawborn, "Plasma concentration and urinary excretion of guanidine derivatives in normal subjects and patients with renal failure," *Clinical and Experimental Pharmacology & Physiology,* vol. 2, pp. 1-15, 1975.

[89] M. Göbel and T. M. Klapötke, "First structural characterization of guanidine, HN [double bond, length as m-dash] C (NH 2) 2," *Chemical communications*, pp. 3180-3182, 2007.

[90] T. Yamada, X. Liu, U. Englert, H. Yamane, and R. Dronskowski, "Solid-state structure of free base guanidine achieved at last," *Chemistry–A European Journal*, vol. 15, pp. 5651-5655, 2009.

[91] P. K. Sawinski, M. Meven, U. Englert, and R. Dronskowski, "Single-crystal neutron diffraction study on guanidine, CN3H5," *Crystal growth & design*, vol. 13, pp. 1730-1735, 2013.

[92] S. Aliyev, R. Ismailova, Z. Asgerova, and A. Zalov, "Research into complex formation of cobalt (II) and nickel (II) with 2-hydroxy-5-nitrothiophenol and diphenylguanidine," *Kimya Problemleri*, pp. 196-204, 2018.

[93] G. R. Hanson, T. A. Kabanos, A. D. Keramidas, D. Mentzafos, and A. Terzis, "Oxovanadium (IV)-amide binding. Synthetic, structural, and physical studies of {N-[2-(4-oxopent-2-en-2-ylamino) phenyl] pyridine-2-carboxamido} oxovanadium (IV) and {N-[2-(4-phenyl-4-oxobut-2-en-2-ylamino) phenyl] pyridine-2-carboxamido} oxovanadium (IV)," *Inorganic Chemistry*, vol. 31, pp. 2587-2594, 1992.

[94] S. Horikoshi and N. Serpone, "Photochemistry with microwaves: Catalysts and environmental applications," *Journal of Photochemistry and Photobiology C: Photochemistry Reviews*, vol. 10, pp. 96-110, 2009.

[95] T.-H. Huang, M.-H. Zhang, M.-L. Tao, and X.-J. Wang, "Synthesis, Structural Characterization, Spectroscopic Properties of Copper (I) Complexes [Cu2 (CH3CN) 4 (dppm) 2](BF4) 2 and [Cu2 (pmk)(dppm) 2](BF4) 2 (dppm= bis (diphenylphosphino) methane, pmk= bis (2-pyridylmethyl) ketazine)," *Synthesis and Reactivity in Inorganic, Metal-Organic, and Nano-Metal Chemistry*, vol. 44, pp. 986-990, 2014.

[96] P. Gushchin, M. Haukka, N. Bokach, and V. Y. Kukushkin, "Platinum (iv)-mediated nucleophilic addition of 1, 3-diphenylguanidine to propiononitrile," *Russian Chemical Bulletin*, vol. 57, pp. 2125-2131, 2008.

[97] S. A. Katkova, M. A. Kinzhalov, P. M. Tolstoy, A. S. Novikov, V. P. Boyarskiy, A. Y. Ananyan, *et al.*, "Diversity of isomerization patterns and protolytic forms in aminocarbene PdII and PtII complexes formed upon addition of N, N′-

diphenylguanidine to metal-activated isocyanides," *Organometallics,* vol. 36, pp. 4145-4159, 2017.

[98] S. K. Bjelogrlić, T. R. Todorović, M. Kojić, M. Senćanski, M. Nikolić, A. Višnjevac, *et al.*, "Pd (II) complexes with N-heteroaromatic hydrazone ligands: Anticancer activity, in silico and experimental target identification," *Journal of Inorganic Biochemistry,* vol. 199, p. 110758, 2019.

[99] X.-D. Yin, K.-Y. Ma, Y.-L. Wang, Y. Sun, X.-F. Shang, Z.-M. Zhao, *et al.*, "Design, synthesis, and antifungal evaluation of 8-hydroxyquinoline metal complexes against phytopathogenic fungi," *Journal of Agricultural and Food Chemistry,* vol. 68, pp. 11096-11104, 2020.

[100] A. S. Attia, A. A. A. Aziz, K. A. Alfallous, and M. El-Shahat, "A novel bonding of 6, 7-dichloroquinoxlaine-2, 3-dione, DCQX, to two molybdenum (0) metal centers: Synthesis, characterization, biological activity studies and semiempirical calculations of [(bpy) 2Mo (μ2-κ2: η6-DCQX) Mo (CO) 3] complex," *Polyhedron,* vol. 44, pp. 238-244, 2012.

[101] J. Kumari and P. Mangala, "Fabrication and Characterization of Molybdenum Trioxide Nanoparticles and their Anticancer, Antibacterial and Antifungal Activities," *Malaysian Journal of Chemistry,* vol. 24, pp. 36-53, 2022.

[102] W. Xu, L. Maser, L. Alig, and R. Langer, "Rhodium carbonyl complexes featuring carbodiphosphorane-based pincer ligands," *Polyhedron,* vol. 196, p. 115018, 2021.

[103] S.-H. Zhou, W.-H. Liao, Y. Yang, W. Li, Y.-y. Wu, T.-T. Wu, *et al.*, "(8-Hydroxyquinoline) Gallium (III) Complex with High Antineoplastic Efficacy for Treating Colon Cancer via Multiple Mechanisms," *ACS omega,* vol. 8, pp. 6945-6958, 2023.

[104] P. Pandey, B. Kharediya, B. Elrez, J. Sutter, G. Bhargavi, M. Rajasekharan, *et al.*, "Ligand directed structural diversity and magnetism in copper (II)–azido assemblies with isomeric aminopyridines: Synthesis, structure, magnetism and theoretical studies," *Dalton Transactions,* vol. 46, pp. 15908-15918, 2017.

الملخص

تم استخدام المسار الأخضر بمساعدة الميكروويف بنجاح لتخليق سلسلة من المعقدات الجديدة من كربونيلات السلسلة الأولى والثانية للفلزات الانتقالية، والتي تحتوي على الليجاند المخلبي bis-(diphenylphosphinemethane (dppm)) . إلى جانب ليجاندات أخرى تشمل: diphenylguanidine (DPG)، 2-aminopyridine (2-aminoPy) 8-hydroxyquinoline (8-HQ) ، بالتناسق مع $[Cr(CO)_6]$ و $[Mo(CO)_6]$عبر مجموعة (C=O) ، وقد تم الحصول على المعقدات الجديدة من الانواع التالية : $[M(CO)_2(dppm)(dpg)]$، $[M(CO)_2(dppm)(8\text{-}HQ)]$، $[M(CO)_2(dppm)(2\text{-aminopy})]$ حيث (M= Cr, Mo).

تم تشخيص هذه المعقدات باستخدام مطيافية الأشعة فوق البنفسجية(UV) ، والأشعة تحت الحمراء (IR)، وأطياف الكتلة (Mass Spectrum) ، والتحليل الدقيق للعناصر(CHN) ، بالإضافة إلى أطياف ^{1}HNMR.، كما تم تقييم النشاط البيولوجي للمعقدات ضد خط خلايا سرطان الكبد(HEPG-2) ، وأظهرت جميع المركبات تأثيرات مثبطة لنمو الخلايا، وكان المركب (F5, F3) الأكثر فعالية بقيمة IC_{50} بلغت (180، 207 ميكرومول) على التوالي، مما يشير إلى إمكانية استخدام هذه المركبات كأساس لتطوير عوامل علاجية جديدة مضادة للسرطان.

علاوة على ذلك ، تم تطبيق نظرية دالة الكثافة (DFT) على معقدات المولبيدنيوم والكروم لتقدير الطاقة الكلية للنظام من خلال تقريب الطاقة إلى الكثافة الإلكترونية . وأظهرت دراسات الالتحام الجزيئي (Molecular Docking) لجميع المجمعات (F1–F6) على مستقبل الإستروجين (PDB ID: 4PYP) أن المعقدات (F1, F4, F6) تمتلك أعلى قدرة على الارتباط بالموقع النشط، بقيم طاقة ربط بلغت (–8.43 و–8.54 و–8.85) كيلو كالوري/مول على التوالي، مما يشير إلى ثبات أعلى وتفاعل أقوى مقارنةً ببقية المعقدات. وقد ساهمت المحاكاة الحاسوبية في توفير فهم أدق لطبيعة التفاعلات وآلية التأثير المحتملة على الخلايا السرطانية. كما تم تقييم النشاط البيولوجي للمعقدات ضد خط خلايا سرطان الكبد.(HEPG-2) .

الجامعة الأسمرية الإسلامية
كلية العلوم
قسم الكيمياء

دراسات تجريبية ومحاكاة خصائص الترابط لبعض المعادن الانتقالية المحتوية على الكربونيل من الصف الأول والثاني وتطبيقاتها البيولوجية

إعداد الطالبة: فتحية محمد احمد التريكي

إشراف

أ.د: سالم التهامي عاشور
الدرجة العلمية: أستاذ

أ.د: خليفة عبدالسلام علي الفلوس
الدرجة العلمية: أستاذ

قدّمت هذه الدراسة استكمالاً لمتطلبات الحصول على درجة الإجازة العالية (الماجستير) في العلوم للعام الجامعي (2024-2025)